

**Discoveries of anti-Müllerian hormone and anti-Müllerian hormone  
receptor type 2 in bovine GnRH neurons and gonadotrophs**

ウシ視床下部とゴナドトロフにおけるアンチミュラーホルモン  
とアンチミュラーホルモン2型受容体の発見

**The United Graduate School of Veterinary Science  
Yamaguchi University**

**Onalenna KEREILWE**

**March 2021**

**Discoveries of anti-Müllerian hormone and anti-Müllerian hormone  
receptor type 2 in bovine GnRH neurons and gonadotrophs**

**A Dissertation**

*Submitted by*

**ONALENNA KEREILWE**

in Partial Fulfillment of the Requirement for the Degree of

**DOCTOR OF PHILOSOPHY**

**(Reproductive Physiology and Management)**



**The United Graduate School of Veterinary Science**

**Yamaguchi University**

**JAPAN**

**March, 2021**

## Acknowledgements

I am highly grateful to the Government of Japan, the Ministry of Education, Culture, Sports, Science and Technology, for sponsoring my study by providing me the *Monbukagakusho (MEXT) Scholarship*.

This dissertation work was carried out at the Laboratory of Reproduction, Department of Veterinary Clinical Sciences, The United Graduate School of Veterinary Science, Yamaguchi University. This work has been realized through the intensive efforts and participation of many people. It is my pleasure to thank the many people who made my study and research possible.

First and foremost, I would like to thank my supervisor, Associate Prof. Dr. Hiroya Kadokawa for his excellent knowledge, guidance, wisdom, unfaltering enthusiasm and patience. I am indebted to him for his continuous help and encouragement throughout the years not only in the academic aspects but also in my daily life. He and his wife, Yukie's positive approach to life and kindness are highly appreciated. They often went beyond the call of their duties to help patiently when I need help.

I am greatly thankful to my co-supervisors Prof. Dr. Mitsuhiro Takagi, Prof. Dr. Naoki Sasaki, Prof. Dr. Ken Kusakabe, and Prof. Dr. Mitsugu Hishinuma for their valuable comments, suggestions and guidance that made my preparation of this dissertation a reality. I am also thankful to all my teachers and office staffs for their kind support and help during my study.

I am highly grateful to the Yamaguchi Prefectural Government for allowing me to use their slaughter houses facilities and beef cattle farmers for allowing using their animals as sources of main data for the purpose of my study.

I would also like to thank Prof. Vitaliano Borromeo, Dipartimento di Medicina Veterinaria, Università degli Studi di Milano, Italy, for providing various antibodies for my study and for valuable suggestions as a co-author in my paper.

I am also thankful to my laboratory colleagues: Asrafun Nahar, Kiran Pandey, Raihana Nasrin Ferdousy, and Risa Saito for their friendly assistance, encouragement and support in my studies. I also express my sincere thanks to my international, Japanese and African friends and their families, Hirakawa-no-Kaze-no Kai, Yamaguchi Red Cross, Yamaguchi city office and many other people and organizations that are not mentioned here, for their support to make my stay in Japan homely. I also acknowledge with thanks the great cooperation I received from the entire university community in terms of academic and social life during my study.

I would like to express my deepest appreciation and love to my parents, brothers, sisters, in-laws and all my family members for their everlasting encouragement, sacrifices, and kindness. Finally, I would like to thank my wife Dineo and our sons, for their unending love, sacrifices, patience, support and encouragement during my study. I would like to dedicate this dissertation to my mother who have been the source of my motivation for higher education.

## Abstract

Fertility decreases during aging in human and bovine females, but the exact pathophysiological mechanisms in the pituitaries and hypothalamus are not clarified yet. Anti-Müllerian hormone (AMH) is a glycoprotein that belongs to the transforming growth factor (TGF)- $\beta$  superfamily. Plasma AMH concentrations can predict the fertility of adult female goats, ewes, cows, and women via unknown physiological mechanisms. This thesis study attempted to clarify whether AMH, and the main receptor for AMH, AMH receptor type 2 (AMHR2) are expressed in pituitaries and hypothalamus, and whether AMH and AMHR2 have important roles for the age-related infertility.

Preantral and small antral follicles may secrete AMH to control gonadotrophin secretion from ruminant gonadotrophs. In first, I investigated whether AMHR2 is expressed in gonadotrophs of postpubertal heifers to control gonadotrophin secretion. Expression of *AMHR2* mRNA was detected in anterior pituitaries (APs) of postpubertal heifers using reverse transcription–polymerase chain reaction (RT-PCR). An anti-AMHR2 chicken antibody was developed against the extracellular region near the N-terminus of bovine AMHR2. Western blotting using this antibody detected the expression of AMHR2 protein in APs. Immunofluorescence microscopy using the same antibody visualised colocalisation of AMHR2 with gonadotrophin-releasing hormone (GnRH) receptor on the plasma membrane of gonadotrophs. AP cells were cultured for 3.5 days and then treated with increasing concentrations (0, 1, 10, 100, or 1000 pg mL<sup>-1</sup>) of AMH. AMH (10–1000 pg mL<sup>-1</sup>) stimulated ( $P < 0.05$ ) basal FSH secretion. In addition, AMH (100–1000 pg mL<sup>-1</sup>) weakly stimulated ( $P < 0.05$ ) basal LH secretion. AMH (100–1000 pg mL<sup>-1</sup>) inhibited GnRH-induced FSH secretion, but

not GnRH-induced LH secretion, in AP cells. I also compared expression levels between old Holsteins ( $79.2 \pm 10.3$  months old) and young ( $25.9 \pm 0.6$  months old) and old Japanese Black females ( $89.7 \pm 20.3$  months old), but no significant differences were observed among the groups. Therefore, AMHR2 is expressed in gonadotrophs of postpubertal heifers to control gonadotrophin secretion.

Other important hormones for endocrinological gonadotroph regulation (e.g. GnRH, inhibin and activin) have paracrine and autocrine roles. Therefore, in the next study, I evaluated AMH expression in bovine gonadotroph cells and the relationships between AMH expression in the bovine AP and oestrous stage, age and breed. *AMH* mRNA expression was detected in APs of postpubertal heifers (26 months old) by RT-PCR. Based on western blotting using an antibody to mature C-terminal AMH, AMH protein expression was detected in APs. Immunofluorescence microscopy utilising the same antibody indicated that AMH is expressed in gonadotrophs. The expression of *AMH* mRNA and protein in APs did not differ between oestrous phases ( $P > 0.1$ ). I compared expression levels between old Holsteins ( $79.2 \pm 10.3$  months old) and young ( $25.9 \pm 0.6$  months old) and old Japanese Black females ( $89.7 \pm 20.3$  months old). The APs of old Holsteins exhibited lower *AMH* mRNA levels ( $P < 0.05$ ), but higher AMH protein levels than those of young Japanese Black females ( $P < 0.05$ ). Therefore, bovine gonadotrophs express AMH and this AMH expression may be breed-dependent.

Circulating concentrations of AMH can indicate fertility in various animals, but the physiological mechanisms underlying the effect of AMH on fertility remain unknown. I recently discovered that AMH has extragonadal functions via its main receptor, AMHR2. Specifically, AMH stimulates the secretion of LH and FSH from bovine gonadotrophs. Moreover, gonadotrophs themselves express AMH to exert paracrine/autocrine functions, and AMH can activate GnRH neurons in mice. The next

study aimed to evaluate whether AMH and AMHR2 are detected in areas of the brain relevant to neuroendocrine control of reproduction: the preoptic area (POA), arcuate nucleus (ARC), and median eminence (ME), and in particular within GnRH neurons. RT-PCR detected both *AMH* and *AMHR2* mRNA in tissues containing POA, as well as in those containing both ARC and ME, collected from postpubertal heifers. Western blotting detected AMH and AMHR2 protein in the collected tissues. Triple fluorescence immunohistochemistry revealed that most cell bodies or fibers of GnRH neurons were AMHR2-positive and AMH-positive, although some were negative. Immunohistochemistry revealed that 75% to 85% of cell bodies and fibers of GnRH neurons were positive for both AMH and AMHR2 in the POA, ARC, and both the internal and external zones of the ME. The cell bodies of GnRH neurons were situated around other AMH-positive cell bodies or fibers of GnRH and non-GNRH neurons. Therefore, AMH and AMHR2 are detected in most cell bodies or fibers of GnRH neurons in the POA, ARC, and ME of heifer brains.

Cow fertility decreases with age, but the hypothalamic pathomechanisms are not understood. AMH stimulates GnRH neurons via AMHR2 in rodent, and most GnRH neurons in the POA, ARC, and ME express AMH and AMHR2. Therefore, in my thesis study I hypothesized that both protein amounts would differ in the anterior hypothalamus (including POA) and posterior hypothalamus (including ARC and ME) between young post-pubertal heifers and old cows. Western blot analysis showed lower ( $P < 0.05$ ) expressions of AMH and AMHR2 in the posterior hypothalamus, but not in the anterior hypothalamus, of old Holstein cows and old Japanese Black cows compared to young heifers. Therefore, AMH and AMHR2 were decreased in the posterior hypothalami of old cows, suggesting decreased AMH and AMHR2 in ARC and/or ME.

In conclusion, this thesis study discovered and revealed AMH and AMHR2 expression in gonadotrophs and GnRH neurons, which have important contribution for the age-related infertility.

## Table of Contents

<b>Acknowledgements</b>	<b>i</b>
<b>Thesis Abstract</b>	<b>iii</b>
<b>Table of Contents</b>	<b>vii</b>
<b>List of Tables</b>	<b>xii</b>
<b>List of Figures</b>	<b>xiv</b>
<b>List of Abbreviations</b>	<b>xxi</b>
<b>List of Companies</b>	<b>xxiv</b>
<b>CHAPTER I</b>	
<b>General Introduction</b>	<b>1-5</b>
<b>CHAPTER II</b>	
<b>Review of Literature</b>	<b>6-13</b>
2.1. Hypothalamus, pituitary and gonads axis	7
2.2. Hypothalamic control of reproduction	7
2.3. Anterior pituitary	8
2.4. Gonadotrophs	8
2.5. AMH and AMHR2	10
2.6. Infertility in aged animals and dairy cows	11
2.7. Issues of Age-related infertility	12
2.8. Hypothalamus-pituitary role in age-related infertility	12
<b>CHAPTER III (Study I)</b>	
<b>Anti- Müllerian hormone receptor type 2 is expressed in gonadotrophs of postpubertal heifers to control gonadotrophin secretion</b>	<b>14-57</b>
Abstract	15
3.1. Introduction	16
3.2. Materials and methods	19
3.2.1. Animals and treatments	19
3.2.2. AP and ovary sample collection	19
3.2.3. RT-PCR sequencing of amplified products and homology search in gene databases	20

3.2.4. Development anti-AMHR2 chicken antibody	23
3.2.5. Other antibodies used in the present study	24
3.2.6. Western blotting for AMHR2	25
3.2.7. Fluorescent immunohistochemistry and confocal microscopic observation	26
3.2.8. AP cell culture and immunocytochemical analysis of cells	27
3.2.9. Pituitary cell culture and analysis of the effects of AMH on LH and FSH secretion	29
3.2.10. RIA to measure gonadotrophin concentrations in culture media	30
3.2.11. AP sample collection for comparisons between oestrous stages	31
3.2.12. AP sample collection for comparisons between age or breeds	31
3.2.13. RT-qPCR to evaluate the factors affecting AMHR2 expression	32
3.2.14. Western blotting to evaluate the factors affecting AMHR2 expression	35
3.2.15. Analysis of the <i>AMHR2</i> gene 5'- flanking region	35
3.2.16. Statistical analysis	36
3.3. Results	37
3.3.1. Expression of <i>AMHR2</i> mRNA in the AP of postpubertal heifers	37
3.3.2. Western blotting for AMHR2	37
3.3.3. Immunofluorescence analysis of AMHR2 expression in bovine granulosa cells	38
3.3.4. Immunofluorescence analysis of AMHR2 expression in bovine AP tissue	38
3.3.5. AMHR2 and GnRHR aggregate on the surface of cultured AP cells	38
3.3.6. AMHR2 expression in cultured gonadotrophs	39

3.3.7. Effects of AMH on gonadotrophin secretion from cultured AP cells	39
3.3.8. Relationship between AMHR2 in APs and the estrous phase	39
3.3.9. AMHR2 expression in APs of Holstein cows, Japanese black heifers, and Japanese black cows	40
3.3.10. ERE, and PRE in the 5'-flanking region of bovine <i>AMHR2</i> gene	40

3.4. Discussion	53
-----------------	----

## CHAPTER IV (Study II)

### **Bovine gonadotrophs express anti- Müllerian hormone (AMH): comparison of AMH mRNA and protein expression levels between old Holsteins and young and old Japanese Black females**

Abstract	59
4.1. Introduction	60
4.2. Materials and methods	62
4.2.1. Antibodies used in this study	62
4.2.2. AP and ovary sample collection for RT-PCR, western blotting and IHC	63
4.2.3. Analysis of the <i>AMH</i> gene 5'- flanking region	65
4.3. Results	66
4.3.1. Expression of <i>AMH</i> mRNA in APs of post-pubertal heifers	66
4.3.2. AMH protein expression in APs	66
4.3.3. Immunofluorescence analysis of AMH expression in bovine small follicles and AP tissues	66
4.3.4. Relationship between AMH in APs and the estrous phase	67
4.3.5. AMH expression in APs of Holstein cows, Japanese black heifers, and Japanese black cows	67

4.3.6. ERE, and PRE in the 5'-flanking region of bovine *AMH* gene 68

4.4. Discussion 77

## **CHAPTER V (Study III)**

### **Anti-Müllerian hormone and its receptor are detected in most gonadotropin-releasing-hormone cell bodies and fibers in heifer brains 80-116**

Abstract	81
5.1. Introduction	82
5.2. Materials and methods	84
5.2.1. Antibodies used in this study	84
5.2.2. Brain and ovary sample collection	84
5.2.3. Western Blotting and RT-PCR for <i>AMH</i> or <i>AMHR2</i> detection	89
5.2.4. Fluorescent immunohistochemistry and confocal microscopy	91
5.3. Results	94
5.3.1. Detection of <i>AMH</i> and <i>AMHR2</i> mRNA in POA and ARC&ME tissues	94
5.3.2. Detection of AMH and AMHR2 protein in POA and ARC&ME tissues	94
5.3.3. Immunofluorescence analysis of AMH and AMHR2	95
5.4. Discussion	114

## **CHAPTER VI (Study IV)**

### **Decreased anti-Müllerian hormone and anti-Müllerian hormone receptor type 2 in Hypothalami of Old Cows 117-131**

Abstract	118
6.1. Introduction	119
6.2. Materials and methods	120
6.3. Results	121
6.4. Appendix	126
6.5. Discussion	130

<b>CHAPTER VII</b>	
<b>General Discussion and Conclusion</b>	<b>132-135</b>
7.1. General Discussion	133
7.2. Conclusion	135
<b>References</b>	<b>136-153</b>

## List of Tables

### CHAPTER III (Study I)

- Table 3.1 Details of the three primers used for PCR to detect *AMHR2* mRNA in bovine anterior pituitaries. 22
- Table 3.2 Name, accession number, and details of the primers used for RT-qPCRs 34

### CHAPTER IV (Study II)

- Table 4.1. Name, accession number, and details of the primers used for RT-qPCRs 64

### CHAPTER V (Study III)

- Table 5.1 Details concerning the primers used for PCR to detect mRNA of *anti-Müllerian hormone (AMH)* and *anti-Müllerian hormone receptor type 2 (AMHR2)*. 90
- Table 5.2 Mean  $\pm$  SEM of the number of examined GnRH-positive, AMHR2-positive, or AMH-positive cell bodies (round or polygonal shape, diameter is more than 8  $\mu$ m) and fibers (axon shown as continuous line of immunopositive signal, or varicosity shown as dotted line) in the preoptic area. 98
- Table 5.3 Mean  $\pm$  SEM of the percentage of GnRH cells that co-localize AMHR2 or AMH, the percentage of AMHR2 or AMH cells that co-localize GnRH in the POA. 99
- Table 5.4 Mean  $\pm$  SEM of the percentage of GnRH fibers that co-localize AMHR2 or AMH, the percentage of AMHR2 or AMH fibers that co-localize GnRH in the POA. 100
- Table 5.5 Mean  $\pm$  SEM of the number of examined GnRH-positive, AMHR2-positive, or AMH-positive fibers in the ARC or iME or eME. 101

Table 5.6	Mean $\pm$ SEM of the percentage of GnRH fibers that co-localize AMHR2 or AMH, the percentage of AMHR2 or AMH fibers that co-localize GnRH in the ARC, iME, or eME.	102
-----------	---	-----

#### **CHAPTER VI (Study IV)**

Table 6.1.	Name, accession number, and details of the primers used for RT-qPCRs	127
------------	--	-----

## List of Figures

### CHAPTER III (Study I)

- Fig. 3.1 Expression of *AMHR2* mRNA detected by RT-PCR. 41  
Electrophoresis of PCR-amplified DNA products using 1 of 3 pairs of primers for bovine *AMHR2* and cDNA derived from AP of post-pubertal heifers.
- Fig. 3.2 Results of western blotting using extracts (4, 8, or 16  $\mu$ g of total 42  
protein) from the AP or ovary of post-pubertal heifers and anti-*AMHR2* antibody (A) or anti- $\beta$ -actin antibody (B).
- Fig. 3.3 Fluorescence immunocytochemistry was used to confirm the 43  
expression of *AMHR2* on the surface of granulosa cells of small (approximately 5 mm) follicles in the ovaries of post-pubertal heifers.
- Fig. 3.4 Triple-fluorescence immunohistochemistry of AP tissue of post- 44  
pubertal heifers for *AMHR2*, GnRHR and either LH (A) or FSH (B). Images were captured by laser confocal microscopy for *AMHR2* (red), GnRHR (green) and LH or FSH (light blue) with counter-staining by DAPI (dark blue).
- Fig. 3.5 Fluorescence immunocytochemistry was used to confirm the 45  
colocalization (yellow in the merge panel) of *AMHR2* and GnRHR on the surface of cultured AP cells (prepared by CellCover method) of post-pubertal heifers. Images were captured by laser confocal microscopy for *AMHR2* (red), GnRHR (green), DNA (dark blue), and DIC on cultured AP cells which did not receive Triton X-100 treatment for antibody penetration.
- Fig. 3.6 Triple-fluorescence immunocytochemistry of cultured AP cells 46  
(prepared by PFA-Triton method) of post-pubertal heifers for *AMHR2*, GnRHR and either LH (A) or FSH (B). Images were captured by laser confocal microscopy for *AMHR2* (green), GnRHR (light blue) and LH or FSH (red) with counter-staining by DAPI (dark blue). Yellow (shown by arrows) indicates the

colocalization of AMHR2 and LH of FSH in LH-positive cells (A) and FSH-positive cells (B).

- Fig. 3.7 Comparison of the effects of various concentrations of AMH in media with (A) and without (B) 1 nM GnRH on LH secretion from cultured AP cells of post-pubertal heifers. 47
- Fig. 3.8 Comparison of the effects of various concentrations of AMH in media with (A) and without (B) 1 nM GnRH on FSH secretion from cultured AP cells of post-pubertal heifers. 48
- Fig. 3.9 Relative *AMHR2* mRNA levels (mean  $\pm$  SEM) in bovine APs during pre-ovulation [day 19 to 21 (day 0 = day of estrus)], early luteal (day 2 to 5), mid-luteal (day 8 to 12), or late luteal (day 15 to 17) phases, as determined by real-time PCR. 49
- Fig. 3.10 (A) Representative AMHR2 (as full length monomer form) and  $\beta$ -actin protein expression in bovine AP tissues obtained during the pre-ovulation, early luteal, mid luteal, or late luteal phases of estrous, as detected by western blotting. 50  
(B) AMH protein expression level of AMH normalized to that of  $\beta$ -actin in healthy post-pubertal heifer AP tissues obtained during pre-ovulation (n =5), early luteal (n =5), mid-luteal (n =6), and late luteal (n = 5) phases.
- Fig. 3.11 Relative *AMHR2* mRNA levels (mean  $\pm$  SEM) in bovine AP tissues obtained from healthy young Japanese heifers (young JB), old Japanese black cows (old JB), and old Holsteins cows (old Hol), as determined by RT-qPCR. 51
- Fig. 3.12 (A) Representative AMH (as full length monomer form) and  $\beta$ -actin protein expression in bovine AP tissues obtained from young JB, old JB, and old Hol. 52  
(B) Protein expression level of AMH normalized to that of  $\beta$ -actin in bovine AP tissues obtained from young JB, old JB, and old Hol.

#### CHAPTER IV (Study II)

- Fig. 4.1 Expression of *AMH* mRNA, as detected by RT-PCR. 69  
Electrophoresis of PCR-amplified DNA products using the primer

pair for bovine *AMH* and cDNA derived from the AP of post-pubertal heifers.

- Fig. 4.2 Western blotting results using extracts (2, 4, 8, or 16  $\mu$ g of total protein) from the APs or ovaries of post-pubertal heifers and an anti-AMH rabbit antibody (A) or anti- $\beta$ -actin mouse antibody (B). 70
- Fig. 4.3 Fluorescence immunohistochemical analysis of AMH on small antral follicles in ovaries of post-pubertal heifers. Images were captured by laser confocal microscopy for AMH (green) with counter-staining by DAPI (dark blue, indicating DNA) and differential interference contrast (DIC). 71
- Fig. 4.4 Triple-fluorescence immunohistochemistry of AP tissues in post-pubertal heifers for the detection of GnRHR, AMH, and LH (A) or FSH (B). Images were captured by laser confocal microscopy for GnRHR (cyan), AMH (red), and LH or FSH (green) with counter-staining by DAPI for DNA (dark blue). 72
- Fig. 4.5 Relative *AMH* mRNA levels (mean  $\pm$  SEM) in bovine APs during pre-ovulation [day 19 to 21 (day 0 = day of estrus)], early luteal (day 2 to 5), mid-luteal (day 8 to 12), or late luteal (day 15 to 17) phases, as determined by RT-qPCR. 73
- Fig. 4.6 (A) Representative AMH (as mature C-terminal form) and  $\beta$ -actin protein expression in bovine AP tissues obtained during the pre-ovulation, early luteal, mid luteal, or late luteal phases of estrous, as detected by western blotting. 74
- (B) AMH protein expression level of AMH normalized to that of  $\beta$ -actin in healthy post-pubertal heifer AP tissues obtained during pre-ovulation (n =5), early luteal (n =5), mid-luteal (n =6), and late luteal (n = 5) phases.
- Fig. 4.7 Relative *AMH* mRNA levels (mean  $\pm$  SEM) in bovine AP tissues obtained from healthy young Japanese heifers (young JB), old Japanese black cows (old JB), and old Holsteins cows (old Hol), as determined by RT-qPCR. 75

- Fig. 4.8 (A) Representative AMH (in the mature C-terminal form) and  $\beta$ -actin protein expression in bovine AP tissues obtained from young JB, old JB, and old Hol. 76
- (B) Protein expression level of AMH normalized to that of  $\beta$ -actin in bovine AP tissues obtained from young JB, old JB, and old Hol.

## CHAPTER V (Study III)

- Fig. 5.1 Schematic illustration of brain tissue sampling from bovine brain to yield POA and ARC&ME blocks. 88
- Fig. 5.2 Detection of *AMH* mRNA (A) and *AMHR2* mRNA (B) by RT-PCR. Electrophoresis of PCR-amplified DNA products using primers for bovine *AMH* or *AMHR2* and cDNA derived from the ovary, tissues containing the POA tissue or ARC&ME tissue of post-pubertal heifers. The lanes labeled as AMH or AMHR2 demonstrate that the sizes of the obtained DNA products met expectations: 328 or 320 bp, respectively. The Marker lane indicates the DNA marker. 103
- Fig. 5.3 Results of western blotting using extracts from the ovary, POA, or ARC&ME tissue of post-pubertal heifers and anti-AMH antibody (A), anti-AMHR2 antibody (B), or anti- $\beta$ -actin antibody (A' and B'). Bovine AMH bands were defined based on size as either precursors or mature C-terminal proteins. Bovine AMHR2 bands were defined based on size as either full-length or cleaved monomers. 104
- Fig. 5.4 Immunocytochemical distribution of GnRH, AMH and AMHR2 in coronal sections containing POA (A, B, C), or ARC and ME (D, E, F) drawn on the corresponding region of the bovine brain atlas (Okamura 2002). The crosses, lines, and triangles indicate cell body, and longitudinal and cross-section of fibers, respectively. The green ones indicate GnRH-positive, AMH-positive and AMHR2-positive (triple positive). The red ones indicate GnRH-positive AMH-negative and AMHR2-negative. The purple ones indicate lack of colocalization of AMH and GnRH. 105

- Fig. 5.5 Triple-fluorescence photomicrographs of AMH, AMHR2, and GnRH in the POA (A, B, C, D) of post-pubertal heifers. Images were captured with laser confocal microscopy for AMH (light blue), AMHR2 (green), and GnRH (red). In the merged photos, CB, Axon, V indicate cell body, axon, and varicosity of neuron. The yellow arrows, CB, Axon, and V indicate the colocalization of AMH, AMHR2, and GnRH. Light blue ones indicate lack of colocalization of AMH and GnRH. Red ones indicate lack of colocalization of GnRH and AMH or AMHR2. 106
- Fig. 5.6 Transparent projection of the z-stack images of triple-stained cell bodies and fibers in the POA (A, B) of post-pubertal heifers. The images were captured using a laser confocal microscope. AMH, AMHR2, and GnRH are depicted in blue, green, and red, respectively. Note that the color indicating DNA has been excluded because the large number of cell nuclei containing DNA would have masked the main objects. 107
- Fig. 5.7 Triple-fluorescence photomicrographs of ARC (A, B, C, D) tissue obtained from post-pubertal heifers. Images were captured with laser confocal microscopy for AMH (light blue), AMHR2 (green), and GnRH (red). In the merged photos, the yellow arrows CB, and Axon indicate the colocalization of AMH, AMHR2, and GnRH. 108
- Fig. 5.8 Triple-fluorescence photomicrographs of ME (A, B) tissue obtained from post-pubertal heifers. Images were captured with laser confocal microscopy for AMH (light blue), AMHR2 (green), and GnRH (red). The orange rectangle within the low magnification image indicates the position of high magnification. In the merged photos, the yellow arrows and V indicate the colocalization of AMH, AMHR2, and GnRH; the red arrows and V indicate the lack of colocalization of GnRH and AMH or AMHR2. Scale bars are 50  $\mu\text{m}$  in the low-magnification photos of (A, B), and 20  $\mu\text{m}$  in the high magnification photos of (A,B). White arrows labeled as 3V, Arc, or Pituitary indicate the direction of the third ventricle, arcuate nucleus, and pituitary, respectively. 109

Fig. 5.9 Triple-fluorescence photomicrographs of other parts of ME (A, 111  
 B) tissue obtained from post-pubertal heifers. Images were  
 captured with laser confocal microscopy for AMH (light blue),  
 AMHR2 (green), and GnRH (red). The orange rectangle within  
 the low magnification image indicates the position of high  
 magnification. Vessel indicate the position of vessel. In the  
 merged photos, the yellow arrows indicate the colocalization of  
 AMH, AMHR2, and GnRH; the light blue arrows indicate the  
 lack of colocalization of AMH and GnRH; the red arrows and V  
 indicate the lack of colocalization of GnRH and AMH or  
 AMHR2. Scale bars are 100  $\mu\text{m}$  in the low-magnification photos  
 of (A) and high-magnification photos of (B), 20  $\mu\text{m}$  in the high  
 magnification photos of (A), and 200  $\mu\text{m}$  in the low-  
 magnification photos of (B). White arrows labeled as 3V, or  
 Pituitary indicate the direction of the third ventricle, and pituitary,  
 respectively.

Fig. 5.10 Transparent projection of the z-stack images of triple-stained 113  
 fibers (A) and terminal (B) in the eME of post-pubertal heifers.  
 The images were captured using a laser confocal microscope.  
 AMH, AMHR2, and GnRH are depicted in blue, green, and red,  
 respectively. Note that the color indicative of DNA has been  
 excluded because the large number of cell nuclei containing DNA  
 would have masked the main objects.

## CHAPTER VI (Study IV)

Fig. 6.1 Representative AMH (in mature C-terminal form) and  $\beta$ -actin 122  
 immunoreactive protein bands in POA tissues (A) obtained from  
 Japanese black young heifers (young JB), old Japanese black cows  
 (old JB) and old Holstein cows (old Hol). Comparison of AMH  
 protein expression normalized to that of  $\beta$ -actin ( $n=5$  per group) in  
 POA (B).

Fig. 6.2 Representative AMH (in mature C-terminal form) and  $\beta$ -actin 123  
 immunoreactive protein bands in ARC&ME tissues (A) obtained

from young JB, old JB, and old Hol. Comparison of AMH protein expression normalized to that of  $\beta$ -actin ( $n=5$  per group) in ARC&ME (B).

Fig. 6.3 Representative AMHR2 (in full length monomer form) and  $\beta$ -actin immunoreactive protein bands in POA tissues (A) obtained from young JB, old JB, and old Hol. Comparison of AMHR2 protein expression normalized to that of  $\beta$ -actin ( $n=5$  per group) in POA (B). 124

Fig. 6.4 Representative AMHR2 (in full length monomer form) and  $\beta$ -actin immunoreactive protein bands in ARC&ME tissues (A) obtained from young JB, old JB, and old Hol. Comparison of AMHR2 protein expression normalized to that of  $\beta$ -actin ( $n=5$  per group) in ARC&ME (B). 125

Fig. 6.5 Relative *AMH* mRNA levels (mean  $\pm$  SEM) in bovine POA and ARC & ME tissues obtained from young and old JB, as determined by RT-qPCR. Data were normalized to the geometric means of *YWHAZ* and *SDHA* levels. 128

Fig. 6.6 Relative *AMHR2* mRNA levels (mean  $\pm$  SEM) in bovine POA and ARC&ME tissues obtained from young and old JB, as determined by RT-qPCR. Data were normalized to the geometric means of *YWHAZ* and *SDHA* levels.

## List of Abbreviations

<b>ac</b>	: anterior commissure
<b>ACTH</b>	: Adrenocorticotrophic hormone
<b>ANOVA</b>	: Analysis of variance
<b>AMH</b>	: Anti Mullerian hormone
<b>AMHR2</b>	: Anti Mullerian hormone receptor type 2
<b>AP</b>	: Anterior pituitary
<b>AVPV</b>	: Anteroventral periventricular nucleus
<b>BLAST</b>	: Nucleotide basic local alignment search tool
<b>ARC</b>	: Arcuate nucleus
<b>BLAT</b>	: BLAST-like alignment tool
<b>bp</b>	: Base pair
<b>BSA</b>	: Bovine serum albumin
<b>C</b>	: Celsius
<b>cAMP</b>	: Cyclic adenosine monophosphate
<b>CCD</b>	: Charge-coupled device
<b>cDNA</b>	: Complementary deoxyribonucleic acid
<b>CO<sub>2</sub></b>	: Carbon dioxide
<b>CP</b>	: Crude protein
<b>Cq</b>	: Quantification cycle
<b>DAPI</b>	: 4',6-diamidino-2-phenylindole
<b>DIC</b>	: Differential interference contrast
<b>DM</b>	: Dry matter
<b>DMEM</b>	: Dulbecco's modified eagle's medium
<b>DMH</b>	: Dorsomedial hypothalamic nucleus
<b>DNA</b>	: Deoxyribonucleic acid
<b>E2</b>	: Estradiol
<b>ECL</b>	: Enhanced chemiluminescence
<b>EGR1</b>	: Early growth response protein
<b>ERE</b>	: Estrogen-responsive element
<b>ERK</b>	: Extracellular signal-regulated kinase
<b>FBS</b>	: Fetal bovine serum

<b>FITC</b>	: Fluorescein isothiocyanate
<b>FSH</b>	: Follicle stimulating hormone
<b>g</b>	: Gravity
<b>G protein</b>	: Guanine-nucleotide-binding regulatory proteins
<b>Gs</b>	: Stimulatory G protein
<b>GPCR/GPR</b>	: G-protein–coupled receptors
<b>GnRH</b>	: Gonadotropin releasing hormone
<b>GnRHR</b>	: Gonadotropin releasing hormone receptor
<b>h</b>	: Hour
<b>HEPES</b>	: 4-(2-hydroxyethyl)-1-piperazineethanesulfonic acid
<b>HPG</b>	: Hypothalamic-pituitary-gonadal axis
<b>HRP</b>	: Horse radish peroxidase
<b>IgG</b>	: Immunoglobulin G
<b>kDa</b>	: Kilo Dalton
<b>kg</b>	: Kilogram
<b>KLH</b>	: keyhole limpet hemocyanin
<b>LH</b>	: Luteinizing hormone
<b>MAP</b>	: Molecule activity predictor
<b>MAPK</b>	: Mitogen-activated protein kinase
<b>Mcal</b>	: Mega calorie
<b>ME</b>	: Median eminence
<b>min</b>	: Minute
<b>mL</b>	: Mililiter
<b>μg</b>	: Microgram
<b>μL</b>	: Microliter
<b>μm</b>	: Micrometer
<b>mRNA</b>	: Messenger ribonucleic acid
<b>MPOA</b>	: Medial preoptic area
<b>n</b>	: Number
<b>NCBI</b>	: National Center for Biotechnology Information
<b>NIDDK</b>	: National Institute of Diabetes and Digestive and Kidney Diseases
<b>ng</b>	: Nanogram
<b>NGS</b>	: Next generation sequencing

<b>nM</b>	: Nanomolar
<b>nm</b>	: Nanometer
<b>OCH</b>	: optic chiasm
<b>OVL</b>	: Vascular organ of the lamina terminals
<b>P</b>	: Probability
<b>P4</b>	: Progesterone
<b>PBS</b>	: Phosphate buffered saline
<b>PCR</b>	: Polymerase chain reaction
<b>PFA</b>	: Paraformaldehyde
<b>Pe</b>	: Periventricular hypothalamic nucleus;
<b>PKA</b>	: Protein kinase A
<b>PKC</b>	: Protein kinase C
<b>PLSD</b>	: Protected least significant difference
<b>POA</b>	: Preoptic area
<b>PRE</b>	: Progesterone-responsive element
<b>PRL</b>	: Prolactin
<b>PVDF</b>	: Polyvinylidene fluoride
<b>PVN</b>	: Paraventricular hypothalamic nucleus;
<b>RIN</b>	: RNA integrity number
<b>RNA</b>	: Ribonucleic acid
<b>RIA</b>	: Radioimmunoassay
<b>RPKM</b>	: Reads per kilobase of exon model per million mapped reads
<b>RT-qPCR</b>	: Quantitative reverse transcription-polymerase chain reaction
<b>SCH</b>	: Suprachiasmatic nucleus;
<b>sec</b>	: Second
<b>SEM</b>	: Standard error of mean
<b>SMAD</b>	: Small mothers against decapentaplegic
<b>SOLiD</b>	: Sequencing by Oligo Ligation Detection
<b>TGF</b>	: transforming growth factor
<b>TSH</b>	: Thyroid stimulating hormone
<b>vs</b>	: Versus
<b>3V</b>	: Third ventricle
<b>VMH</b>	: Ventromedial hypothalamic nucleus.

## List of Companies Supplying Chemicals or Instruments Used in This Study

<b>Name of company</b>	<b>Address</b>
Agilent Technologies	Santa Clara, CA, USA
Anacyte laboratories UG	Kuhreder, Hamburg, Germany
As One Corporation	Osaka, Japan
Beckman Coulter Inc.	Brea, CA, USA
Bethyl laboratories, Inc.	Montgomery, TX, USA
Bio-Rad	Hercules, CA, USA
Biorbyt	Cambridge, UK
Carl Zeiss	Göttingen, Germany
Fujifilm	Tokyo, Japan
GE Healthcare	Amersham, UK
Genetyx	Tokyo, Japan
Gelstar, Lonza	Allendale, NJ
Gibco	Grand Island, NY, USA
Ibidi	Planegg, Germany
Kamar Product Inc.	Zionville, IN, USA
Kirkegaard & Perry Laboratories	Baltimore, MD, USA
Leica Microsystems PtyLtd.	Wetzlar, Germany
M. Watanabe & Co.	Tokyo, Japan
Matsunami-Glass	Osaka, Japan
Nacalai Tesque Inc.	Kyoto, Japan
NanoDrop Technologies Inc.	Wilmington, DE, USA
NIDDK	Bethesda, CA, USA
Nippon Gene	Tokyo, Japan
Partec GmbH	Gorlitz, Germany
Peptide Institute Inc.	Osaka, Japan
Pfizer	Tokyo, Japan
Pierce Biotechnology	Rockford, IL, USA
Qiagen	Valencia, CA, USA
R&D systems	Minneapolis, MN, US
SAS Institute, Inc.	Cary, NC, USA

Sakura Fine Technical Co. Ltd.	Tokyo, Japan
Santa Cruz Biotechnology, Inc.	Dallas, TX, USA
Scrum Inc.	Tokyo, Japan
Sigma-Aldrich	St. Louis, MO, USA
Stemcell Technologies	<u>Vancouver, Canada</u>
Sumitomo Bakelite	Tokyo, Japan
Takara Bio Inc.	Shiga, Japan
Thermo Fisher Scientific	Rockford, IL, USA
Toyobo	Tokyo, Japan
Vector Laboratories Inc.	Burlingame, CA, USA
Wako Pure Chemicals	Osaka, Japan

# **CHAPTER I**

## **General Introduction**

The hypothalamic-pituitary-gonadal axis drives reproduction and some of the most important components of the axis are the GnRH neurons (Herbison 2016; Nestor *et al.* 2018). GnRH neurons originate in the POA and ARC and project to the ME, the interface between the neural and peripheral endocrine systems, and secrete GnRH into the pituitary portal blood vessels (Clarke *et al.* 1987; Jansen *et al.* 1997). The secreted GnRH binds to the GnRHRs on the lipid raft portion of the plasma membrane of gonadotrophs to stimulate the secretion of LH and FSH (Kadokawa *et al.* 2014). These gonadotrophins regulate important events related to ovulation, such as oocyte maturation, embryo development, and formation and maintenance of the corpus luteum.

The AP receives signals from both the hypothalamus and various peripheral tissues, and secretes the important hormones that control various important functions in multiple organs. Among them the most well-known one is the feedback mechanism by antral follicles and corpora lutea, which secrete steroids and inhibin to control gonadotropin secretion from the AP (Martin *et al.* 1991). It is important to clarify mechanisms controlling the HPG axis, but still little has known for mechanisms. Especially, it is not clear whether hormones secreted from preantral and small antral follicles control gonadotropin secretion from the AP. I had a question whether preantral and small antral follicles are silent majority in ovaries.

Gonadotrophs are controlled by GnRH via the GnRHR that are present in lipid rafts in the plasma membrane of gonadotrophs (Navratil *et al.* 2009; Wehmeyer *et al.* 2014; Kadokawa *et al.* 2014). The lipid rafts are distinct, relatively insoluble regions that have lower density and are less fluid than surrounding membrane (Simons *et al.* 2000; Head *et al.* 2014), and they facilitate signaling by allowing colocalization of membrane receptors and their downstream signaling components (Simons *et al.* 2000;

Head *et al.* 2014). Therefore, gonadotroph lipid rafts containing GnRHR may contain any important receptor.

GnRHRs are present in gonadotroph plasma membrane lipid rafts (Navratil *et al.* 2009; Wehmeyer *et al.* 2014; Kadokawa *et al.* 2014), which are distinct, relatively insoluble regions that have lower density and are less fluid than surrounding membrane (Simons and Tootter 2000; Head *et al.* 2014). Lipid rafts facilitate signaling by allowing colocalization of membrane receptors and their downstream signaling components (Simons and Tootter 2000; Head *et al.* 2014). Lipid rafts containing GnRHR also harbor insulin receptor (Navratil *et al.* 2009) and glucocorticoid receptor (Wehmeyer *et al.* 2014) in the L $\beta$ T2 clonal murine gonadotroph cell line, thus providing a potential means of integrating neuropeptide and energy homeostasis signals to modulate reproductive function. Lipid rafts facilitate signaling by allowing colocalization of membrane receptors and their downstream signaling components. Therefore, gonadotroph lipid rafts containing GnRHR may contain any important receptor that have yet to be identified. Kadokawa *et al.* (2014) previously developed a highly specific antibody that recognizes the extracellular region at the N terminus of bovine GnRHR. This is a useful tool to improve knowledge for GnRHR.

AMH is a dimeric glycoprotein in the TGF- $\beta$  family, and it is well known that AMH is produced by granulosa cells of the preantral and small antral follicles in humans and animals (Bhide and Homburg 2016). AMH regulates follicular development during the gonadotropin-responsive phase (Hernandez-Medrano *et al.* 2012) and to inhibit follicular atresia (Seifer *et al.* 2014). However, plasma AMH concentrations positively correlate with pregnancy rates in dairy cows (Ribeiro *et al.* 2014). Further, circulating AMH concentrations can predict the number of high-quality

embryos produced by a donor goat or cow (Ireland *et al.* 2008; Monniaux *et al.* 2011). Although the primary role of AMH is at the ovary level in female animals, AMH secreted from preantral and small antral follicles into circulating blood may have roles in other organs. The APs of adult rats express mRNA for the main receptor of AMH, AMHR2 (Bédécarrats *et al.* 2003). Also the brains of adult tilapia express AMH (Poonlaphdecha *et al.* 2011). However, little is known for relationship between AMH and the GnRH neurons and gonadotrophs.

Fertility decreases during aging in human and bovine females (Osoro and Wright 1992; Scheffer *et al.* 2018), however, little is known about the exact mechanisms underlying this association in domestic animals. Studies of AMH are promising for understanding these mechanisms. Blood AMH concentrations are highest in pubertal girls and decrease gradually from the age of 25 years until the postmenopausal period (Dewailly *et al.* 2014). In contrast, old Japanese Black cows have higher blood AMH concentrations than postpubertal heifers and young cows (Koizumi and Kadokawa 2017). These data suggest that age may be a determinant of blood AMH concentration.

In the first study, I hypothesized AMHR2 is expressed in gonadotrophs and if it has any role in gonadotrophs function. Other important hormones for endocrinological gonadotroph regulation (e.g. GnRH, inhibin and activin) have paracrine and autocrine roles (Pagesy *et al.* 1992; Miller *et al.* 1996; Popovics *et al.* 2011). Therefore, in the second study, I hypothesized that AMH is expressed in bovine gonadotrophs, and I evaluated the relationship between AMH expression in the bovine AP and oestrous stage, age and breed. In the third study, I hypothesized that AMH and AMHR2 may be detected in the areas of the brain relevant to neuroendocrine control of reproduction:

POA, ARC, and ME of heifers, and especially within GnRH neurons. Then, in the fourth study, I evaluated relation between aging and AMH and AMHR2 expression and in POA, ARC and ME.

This thesis consists of nine chapters. In Chapter I (General Introduction), I explained the background information and main objectives of the study. In Chapter II, I reviewed the literatures directly or indirectly related to my thesis. Chapters III and IV deal with expression of AMHR2 and AMH in gonadotrophs and that their expressions are age related. In Chapter V and VI I determined expression of AMH and AMHR2 in hypothalamus and evaluated if the expression is age-related. Finally, I discussed the main findings of the present study to conclude in chapter VII.

## **CHAPTER II**

### **Review of Literature**

## **2.1. Hypothalamus, pituitary and gonads axis**

Animal reproduction is tightly regulated by the hormones secreted from the hypothalamus, pituitary and gonads. The HPG axis drives reproduction, including sexual development, puberty, gametogenesis and pregnancy. Defects in the HPG axis lead to hypogonadotropic hypogonadism, and to induce abnormal reproductive functions and sterility (Larco *et al.* 2013). Bovine reproductive functions are regulated by several hormones including GnRH of hypothalamus, LH and FSH of AP, and E2 and P4 of ovaries. Some of the most important components of the axis are the GnRH neurons in hypothalamus and gonadotrophs (Herbison 2016; Nestor *et al.* 2018; Kadokawa 2020).

## **2.2. Hypothalamic control of reproduction**

The HPG axis drives reproduction and one of the most important components of the axis are the GnRH neurons (Herbison 2016; Nestor *et al.* 2018). GnRH neurons originate in the POA and ARC and project to the ME, the interface between the neural and peripheral endocrine systems, and secrete GnRH into the pituitary portal blood vessels (Clarke *et al.* 1987; Jansen *et al.* 1997). The secreted GnRH binds to GnRH receptors on the lipid raft portion of the plasma membrane of gonadotrophs to stimulate the secretion of LH and FSH (Kadokawa *et al.* 2014). Given their central role in reproduction, it is important to clarify mechanisms controlling GnRH neurons in the hypothalamus.

As mentioned above, the hypothalamus controls reproduction through the GnRH released from GnRH neurons which originate from the POA, ARC and terminate at the ME. The POA is the center to control GnRH surge which is followed by LH and FSH surge, ARC is the center to control pulsatile GnRH secretion which is followed by

pulsatile LH secretion (Tsutsumi and Webster 2009). It is necessary to clarify factors to regulate GnRH neurons.

### **2.3. Anterior Pituitary**

The bovine pituitary is an orbicular-ovate structure located at the base of the brain and it constitutes the hub of the endocrine system. Pituitary is comprised of three different lobes: the anterior, posterior, and intermediate lobes. Anterior part, AP is the most important endocrine organ for reproduction. The pituitary gland is located outside the blood-brain barrier (Nussey and Whitehead 2001). AP receives various hypothalamic and peripheral inputs. AP releases various hormones to control downstream organs including endocrine glands. Therefore, AP is the most important organ for controlling growth, metabolism, and reproduction. The AP consists of heterogeneous population of highly differentiated endocrine cell types defined by the hormones secreted. Among the various types of endocrine cells, gonadotrophs comprise 10-15% of the total AP cells (Ben-Sholmo and Melmed 2011).

### **2.4. Gonadotrophs**

Gonadotrophs play central important roles in the control of reproductive function. Gonadotrophs secrete gonadotropins, LH and FSH, to regulate follicle growth, ovulation, and corpus luteum formation in ovaries of vertebrates. Acting as a feedback mechanism, antral follicles and corpora lutea secrete steroids and inhibin to control gonadotropin secretion from gonadotrophs (Martin *et al.* 1991). However, it is not clear whether hormones secreted from preantral and small antral follicles control

gonadotropin secretion. I had a question whether preantral and small antral follicles are silent majority in ovaries.

Gonadotrophs are scattered throughout the AP (Kaiser 2011). Size and function of gonadotrophs are various (Childs 1997; Kadokawa *et al.* 2014). All types of gonadotrophs actively secrete LH or FSH in estrus period especially (Childs 1997). They are either LH- or FSH-monohormonal or bihormonal (Kaiser 2011; Kadokawa *et al.* 2014). In the adult male rat pituitary, about 70% of gonadotrophs are bihormonal, and 15% are LH monohormonal, and 15% are FSH monohormonal (Kaiser 2011). Also bovine gonadotroph are heterogeneous, including bihormonal, LH- and FSH-monohormonal (Kadokawa *et al.* 2014).

Plasma membrane of gonadotrophs contains lipid-raft microdomains, which are distinct, relatively insoluble regions that have lower density and are less fluid than surrounding membrane (Simons and Tooter 2000; Head *et al.* 2014) and facilitate signaling by allowing colocalization of membrane receptors and their downstream signaling components (Simons and Tooter 2000; Head *et al.* 2014). Gonadotrophs are controlled by GnRH *via* the GnRHR that are present in lipid rafts in the plasma membrane of gonadotrophs (Navratil *et al.* 2009; Wehmeyer *et al.* 2014; Kadokawa *et al.* 2014). Lipid rafts of gonadotroph containing GnRHR also harbor insulin receptor (Navratil *et al.* 2009) and glucocorticoid receptor (Wehmeyer *et al.* 2014) in the L $\beta$ T2 clonal murine gonadotroph cell line, thus providing a potential means of integrating neuropeptide and energy homeostasis signals to modulate reproductive function. However, gonadotroph lipid rafts containing GnRHR may contain other types of receptor that have yet to be identified. It is well known that GPCR proteins can form functionally active homomers and heteromers with different receptors (Ritter and Hall

2009). Therefore, further studies are required to clarify whether GnRHR form heteromers with any receptors.

## **2.5. AMH and AMHR2**

AMH is a dimeric glycoprotein in the TGF- $\beta$  family, which include other ovarian hormones, inhibin and activin. AMH is a molecule is a 140-kDa dimeric glycoprotein composed of identical 70-kDa monomers (Campbell *et al.* 2012). The best-studied tissue that secretes AMH are the immature granulosa cells in the ovaries of adult humans and animals (Bhide and Homburg 2016), and AMH reportedly plays various important roles to regulate follicular development during the gonadotropin-responsive phase (Hernandez-Medrano *et al.* 2012) and to inhibit follicular atresia (Seifer *et al.* 2014).

Interestingly, plasma AMH concentrations can predict the fertility of adult female goats, ewes, cows, and women (Monniaux *et al.* 2012; Meczekalski *et al.* 2016; Mossa *et al.* 2017). Blood AMH concentrations are also indicative of ovarian aging in women (Bhide and Homburg 2016; Dewailly *et al.* 2014). Plasma AMH concentrations positively correlate with pregnancy rates in dairy cows (Ribeiro *et al.* 2014). Further, circulating AMH concentrations can predict the number of high-quality embryos produced by a donor goat or cow (Ireland *et al.* 2008; Monniaux *et al.* 2011). These data suggest the importance of AMH for proper reproductive function in ruminants.

Although the well-known role of AMH is at the ovary level in female animals, AMH secreted from preantral and small antral follicles into circulating blood may have roles in other organs. Indeed, the APs of adult rats express mRNA for the main receptor of AMH, AMHR2 (Bédécarrats *et al.* 2003). AMH activates LH $\beta$  and FSH $\beta$  gene

expression in L $\beta$ T2 cells—a murine gonadotroph-derived cell line (Bédécarrats *et al.* 2003). Garrel *et al.* (2016) recently reported that AMH stimulates FSH secretion in rats *in vivo*; however, such stimulation is restricted to pre-pubertal female rats. However, there are still no data on the regulatory role of AMH on gonadotropin secretion from gonadotrophs in ruminant species. AMH and AMHR2 were detected by NGS in bovine APs (Pandey *et al.* 2017b). However, which cell express AMH and AMHR2 were remained to be studied, when this thesis studies began.

We previously discovered that two orphan receptors, GPR61 and GPR153, are colocalized with GnRHR in gonadotroph plasma membrane lipid rafts (Pandey *et al.* 2017a, 2018). Therefore, gonadotroph lipid rafts containing GnRHR may contain AMHR2.

Little is known concerning the relationship between AMH and the brain. While the brains of adult tilapia express AMH, the localization of AMH expression in the brain remains unclarified (Poonlaphdecha *et al.* 2011).

## **2.6. Infertility in aged animals and dairy cows**

Old age is associated with decreased fertility in beef cows (Osoro and Wright 1992); however, little is known about the exact mechanisms underlying this association in domestic animals. Studies of AMH are promising for understanding these mechanisms. Blood AMH concentrations are highest in pubertal girls and decrease gradually from the age of 25 years until the postmenopausal period (Dewailly *et al.* 2014). Infertility in Holsteins is an important issue in dairy industries worldwide (Kadokawa and Martin 2006; Adamczyk *et al.* 2017; Gernand and König 2017).

## **2.7. Issues of Age-related infertility**

Surprisingly, little is known for details of mechanism for reproductive longevity, and only a previous review reported the difference between *Bos taurus* and *Bos indicus* (Chenoweth 1994). However, in an early study by Erickson *et al.* (1976), aging was associated with a decrease in the ovarian follicular reserve and 55% of the herd was reported to be infertile by 13 years of age. Also Wathes (2012) reported that culling for infertility remains the main reason for disposal of dairy cows, limiting productive lifespan. Wathes (2012) reported that ovulation is inhibited in extreme cases, preventing the possibility of conception, and more often cows do conceive, but fail to remain pregnant owing to intrinsic problems in the embryo and/or to a poor-quality reproductive tract environment. Wathes (2012) reported that both aspects have a genetic component and are also influenced by management practices affecting nutrition and health, furthermore, the relative importance of these factors varies among heifers, first-lactation and older cows. Therefore, clarifying mechanism of reproductive aging is very important.

## **2.8. Hypothalamus-pituitary role in age-related infertility**

Little information is available on reproductive aging in cattle, however, Malhi *et al.* (2006) reported that preovulatory LH surge in response to estradiol treatment was significantly delayed in old (13-14 year old ) than young (1-4 year old) cows. Bryner *et al.* (1990) compared patterns of concentrations of LH and FSH during an estrous cycle between 5 to 7 years lactating beef cows 12 years or older ones. Length of estrous cycle did not differ between young and old cows ( $P = 0.06$ ). No differences due to age were found for LH, because their experiment design was based on only 12-hours interval blood sampling while LH secretions are pulsatile which require every 10-min interval

collection (Kadokawa and Yamada 1999, 2000; Kadokawa *et al.* 2006), or surge which require every 15-min interval collection (Kadokawa *et al.* 1998; 2008a; Kadokawa, 2007). Patterns of concentrations of FSH during days 6 through 12 differed with age (P less than 0.05). An earlier (P less than 0.025) midcycle elevation of FSH was associated with an earlier rise during the follicular phase in old than in young cows. For the relationship between FSH secretion and aging in women, Ko and Kim (2018) recently did literature review using 23 selected previous papers. They reported that blood FSH concentration in women toward menopause decrease in 21 previous papers (Ko and Kim 2018). Therefore, we need to study hypothalamus-pituitary level in order to clarify pathological mechanisms of age-related infertility.

## **CHAPTER III**

**(Study I)**

**Anti-Müllerian hormone receptor type 2 is expressed in  
gonadotrophs of post-pubertal heifers to control gonadotropin  
secretion**

## **Abstract**

Preantral and small antral follicles may secrete AMH to control gonadotropin secretion from ruminant gonadotrophs. This study investigated whether the main receptor for AMH; AMHR2, is expressed in gonadotrophs of post-pubertal heifers to control gonadotropin secretion. RT-PCR detected expressions of AMHR2 mRNA in APs of post-pubertal heifers. An anti-AMHR2 chicken antibody against the extracellular region near the N terminus of bovine AMHR2 was developed. Western blotting utilizing this antibody detected the expressions of AMHR2 protein in APs. Immunofluorescence microscopy utilizing the same antibody visualized colocalization of AMHR2 with GnRH receptor on the plasma membrane of gonadotrophs. I cultured the AP cells for 3.5 days, and then treated them with increasing concentrations (0, 1, 10, 100, or 1000 pg/ml) of AMH. AMH (10–1000 pg/ml) stimulated ( $P < 0.05$ ) basal FSH secretion. The hormone (100–1000 pg/ml) also stimulated ( $P < 0.05$ ) basal LH secretion weakly. However, AMH (100–1000 pg/ml) inhibited GnRH-induced FSH secretion, but not GnRH-induced LH secretion, in AP cells. The expression of AMHR2 mRNA and protein in APs did not differ between oestrous phases ( $P > 0.1$ ). I compared expression levels between old Holsteins ( $79.2 \pm 10.3$  months old) and young ( $25.9 \pm 0.6$  months old) and old Japanese Black females ( $89.7 \pm 20.3$  months old), but no significant differences were observed among the groups. In conclusion, AMHR2 is expressed in gonadotrophs of post-pubertal heifers to control gonadotropin secretion.

### 3.1. Introduction

Gonadotrophs in the APs secrete gonadotropins, LH and FSH, to regulate follicle growth, ovulation, and corpus luteum formation in ovaries of vertebrates. Acting as a feedback mechanism, antral follicles and corpora lutea secrete steroids and inhibin to control gonadotropin secretion from the AP (Martin *et al.* 1991). This pituitary-ovary axis is one of the most important fundamental mechanisms for reproduction. However, it is not clear whether hormones secreted from preantral and small antral follicles control gonadotropin secretion from the AP. I have a question whether preantral and small antral follicles are silent majority in ovaries.

AMH is a dimeric glycoprotein in the TGF- $\beta$  family, and AMH is produced mainly by granulosa cells of the preantral and small antral follicles in humans and animals (Bhide and Homburg 2016). AMH regulates follicular development during the gonadotropin-responsive phase (Hernandez-Medrano *et al.* 2012) and to inhibit follicular atresia (Seifer *et al.* 2014). Blood AMH concentrations are indicative of ovarian aging in women (Bhide and Homburg 2016; Dewailly *et al.* 2014). Plasma AMH concentrations positively correlate with pregnancy rates in dairy cows (Ribeiro *et al.* 2014). Further, circulating AMH concentrations can predict the number of high-quality embryos produced by a donor goat or cow (Ireland *et al.* 2008; Monniaux *et al.* 2011). These data suggest the importance of AMH for proper reproductive function in ruminants after puberty.

Although the primary role of AMH is at the ovary level in female animals, AMH secreted from preantral and small antral follicles into circulating blood may have roles in other organs. Indeed, the APs of adult rats express mRNA for the main receptor of AMH; AMHR2 (Bédécarrats *et al.* 2003). AMH activates LH $\beta$  and FSH $\beta$  gene expression in L $\beta$ T2 cells—a murine gonadotroph-derived cell line (Bédécarrats *et al.*

2003). Garrel *et al.* (2016) recently reported that AMH stimulates FSH secretion in rats *in vivo*; however, such stimulation is restricted to pre-pubertal female rats. However, there are still no data on the regulatory role of AMH on gonadotropin secretion from gonadotrophs in ruminant species.

Gonadotrophs are controlled by GnRH *via* GnRHR that are present in lipid rafts in the plasma membrane of gonadotrophs (Navratil *et al.* 2009; Wehmeyer *et al.* 2014; Kadokawa *et al.* 2014). The lipid rafts are distinct, relatively insoluble regions that have lower density and are less fluid than surrounding membrane (Simons *et al.* 2000; Head *et al.* 2014), and they facilitate signaling by allowing colocalization of membrane receptors and their downstream signaling components (Simons *et al.* 2000; Head *et al.* 2014). Pandey *et al.* (2017a, 2018) discovered that two orphan receptors, GPR61 and GPR153, are colocalized with GnRHR in gonadotroph plasma membrane lipid rafts. Therefore, gonadotroph lipid rafts containing GnRHR may contain AMHR2.

Old age is associated with decreased fertility in beef cows (Osoro and Wright 1992), however, little is known about the exact mechanisms underlying this association in domestic animals. Studies of AMH are promising for understanding these mechanisms. Blood AMH concentrations are highest in pubertal girls and decrease gradually from the age of 25 years until the postmenopausal period (Dewailly *et al.* 2014). In contrast, old Japanese Black cows have higher blood AMH concentrations than postpubertal heifers and young cows (Koizumi and Kadokawa 2017). These data suggest that age may be a determinant of blood AMH concentration.

In the present study, I tested the hypothesis that AMHR2 is expressed in the gonadotrophs of post-pubertal heifers to control gonadotropin secretion. Infertility in Holsteins is an important issue in dairy industries worldwide (Kadokawa and Martin 2006; Adamczyk *et al.* 2017; Gernand and König 2017). Therefore, I also evaluated the

relationship between AMHR2 expression in APs and various physiological factors, i.e. stage of the oestrous cycle, age and breed.

## **3.2. Materials and methods**

### **3.2.1. Animals and treatments**

All experiments were performed according to the Guiding Principles for the Care and Use of Experimental Animals in the Field of Physiological Sciences (Physiological Society of Japan) and approved by the Committee on Animal Experiments of the School of Veterinary Medicine, Yamaguchi University.

### **3.2.2. AP and ovary sample collection**

AP tissues were obtained from post-pubertal (26 months of age) Japanese Black heifers at a local abattoir, using a previously described method (Kadokawa *et al.* 2014). The heifers were in the middle luteal phase, i.e., 8 to 12 days after ovulation, as determined by macroscopic examination of the ovaries and uterus (Miyamoto *et al.* 2000); the AP show the highest LH and GnRHR concentrations in this phase (Nett *et al.* 1987).

Granulosa cells in small antral follicles express *AMHR2* mRNA (Poole *et al.* 2016). Therefore, I also collected ovary tissue samples from the same heifers to use as positive controls of *AMHR2* in western blotting and immunohistochemistry assays.

The AP and ovary samples for RNA or protein (n = 3) extraction were immediately frozen in liquid nitrogen and stored at -80°C. The AP and ovary samples for immunohistochemistry (n = 5) were fixed with 4% paraformaldehyde at 4°C for 16 h. The AP samples meant for cell culture followed by immunocytochemical analysis (n = 5) and those that were to be used for cell culture to evaluate the effect of AMH on LH and FSH secretion (n = 8) were stored in ice-cold 25 mM HEPES buffer (pH 7.2) containing 10 mM glucose and transported on ice to the laboratory.

### **3.2.3. RT-PCR, sequencing of amplified products, and homology search in gene databases**

Total RNA was extracted from the AP samples ( $n = 3$ ) using RNAiso Plus (Takara Bio Inc) according to the manufacturer's protocol. The extracted RNA samples were treated with ribonuclease-free deoxyribonuclease (Toyobo) to eliminate possible genomic DNA contamination. Using a NanoDrop ND-1000 spectrophotometer (NanoDrop Technologies Inc.), the concentration and purity of each RNA sample were evaluated to ensure the  $A_{260}/A_{280}$  nm ratio was in the acceptable range of 1.8–2.1. The mRNA quality of all samples was verified by electrophoresis of total RNA followed by staining with ethidium bromide, and the 28S:18S ratios were 2:1. The cDNA was synthesized from 0.5  $\mu$ g of the total RNA per AP using ReverTra Ace qPCR RT Master Mix (Toyobo) according to the manufacturer's protocol.

In order to determine the expression of *AMHR2* mRNA in the AP, PCR was conducted using one of three pairs of primers designed by Primer3 based on reference sequence of bovine AMHR2 [NCBI reference sequence of bovine AMHR2 is NM\_001205328.1], as one of PCR primers must span exon-exon junction. Table 3.1 shows the details of the primers, and the expected PCR-product sizes of the AMHR2 were 340 bp, 320 bp, and 277 bp. Using a Veriti 96-Well Thermal Cycler (Thermo Fisher Scientific), PCR was performed using 20 ng of cDNA and polymerase (Tks Gflex DNA Polymerase, Takara Bio Inc.) under the following thermocycles: 94 °C for 1 min for pre-denaturing followed by 35 cycles of 98°C for 10 s, 60°C for 15 s, and 68°C for 30 s. PCR products were separated on 1.5% agarose gel by electrophoresis with a molecular marker [Gene Ladder 100 (0.1-2kbp), Nippon Gene], stained with fluorescent stain (Gelstar, Lonza), and observed using a CCD imaging system (GelDoc; Bio-Rad). The PCR products were purified with the NucleoSpin Extract II kit (Takara

Bio Inc.) and then sequenced with a sequencer (ABI3130, Thermo Fisher Scientific) using one of the PCR primers and the Dye Terminator v3.1 Cycle Sequencing Kit (Thermo Fisher Scientific). The sequences obtained were used as query terms with which to search the homology sequence in the DDBJ/GenBank™/EBI Data Bank using the BLAST optimized for highly similar sequences (available on the NCBI website).

**Table 3.1.** Details of the three primers used for PCR to detect *AMHR2* mRNA in bovine anterior pituitaries.

Primer pair	Sequence	5'-3'	Position		Size (bp)
			Nucleotide	Exon	
1st	up	GATTTGCGACCTGACAGCAG	1273-1292	9-10	340
	down	CGGGAGGAGTGGAGAAATGG	1593-1612	11	
2nd	up	AGATTTGCGACCTGACAGCAG	1272-1292	9-10	320
	down	CTTCCAGGCAGCAAAGTGAG	1572-1591	11	
3rd	up	GTGCTTCTCCCAGGTCATACG	606-626	5-6	277
	down	GGTGTGCTGGGTCAAGTAGT	863-882	7	

#### 3.2.4. Development anti-AMHR2 chicken antibody

SOSUI v.1.11 algorithm (Hirokawa *et al.* 1998; <http://harrier.nagahama-i-bio.ac.jp/sosui/>) was used to determine that bovine AMHR2 protein [543 amino acids; accession number NP\_001192257.1 in NCBI reference bovine sequences] contains one hydrophobic transmembrane domains (amino acid 146–168) linked by hydrophilic extracellular and intracellular regions. This structure is the same as the reported structure of mouse AMHR2 (Sakalar *et al.* 2015).

Genetyx ver. 11 (Genetyx) was utilized to predict antigenic determinants based on an algorithm derived by Hopp and Woods (1981). For antibody production, a peptide corresponding to amino acids 31–45 (GVRGSTQNLGKLLDA), an extracellular region that is located near the N terminus of the AMHR2, was used for three reasons. First, this peptide has no homology to the corresponding region of chicken AMHR2 (XP\_015145444.1). Second, the peptide sequences are in downstream region of the signal peptide of bovine AMHR2 (amino acid 1–17). Third, there was no other protein encoded in the bovine genome exhibited homology to the peptide sequences of the AMHR2 by comparison with the sequences retrieved from DDBJ/GenBank™/EBI Data Bank, using the protein BLAST.

A commercial service (Scrum Inc.) was utilized for synthesis of antigen peptide (C-GVRGSTQNLGKLLDA), conjugation with KLH, immunization, and antibody purification. Briefly, the peptide was synthesized and the purity verified (>99.0%) using high-performance liquid chromatography followed by mass spectrometry. Then, KLH was conjugated to the sulfhydryl group of the cysteine to produce an immunogen that was then emulsified with Complete Freund's adjuvant and injected into chickens five times at 14-day intervals. Blood was collected 7 days after the final immunization and

the antibody was purified by affinity column chromatography (PD10; GE Healthcare) containing an antigen-conjugated gel prepared with the SulfoLink Immobilization Kit (Thermo Fisher Scientific).

### **3.2.5. Other antibodies used in this study**

A guinea pig polyclonal antibody that recognizes the N-terminal extracellular domain (corresponding to amino acids 1–29; MANSDSPEQNENHCSAINSSIPLTPGSLP) of GnRHR (anti-GnRHR) was previously developed. The specificity of the anti-GnRHR antibody was verified by western blotting, and pretreatment with anti-GnRHR antibody inhibited GnRH-induced LH secretion from cultured bovine gonadotroph (Kadokawa *et al.* 2014). Additionally, the anti-GnRHR antibody was used for immunofluorescence detection of GnRHR in plasma membrane of bovine gonadotroph (Kadokawa *et al.* 2014; Pandey *et al.* 2016). A strong and localized GnRHR-positive staining signal was observed as aggregation on the plasma membrane of gonadotrophs (Kadokawa *et al.* 2014). The anti-GnRHR as well as a mouse monoclonal anti-LH  $\beta$  (LH $\beta$ ) subunit antibody (clone 518-B7; Matteri *et al.* 1987) was used for immunohistochemical analysis of AP tissue and cultured AP cells. This antibody does not cross-react with other pituitary hormones (Iqbal *et al.* 2009). A mouse monoclonal anti-FSH  $\beta$  (FSH $\beta$ ) subunit antibody (clone A3C12) was also used, and that does not cross-react with other pituitary hormones (Borromeo *et al.* 2004) for immunohistochemical analysis of AP tissue.

### 3.2.6. Western Blotting for AMHR2

I extracted protein from the samples of AP (n = 3) or ovary (n = 3, used as positive control) and performed western blotting following a previously described method (Kadokawa *et al.* 2014). The extracted protein (33.4 µg of total protein in 37.5 µl) was mixed in 12.5 µl of 4x Laemmli sample buffer (Bio-rad) containing 10% (v/v) β-mercaptoethanol, then boiled for 3 min at 100 °C. Boiled protein samples were quickly cooled in ice, then 4, 8, or 16 µg of total protein were loaded onto sodium dodecyl sulfate polyacrylamide gels, along with a molecular weight marker (Precision Plus Protein All Blue Standards; Bio-Rad), for resolution by electrophoresis at 100 V for 90 min. Proteins were then transferred to PVDF membranes for immunoblotting with the anti-AMHR2 chicken antibody (1:25,000 dilution) after blocking with 0.1% Tween 20 and 5% non-fat dry milk for 1 h at 25 °C. The membranes were incubated overnight at 4 °C with the primary antibody, washed with 10 mM Tris-HCl (pH 7.6) containing 150 mM NaCl and 0.1% Tween 20, and incubated with HRP-conjugated anti-chicken IgG goat antibody (Bethyl laboratories, Inc.; 1:50,000 dilution) at 25 °C for 1 h. Protein bands were visualized using an ECL-Prime chemiluminescence kit (GE Healthcare) and CCD imaging system (Fujifilm). Previous studies utilizing western blotting for AMHR2 reported that human and mouse AMHR2 are present as dimers, full-length monomers, or cleaved monomers (Faure *et al.* 1996; Hirschhorn *et al.* 2015). Thus, I defined bovine AMHR2 bands based on mobility as one of these structure types. After antibodies were removed from the PVDF membrane with stripping solution (Nacalai Tesque Inc.), the membrane was used for immunoblotting with the anti-β-actin mouse monoclonal antibody (A2228, 1:50,000 dilution; Sigma-Aldrich).

### 3.2.7. Fluorescent immunohistochemistry and confocal microscopic observation

After storage in 4% PFA-PBS at 4°C for 16 h, the AP (n = 5) or ovary (n = 5) tissue blocks were placed in 30% sucrose-PBS until the blocks were infiltrated with sucrose. The methods for immunofluorescence analysis of AP tissue have been described previously (Kadokawa *et al.* 2014). Briefly, I prepared 15- $\mu$ m sagittal sections were cut using a cryostat (CM1900, Leica Microsystems Pty Ltd.) and mounted them on slides. The sections were treated with 0.3 % Triton X-100 in PBS for 15 min, then, incubated with 0.5 mL of PBS containing 10% normal goat serum (Wako Pure Chemicals) for blocking for 1 h. Incubation with a cocktail of primary antibodies (anti-GnRHR guinea pig antibody, anti-AMHR2 chicken antibody, and either anti-LH $\beta$  or anti-FSH $\beta$  mouse antibody [all diluted as 1:1,000]) for 12 h at 4°C was followed by incubation with a cocktail of fluorochrome-conjugated secondary antibodies (Alexa Fluor 488 goat anti-chicken IgG, Alexa Fluor 546 goat anti-mouse IgG, and Alexa Fluor 647 goat anti-guinea pig IgG [all from Thermo Fisher Scientific and diluted as 1  $\mu$ g/mL]) and 1  $\mu$ g/mL of 4', 6'-diamino-2-phenylindole (DAPI; Wako Pure Chemicals) for 2 h at room temperature. Moreover, I prepared 15- $\mu$ m ovary sections, incubated with anti-AMHR2 chicken antibody (1:1,000), and then incubated with 1  $\mu$ g/mL Alexa Fluor 488 goat anti-chicken IgG and DAPI to use as positive controls to verify the anti-AMHR2 antibody.

The stained sections on slides were observed with a confocal microscope (LSM710; Carl Zeiss) equipped with diode (405 nm), argon (488 nm), HeNe (533 nm) and HeNe (633 nm) lasers. Images obtained by fluorescence microscopy were scanned with a 40 $\times$  or 63 $\times$  oil-immersion objective and recorded by a CCD camera system controlled by ZEN2012 black edition software (Carl Zeiss). GnRHR, AMHR2, and

LH $\beta$  or FSH $\beta$  localization were examined in confocal images of triple-immunolabeled specimens. In the confocal images obtained after immunohistochemistry analysis, the GnRHR is shown in green, AMHR2 is shown in red, and LH $\beta$  or FSH $\beta$  is shown in light blue. Therefore, the yellow coloration on the surface of light blue-colored cells indicates the colocalization of AMHR2 and GnRHR. The percentage of AMHR2 single (red)-labeled light blue-colored cells, or the percentage of double (yellow)-labeled light blue-colored cells, among all of the AMHR2-positive light blue-colored cells (sum of the numbers of red-labeled and yellow-labeled light blue-colored cells), were determined from 12 representative confocal images per pituitary gland. Moreover, the percentage of GnRHR single (green)-labeled light blue-colored cells, or the percentage of double (yellow)-labeled light blue-colored cells, among all of the GnRHR-positive light blue-colored cells (sum of the numbers of green-labeled and yellow-labeled light blue-colored cells), were determined from 12 representative confocal images per pituitary gland. To verify the specificity of the signals, I included several negative controls in which the primary antiserum had been omitted or pre-absorbed with 5 nM of the same antigen peptide, or in which normal chicken IgG (Wako Pure Chemicals) was used instead of the primary antibody.

### **3.2.8. AP cell culture and immunocytochemical analysis of cells**

The AP cells from 5 heifers were enzymatically dispersed using the method of Suzuki *et al.* (2008), and cell viability was confirmed to be greater than 90% by Trypan blue exclusion. Total cell yield was  $19.8 \times 10^6 \pm 0.8 \times 10^6$  cells per pituitary gland. The dispersed cells were then suspended in DMEM (Thermo Fisher Scientific) containing  $1 \times$  nonessential amino acids (Thermo Fisher Scientific), 100 U/mL penicillin, 50  $\mu$ g/mL streptomycin, 10% horse serum (Thermo Fisher Scientific), and 2.5% fetal

bovine serum (Thermo Fisher Scientific). The cells ( $2.5 \times 10^5$  cells/mL, total = 0.15 mL per lane) were cultured in the culture medium at 37 °C in 5% CO<sub>2</sub> for 82 h, using a microscopy chamber ( $\mu$ -Slide VI 0.4, Ibidi). I cultured the AP cells for 82 h (3.5 days), as previously described (Hashizume *et al.* 2003; Kadokawa *et al.* 2008b; Hashizume *et al.* 2009; Kadokawa *et al.* 2014; Nakamura *et al.* 2015). I supplied recombinant human activin A (final concentration, 10 ng/ml; R&D systems) to stimulate FSH synthesis at 24 h prior to fixation. Mature activin A of bovines (NP\_776788.1) and ovines (NP\_001009458.1) have 100% homology with that of humans (CAA40805.1), and the 24 h culture with the same concentration of same recombinant human activin A product stimulates FSH expression in cultured ovine AP cells (Young *et al.* 2008).

I fixed and treated the cultured cells using either 4% PFA for 3 min followed by 0.1% Triton X-100 treatment for 1 min (PFA-Triton method), or fixation for 2 min with CellCover (Anacyte Laboratories UG), instead of 4% PFA, and no Triton X-100 treatment (CellCover method), as described by Kadokawa *et al.* (2014). Briefly, one of the aforementioned methods was used to treat the cells attached to the bottom of the microscopy chamber. For the PFA-Triton method, the fixed cells were incubated with 0.1 mL of the same cocktail of primary antibodies for 2 h at room temperature. Incubation with Triton X-100 allowed both anti-GnRHR and anti-AMHR2 antibodies to bind to target proteins in the cytoplasm and at the cell surface. For the CellCover method, the fixed cells were incubated with only guinea pig anti-GnRHR and chicken anti-AMHR2 (both 1:1,000) for 2 h at room temperature. The cells were not treated with Triton X-100, so the antibodies bound only to the extracellular domains of the respective receptors in most cells, although some cytoplasmic labeling occurred in broken cells. For both PFA-Triton and CellCover methods, cells were incubated with fluorochrome-conjugated secondary antibody cocktail and DAPI, and subjected to

confocal microscopy to produce fluorescence micrographs and DIC images on a single plane. Signal specificity was confirmed using negative controls in which the primary antiserum was omitted or pre-absorbed with 5 nM antigen peptide, or in which the normal chicken IgG replaced the primary antibody. Eight randomly selected images of cells prepared by CellCover method were analyzed for co-localization utilizing the ZEN 2012 black edition software (Carl Zeiss) to calculate overlap coefficients (Manders *et al.* 1993) for the Alexa Fluor 488 and Alexa Fluor 647 fluorophores.

### **3.2.9. Pituitary cell culture and analysis of the effects of AMH on LH and FSH secretion**

The AP cells derived from 8 heifers were prepared using the protocol described above. After the cells ( $2.5 \times 10^5$  cells/mL, total 0.3 mL) had been plated in 48-well culture plates (Sumitomo Bakelite), they were maintained at 37°C in a humidified atmosphere of 5% CO<sub>2</sub> for 82 h. I supplied the recombinant human activin A (final concentration, 10 ng/ml) to stimulate FSH synthesis at 24 h prior to the AMH test.

In the test to evaluate the effect of AMH in the absence of GnRH, the old medium was replaced by 295 µL DMEM containing 0.1% BSA and 10 ng/ml activin A and incubated for 2 h. Treatment was performed by adding 5 µL of DMEM alone or 5 µL of DMEM containing various concentrations of human recombinant AMH (R & D systems; final concentration of 0, 1, 10, 100, or 1000 pg/ml AMH).

The bioactive region in the carboxyl-terminal region of mature AMH (Belville *et al.* 2004) of bovines (NP\_776315.1) and goat (XP\_017906255.1) has 96% homology with that of humans (NP\_000470.2), and the same recombinant human AMH product shows the biological effect for goat follicles (Rocha *et al.* 2016).

After incubation for further 2 h, the medium from each well was collected for RIA analyses of LH and FSH levels. The physiological concentration of AMH in blood ranged between 5 and 300 pg/ml in Japanese Black cows in a previous study (Koizumi and Kadokawa 2017). Therefore, I used the above-mentioned AMH concentration in this study.

In the test to evaluate the effect of AMH in the presence of GnRH, the old medium was replaced by 290  $\mu$ L DMEM containing 0.1% BSA and 10 ng/ml activin A and incubated at 37°C for 2 h. Pretreatment was performed by adding 5  $\mu$ L of DMEM alone or 5  $\mu$ L of DMEM containing various concentrations (0, 60, 600, 6000, and 60000 pg/ml) of the human recombinant AMH. The cells were incubated while gently shaking for 5 min, and then, cells were treated with 5  $\mu$ L of 60 nM GnRH (Peptide Institute Inc.) dissolved in DMEM for 2 h in order to stimulate LH and FSH secretion. The pretreatment plus the GnRH treatment yielded a final concentration of 0, 1, 10, 100, or 1000 pg/ml AMH. The final concentration of GnRH was 1 nM in all treatments (Kadokawa *et al.* 2014), except the “control”. Control wells were treated with 5  $\mu$ L of DMEM, but were not incubated with GnRH. “GnRH” wells were pre-treated with 5  $\mu$ L of DMEM for 5 min and were then incubated with GnRH for 2 h. After incubation for 2 h, the medium from each well was collected for LH and FSH RIAs.

### **3.2.10. RIAs to measure gonadotropin concentration in culture media**

The concentration of LH was measured in duplicate samples of culture media by double antibody RIA using  $^{125}$ I-labeled bLH and anti-oLH-antiserum (AFP11743B and AFP192279, National Hormone and Pituitary Program of the NIDDK). The limit of detection was 0.40 ng/mL. At 2.04 ng/mL, the intra-assay coefficient of variation was 3.6% and inter-assay coefficient of variation was 6.2%. The concentration of FSH

was measured in duplicate samples of culture media by double antibody RIA using  $^{125}\text{I}$ -labeled bFSH, reference grade bFSH, and anti-oFSH antiserum (AFP5318C, AFP5346D, and AFPC5288113, NIDDK). The limit of detection was 0.20 ng/mL. At 4.00 ng/mL, the intra-assay coefficient of variation was 4.3% and inter-assay coefficient of variation was 7.1%.

### **3.2.11. AP sample collection for comparisons between oestrous stages**

AP tissues were collected from the heads of adult (26-month-old) non-pregnant healthy Japanese Black heifers in the pre-ovulation (Days 19–21 (Day 0 = day of oestrus);  $n = 5$ ), early luteal (Days 2–5;  $n = 5$ ), mid-luteal (Days 8–12;  $n = 5$ ) or late luteal (Days 15–17;  $n = 5$ ) phases, as determined by macroscopic examination of the ovaries and uterus (Miyamoto *et al.* 2000). Samples were obtained at a local abattoir as previously described (Rudolf and Kadokawa 2014) and immediately frozen in liquid nitrogen and stored at  $-80^{\circ}\text{C}$  until RNA or protein extraction.

### **3.2.12. AP sample collection for comparisons between ages or breeds**

AP tissues were obtained during the luteal phase from healthy postpubertal Japanese Black heifers ( $25.9 \pm 0.6$  months of age;  $n = 5$ ; young JB group), old Japanese Black cows ( $89.7 \pm 20.3$  months of age;  $5.2 \pm 0.5$  parity;  $n = 5$ ; old JB group) and old Holstein cows ( $79.2 \pm 10.3$  months of age;  $6.6 \pm 0.9$  parity;  $n = 5$ ; old Hol group) from the local abattoir. It was not possible to obtain AP samples from postpubertal Holstein heifers because they are kept in dairy farms for milking purposes. All of the heifers and cows in the three groups were non-lactating and non-pregnant and they had no follicular cysts, luteal cysts or other ovarian disorders based on macroscopic examinations of the ovaries (Kamomae 2012). All cows in the old Hol group had endometritis as determined

by macroscopic examination of the uterus with mucopurulent vaginal discharge (Kamomae 2012). All of their endometritis clinical scores (Sheldon and Dobson 2004) were 1, since the mucus character was clear or translucent with flecks of white pus and the mucus odour was not unpleasant. The old Holstein cows were slaughtered owing to infertility, diagnosed after at least five artificial insemination attempts. The old Japanese Black cows were slaughtered after completing parturition a sufficient number of times, as planned by farmers to obtain beef.

### **3.2.13. RT-qPCR to evaluate the factors affecting *AMHR2* expression**

RT-qPCR was performed to compare *AMHR2* expression between oestrous phases and between the young JB, old JB and old Hol groups. The preparation of high-quality total RNA and cDNA synthesis was performed as described above.

Table 3.2 shows the primers designed for RT-qPCR using Primer Express Software Version 3.0 (Thermo Fisher Scientific) based on the reference sequences. The level of gene expression was measured in duplicate by RT-qPCR analyses with 20 ng cDNA, using the CFX96 Real-Time PCR System (Bio-Rad) and Power SYBR Green PCR Master Mix (Thermo Fisher Scientific) together with a six-point relative standard curve, non-template control and no-reverse-transcription control. Standard 10-fold dilutions of purified and amplified DNA fragments were prepared. Temperature conditions for all genes were as follows: 95°C for 10 min for pre-denaturation; five cycles each of 95°C for 15 s and 66°C for 30 s and 40 cycles each of 95°C for 15 s and 60°C for 60 s. Melting curve analyses were performed at 95°C for each amplicon and each annealing temperature to ensure the absence of smaller non-specific products such as dimers. To optimise the RT-qPCR assay, serial dilutions of a cDNA template were used to generate a standard curve by plotting the log of the starting quantity of the

dilution factor against the Cq value obtained during amplification of each dilution. Reactions with a coefficient of determination ( $R^2$ ) >0.98 and efficiency between 95 and 105% were considered to be optimised. The concentration of PCR products was calculated by comparing Cq values of unknown samples with the standard curve using appropriate software (CFXmanager Version 3.1; Bio-Rad). The gene expression levels for *AMHR2* genes were normalised to the geometric mean of the expression levels of two housekeeping genes, *glyceraldehyde-3-phosphate dehydrogenase (GAPDH)* and *RAN-binding protein (RANBP10)*. I selected these two housekeeping genes from among 20 that have been previously described (Walker *et al.* 2009; Rekawiecki *et al.* 2012) because they had the smallest inter-heifer coefficients of variation of reads per kilobase of transcript per million mapped reads value upon deep sequencing of the transcriptome (Pandey *et al.* 2017b).

**Table 3.2.** Name, accession number, and details of the primers used for RT-qPCRs

Gene name	Accession number	Primer	Sequence 5'-3'	Size (bp)
<i>GAPDH</i>	NM_001034034	Forward	TGGTGAAGGTCGGAGTGAAC	91
		Reverse	ATGGCGACGATGTCCACTTT	
<i>RANBP10</i>	NM_001098125	Forward	CCCAGTCCTACCAGCCTACT	133
		Reverse	CCCCCAGAGTTGAATGACCC	
<i>AMHR2</i>	NM_001205328 Exon 9 10	Forward	TGGGAGATTATGAGTCGCTGC	52
		Reverse	GTGGTGGTCTGCTGTCAGGT	

### **3.2.14. Western blotting to evaluate the factors affecting AMHR2 expression**

Western blotting was performed to compare AMHR2 protein levels in APs between different oestrous phases and between the young JB, old JB and old Hol groups. Sample collection and western blotting were performed as described above. Briefly, 15  $\mu$ L (8  $\mu$ g of total protein) of boiled sample was loaded on a polyacrylamide gel along with the molecular weight marker and four standard samples (2, 4, 8 and 16  $\mu$ g total protein for each of five randomly selected AP samples diluted with protein extraction reagent). MultiGauge Version 3.0 software (Fujifilm) was used to quantify the signal intensity of the protein bands. The intensities of band of AMHR2 (as full length monomers form) for 16-, 8-, 4- and 2- $\mu$ g AP protein samples were set as 100%, 50%, 25% and 12.5% respectively and the intensity of other samples was calculated as a percentage of these standards using MultiGauge software. After antibodies were removed from the PVDF membrane with stripping solution, the membrane was used for immunoblotting with the anti- $\beta$ -actin mouse monoclonal antibody. The intensities of the  $\beta$ -actin band for 16-, 8-, 4- and 2- $\mu$ g AP protein samples were set as 100%, 50%, 25% and 12.5% respectively and the intensity of other samples was calculated as a percentage of these standards using MultiGauge software. AMHR2 expression level was normalised to that of  $\beta$ -actin in each sample.

### **3.2.15. Analysis of the AMHR2 gene 5'- flanking region**

The 5000-nucleotide sequence of the 5' flanking region of the *AMHR2* gene (Chromosome 12: 53,423,855-53,431,672) was obtained using the online Ensembl ([www.ensembl.org](http://www.ensembl.org)) and BLAT Search Genome program (<http://genome.ucsc.edu>) (Cow Jun. 2014, Bos\_taurus\_UMD\_3.1.1/bosTau8). The sequence was analysed using Genetyx software Version 13 (Genetyx) for the presence of consensus response element

(RE) sequences for oestrogen i.e. ERE (5'-GGTCANNNTGACC-3'; Gruber *et al.* 2004) and half ERE (GGTCA, TGACC or TGACT; Liu *et al.* 1995), as well as for progesterone i.e. PRE (5'-G/A G G/T AC A/G TGGTGGTTCT-3'; Geserick *et al.* 2005).

### **3.2.16. Statistical analysis**

The statistical significance of differences were analyzed by one-factor ANOVA followed by *post-hoc* comparisons using Fisher's PLSD test using StatView version 5.0 for Windows (SAS Institute, Inc., Cary, NC, USA). The level of significance was set at  $P < 0.05$ . Data are expressed as mean  $\pm$ SEM.

### **3.3. Results**

#### **3.3.1. Expression of *AMHR2* mRNA in AP of post-pubertal heifers**

The expected PCR products (size 340 bp, 320 bp, and 277 bp) were observed in the agarose gel after electrophoresis (Fig. 3.1). Homology searching in the gene databases for the obtained sequence of amplified products using the first, second and third primer pair respectively revealed that the best match alignment was bovine *AMHR2* (NM\_001205328.1), which had a query coverage of 100%, an e-value of 0.0, and a maximum alignment identity of 99%. No other bovine gene was found to have a homology for the obtained sequences of amplified products, leading to the conclusion that the sequences of the amplified products were identical with the sequence of bovine *AMHR2*.

#### **3.3.2. Western blotting for *AMHR2***

The presence of *AMHR2* in the AP and ovarian tissue was analyzed by western blot, using anti-*AMHR2* antibody (Fig. 3.2). The anti-*AMHR2* antibody revealed similar bands in the two tissues, with few differences (Fig. 3.2A). The major difference was that AP tissue showed weaker bands than ovarian tissue did. Nevertheless,  $\beta$ -actin bands showed weaker staining in both tissue types (Fig. 3.2B). Finally, another difference was that the full-length monomer in the ovary appeared as a single band, whereas in AP cells, it appeared as a doublet (Fig. 3.2A). No bands were observed in the negative control membranes, where the primary antiserum was pre-absorbed with the antigen peptide.

### **3.3.3. Immunofluorescence analysis of AMHR2 expression in bovine granulosa cells**

Fig. 3.3 shows the immunofluorescence in the granulosa cells of small (about 5 mm) follicles in the ovary tissues of post-pubertal heifers. Strong AMHR2 staining appeared to be aggregated, not evenly dispersed.

### **3.3.4. Immunofluorescence analysis of AMHR2 expression in bovine AP tissue**

Expression of LH $\beta$ , FSH $\beta$ , GnRHR, and AMHR2 in bovine AP tissue was investigated by immunohistochemistry (Fig. 3.4). AMHR2 and GnRHR colocalized in the majority of both LH $\beta$ -positive (Fig. 3.4A) and FSH $\beta$ -positive (Fig. 3.4B) cells. Focus depth of the high magnification lens used in this study are thin, thus, the best focus for GnRHR and AMHR2 on plasma membrane was quite different from both the best focus for nucleus and the best focus for cytoplasmic LH $\beta$  or FSH $\beta$ . Thus, I could know both membrane receptors are on the cell-surface. Percentages of single- and double-labeled AMHR2- and GnRHR-positive cells were determined from 12 representative confocal images per pituitary gland. In each pituitary gland, there was an average of  $52.4 \pm 2.4$  GnRHR-positive cells,  $44.6 \pm 1.2$  AMHR2-positive cells, and  $33.6 \pm 1.3$  double-positive cells;  $64.5\% \pm 3.2\%$  of GnRHR-positive cells were AMHR2-positive, whereas  $78.4\% \pm 1.8\%$  of AMHR2-positive cells were GnRHR-positive.

### **3.3.5. AMHR2 and GnRHR aggregate on the surface of cultured AP cells**

In the AP cells prepared by the CellCover method, AMHR2 aggregated on the surface of GnRHR-positive cells (Fig. 3.5). The overlap coefficient between AMHR2 and GnRHR was  $0.76 \pm 0.05$  on the cell surface of cultured AP cells.

### **3.3.6. AMHR2 expression in cultured gonadotrophs**

Among the AP cells prepared by the PFA-Triton method, I observed AMHR2 in both LH $\beta$ -positive and FSH $\beta$ -positive cells (Fig. 3.6).

### **3.3.7. Effects of AMH on gonadotropin secretion from cultured AP cells**

Fig. 3.7 shows the effect of various concentrations of AMH on LH secretion from the AP cells derived from post-pubertal heifers cultured in the absence (A) or presence (B) of GnRH. In the absence of GnRH (Fig. 3.7A), 100 pg/ml and 1000 pg/ml of AMH increased ( $P < 0.05$ ) LH secretion, when compared with the controls ( $17.6 \pm 2.4$  ng/ml). Conversely, there was no effect of AMH on the GnRH-induced LH secretion (Fig. 3.7B).

Fig. 3.8 shows the effect of various concentrations of AMH on FSH secretion from the AP cells derived from post-pubertal heifers cultured in the absence (A) or presence (B) of GnRH. The effect of different concentrations of AMH was significant ( $P < 0.05$ ) in the absence of GnRH (Fig. 3.8A). The wells with 10 pg/ml ( $P < 0.05$ ), 100 pg/ml ( $P < 0.05$ ), and 1000 pg/ml ( $P < 0.05$ ) of AMH, but not 1 pg/ml of AMH, had higher FSH concentrations than those without AMH ( $8.4 \pm 1.2$  ng/ml). The effect of different concentrations of AMH was significant ( $P < 0.05$ ) in the presence of GnRH (Fig. 3.8B). FSH concentrations in the medium of GnRH wells were higher ( $P < 0.05$ ) than those in the medium of control wells. There was no effect of 1 pg/ml or 10 pg/ml of AMH on the GnRH-induced FSH secretion. There was a suppressing effect of 100 pg/ml ( $P < 0.05$ ) and 1000 pg/ml ( $P < 0.05$ ) of AMH on the GnRH-induced FSH secretion.

### **3.3.8. Relationship between AMHR2 in APs and the estrous phase**

I used RT-qPCR and western blotting to evaluate the relationship between the estrous phase and AMHR2 expression at the mRNA and protein levels in APs. There

were no differences among phases of the estrous cycle in AMHR2 expression at the mRNA ( $P > 0.05$ ; Fig. 3.9) or protein levels ( $P > 0.05$ ; Fig. 3.10).

### **3.3.9. AMHR2 expression in APs of Holstein cows, Japanese black heifers, and Japanese black cows**

RT-qPCR and western blotting were used to analyze AMHR2 expression at the mRNA and protein levels in the AP. There was no significant differences ( $P > 0.10$ ) among the groups in expression levels of AMHR2 mRNA (Fig. 3.11) and protein (Fig. 3.12).

### **3.3.10. ERE, and PRE in the 5'-flanking region of bovine AMHR2 gene**

The 5'-flanking region of the bovine *AMHR2* gene was analyzed for EREs, PREs, and similar sequences. There were no ERE, no half ERE, nor PRE sequences.

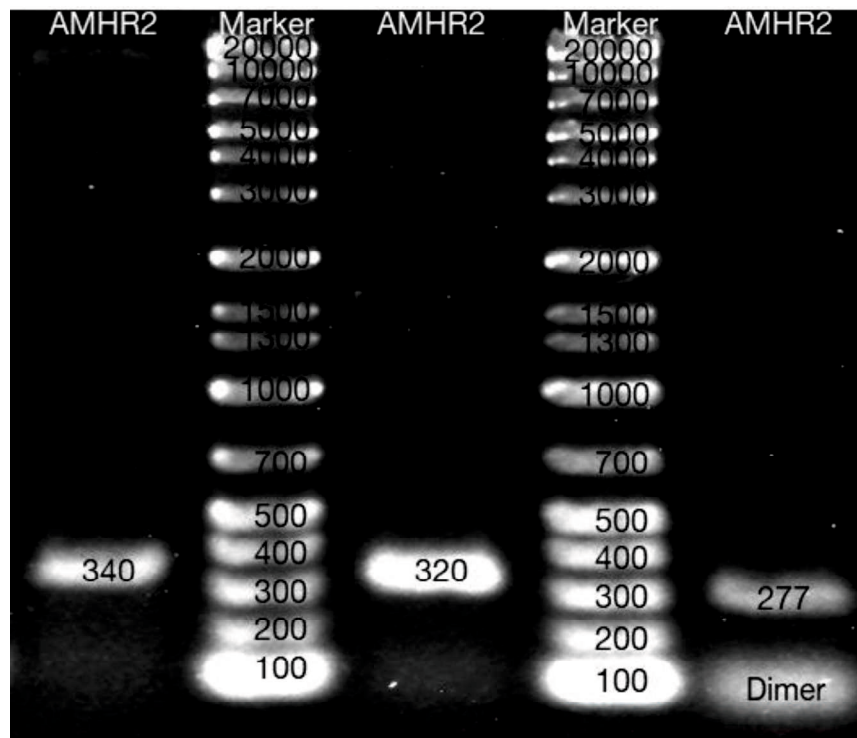


**Fig. 3.1.** Expression of *AMHR2* mRNA detected by RT-PCR. Electrophoresis of PCR-amplified DNA products using 1 of 3 pairs of primers for bovine *AMHR2* and cDNA derived from AP of post-pubertal heifers. The lanes labeled as *AMHR2* demonstrate that the DNA products obtained were of the size that had been expected—340 bp, 320bp, and 277 bp, respectively. Other two lanes (Marker) are the DNA marker.

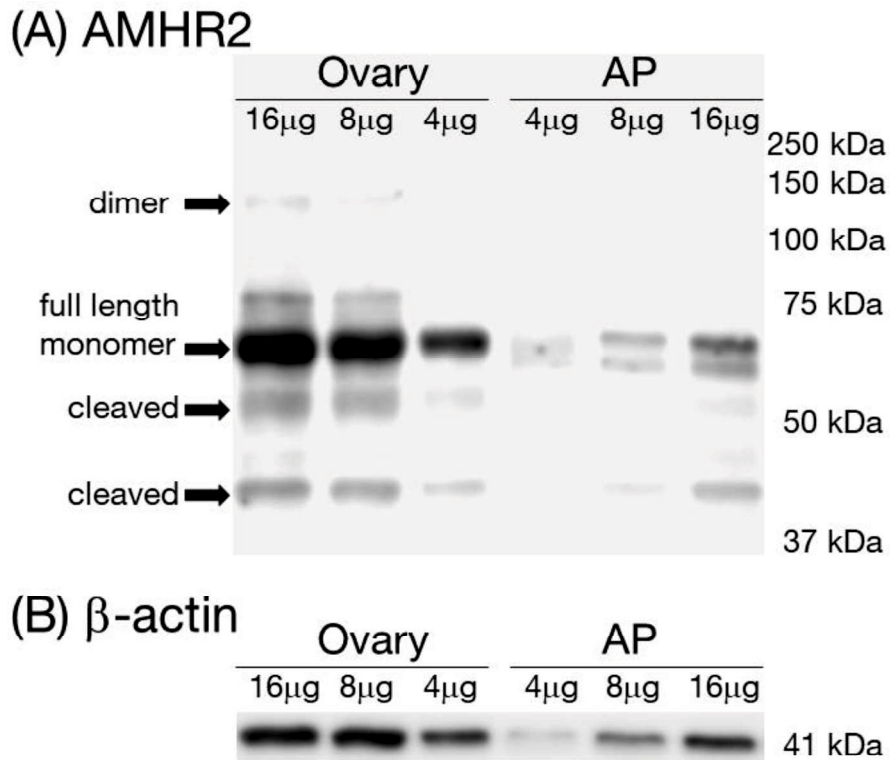


**Fig. 3.2.** Results of western blotting using extracts (4, 8, or 16 µg of total protein) from the AP or ovary of post-pubertal heifers and anti-AMHR2 antibody (A) or anti-β-actin antibody (B). I defined bovine AMHR2 bands based on size as dimers, full length monomers, or cleaved monomers, according to previous studies utilizing western blotting for human and mouse AMHR2 (Faure *et al.* 1996; Hirschhorn *et al.* 2015).

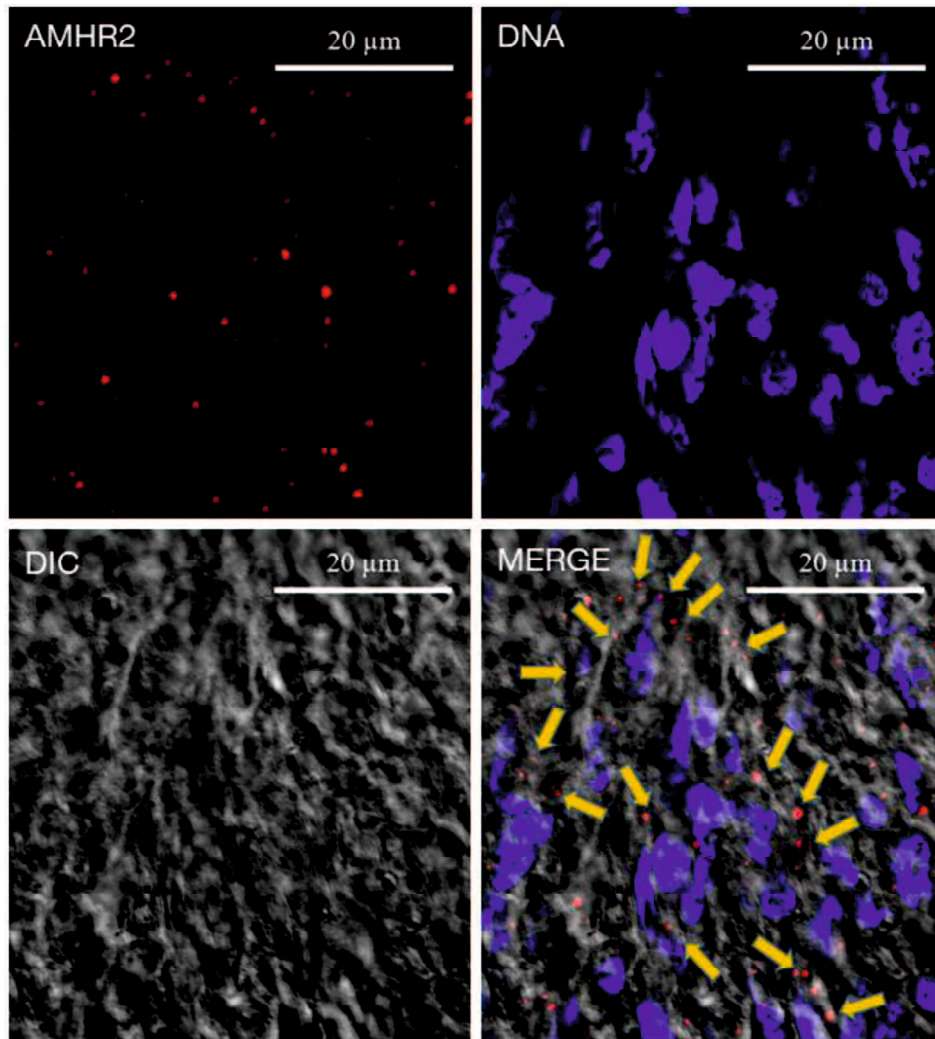


**Fig. 3.3.** Fluorescence immunocytochemistry was used to confirm the expression of AMHR2 on the surface of granulosa cells of small (approximately 5 mm) follicles in the ovaries of post-pubertal heifers. Images were captured by laser confocal microscopy for AMHR2 (red), DNA (dark blue), and differential interference contrast (indicated as DIC). Strong AMHR2 staining appeared to be aggregated (orange arrows), not evenly dispersed. (scale bars = 20 μm).

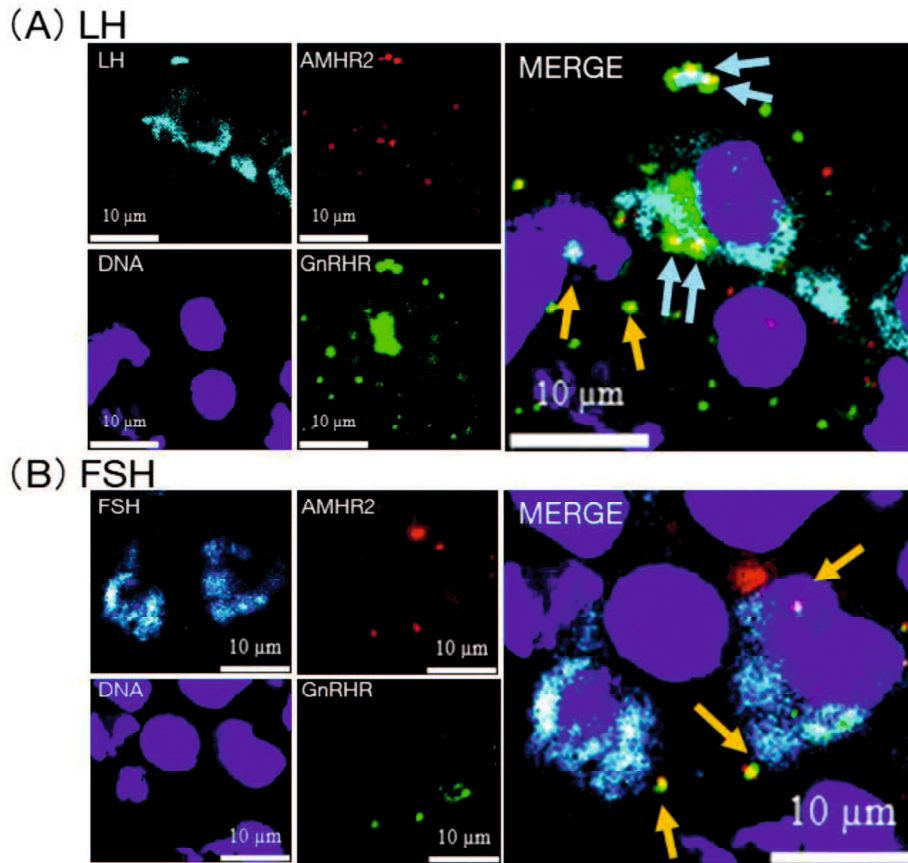


**Fig. 3.4.** Triple-fluorescence immunohistochemistry of AP tissue of post-pubertal heifers for AMHR2, GnRHR and either LH (A) or FSH (B). Images were captured by laser confocal microscopy for AMHR2 (red), GnRHR (green) and LH or FSH (light blue) with counter-staining by DAPI (dark blue). Yellow indicates the colocalization of AMHR2 and GnRHR on the surface of LH-positive cells (blue arrow) and FSH-positive cells (orange arrows). Both AMHR2 and GnRHR appeared to be aggregated, not evenly dispersed. Note that the focus depth of the high magnification lens is thin; thus, the best focus for the membrane receptors was quite different from both the best focus for the nucleus and the best focus for cytoplasmic LH. Therefore, this image was taken using the best focus for the membrane receptors while using strong laser power and strong CCD sensitivity for DAPI and cytoplasmic LH. Scale bars are 10 μm.

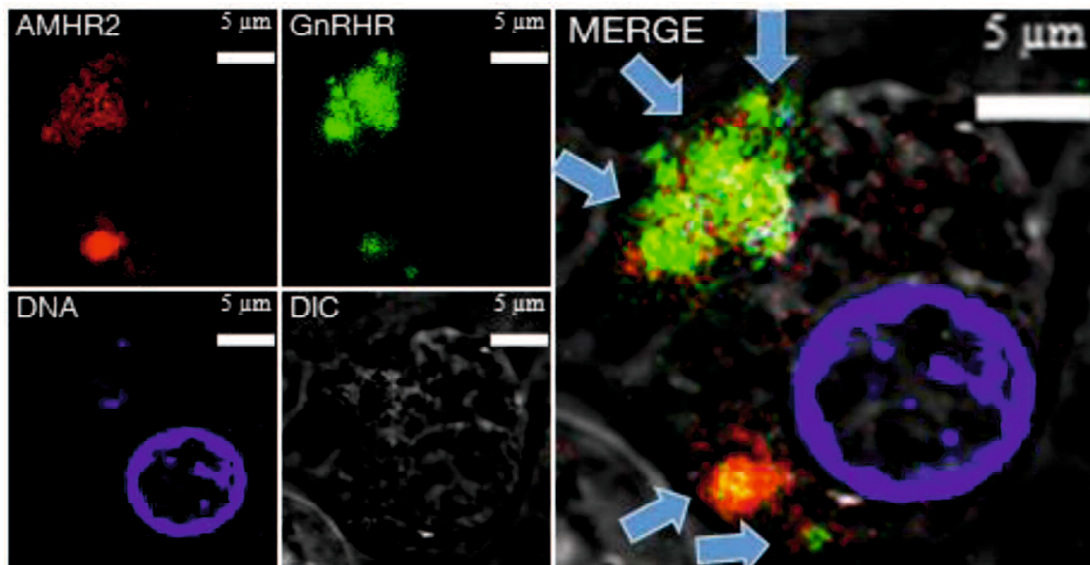
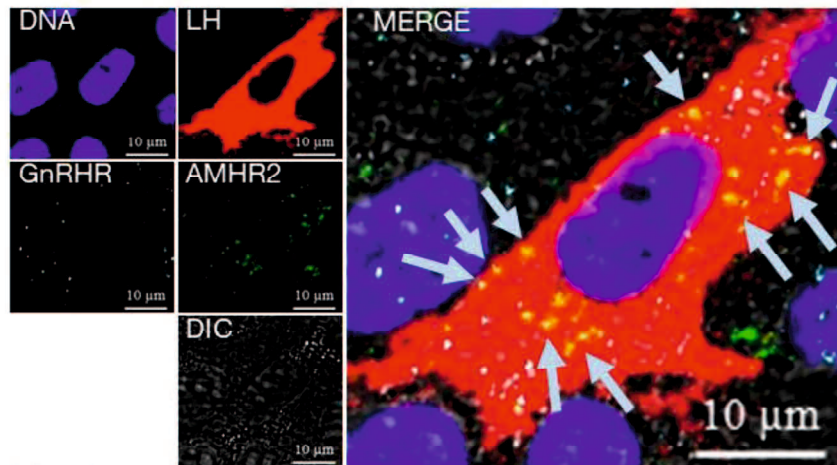


**Fig. 3.5.** Fluorescence immunocytochemistry was used to confirm the colocalization (yellow in the merge panel) of AMHR2 and GnRHR on the surface of cultured AP cells (prepared by CellCover method) of post-pubertal heifers. Images were captured by laser confocal microscopy for AMHR2 (red), GnRHR (green), DNA (dark blue), and DIC on cultured AP cells which did not receive Triton X-100 treatment for antibody penetration. Thus, antibody could only bind AMHR2 and GnRHR on the surface of gonadotrophs. The blue arrows indicate the colocalization of aggregated GnRHR and aggregated AMHR2. (scale bars = 5  $\mu\text{m}$ ).

(A) LH



(B) FSH

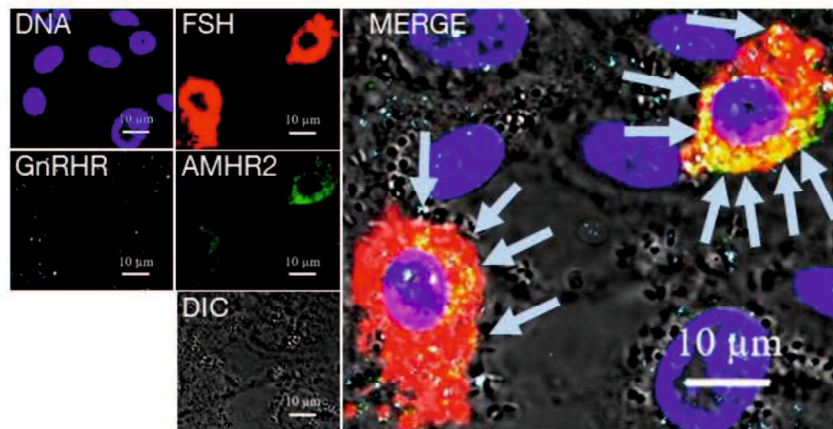


**Fig. 3.6.** Triple-fluorescence immunocytochemistry of cultured AP cells (prepared by PFA-Triton method) of post-pubertal heifers for AMHR2, GnRHR and either LH (A) or FSH (B). Images were captured by laser confocal microscopy for AMHR2 (green), GnRHR (light blue) and LH or FSH (red) with counter-staining by DAPI (dark blue). Yellow (shown by arrows) indicates the colocalization of AMHR2 and LH of FSH in LH-positive cells (A) and FSH-positive cells (B). This image was taken using the best focus for the membrane receptors while using strong laser power and strong CCD sensitivity for DAPI and cytoplasmic LH. Note that the cells prepared by the PFA-triton method are thinner than those prepared by the CellCover method. Scale bars are 10 μm.

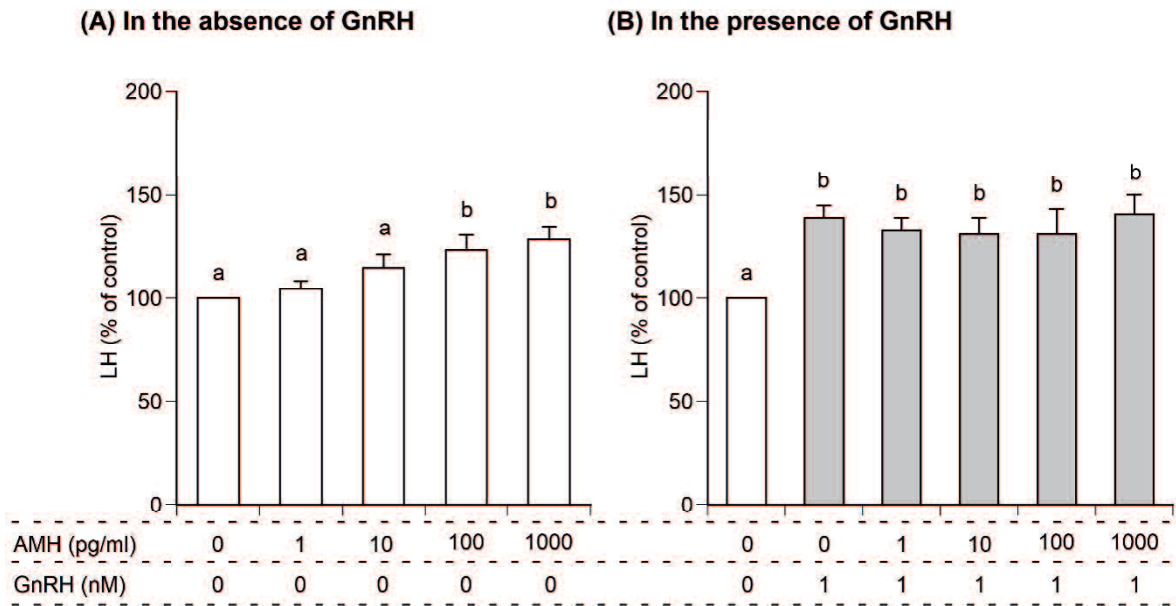


**Fig. 3.7.** Comparison of the effects of various concentrations of AMH in media with (A) and without (B) 1 nM GnRH on LH secretion from cultured AP cells of post-pubertal heifers. The concentrations of LH in the control cells (cultured in medium alone without AMH and GnRH) were averaged and set at 100%, and the mean LH concentration for each treatment group is expressed as a percentage of the control value. Different letters indicate statistical differences ( $P < 0.05$ ).

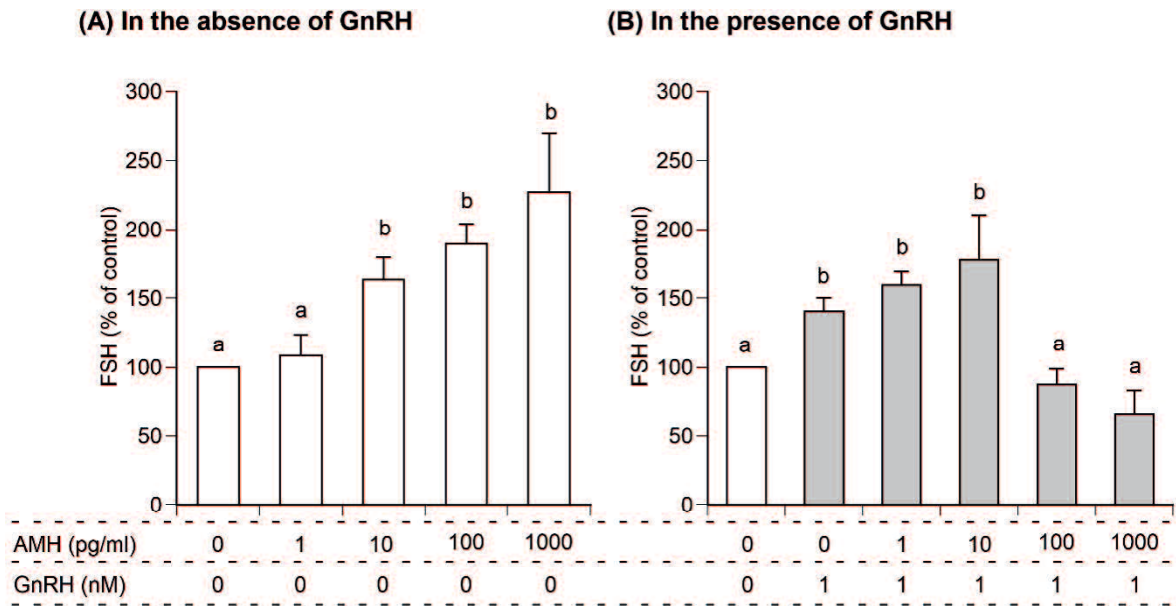


**Fig. 3.8.** Comparison of the effects of various concentrations of AMH in media with (A) and without (B) 1 nM GnRH on FSH secretion from cultured AP cells of post-pubertal heifers. The concentrations of FSH in the control cells (cultured in medium alone without AMH and GnRH) were averaged and set at 100%, and the mean FSH concentration for each treatment group is expressed as a percentage of the control value. Different letters indicate statistical differences ( $P < 0.05$ ).

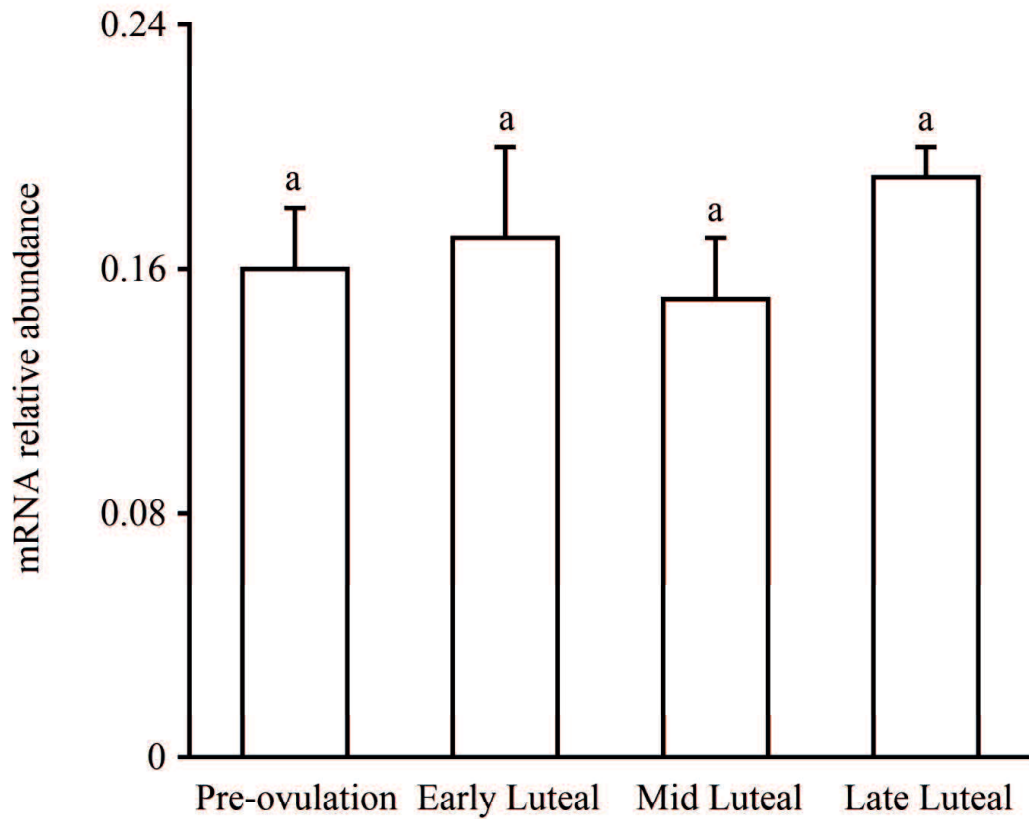


**Fig. 3.9.** Relative *AMHR2* mRNA levels (mean  $\pm$  SEM) in bovine APs during pre-ovulation [day 19 to 21 (day 0 = day of estrus)], early luteal (day 2 to 5), mid-luteal (day 8 to 12), or late luteal (day 15 to 17) phases, as determined by RT-qPCR. Data were normalized to the geometric means of *GAPDH* and *RAN-binding protein (RANBP10)* levels. The same letters indicate no significant differences ( $P > 0.05$ ) across phases.

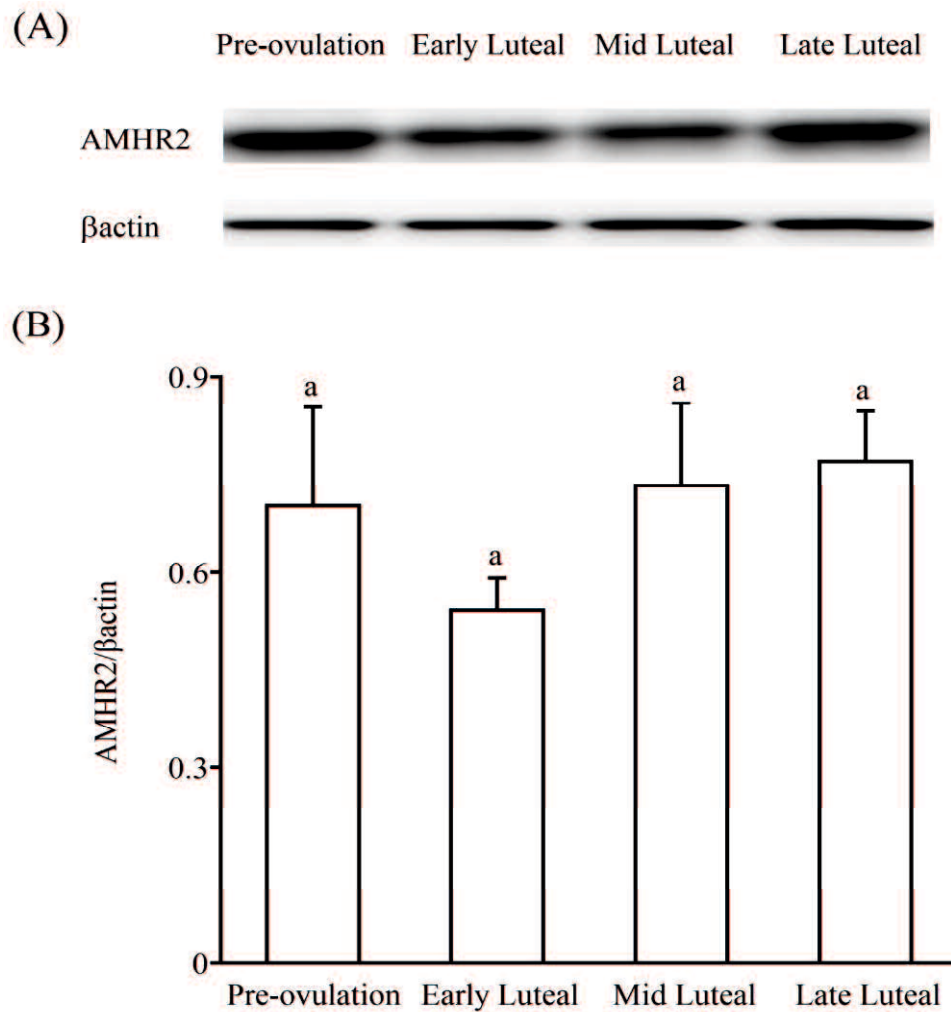


**Fig. 3.10.** (A) Representative AMHR2 (as full length monomer form) and  $\beta$ -actin protein expression in bovine AP tissues obtained during the pre-ovulation, early luteal, mid luteal, or late luteal phases of estrous, as detected by western blotting. (B) AMH protein expression level of AMH normalized to that of  $\beta$ -actin in healthy post-pubertal heifer AP tissues obtained during pre-ovulation (n =5), early luteal (n =5), mid-luteal (n =6), and late luteal (n = 5) phases. The same letters indicate no significant differences ( $P > 0.05$ ) across phases.

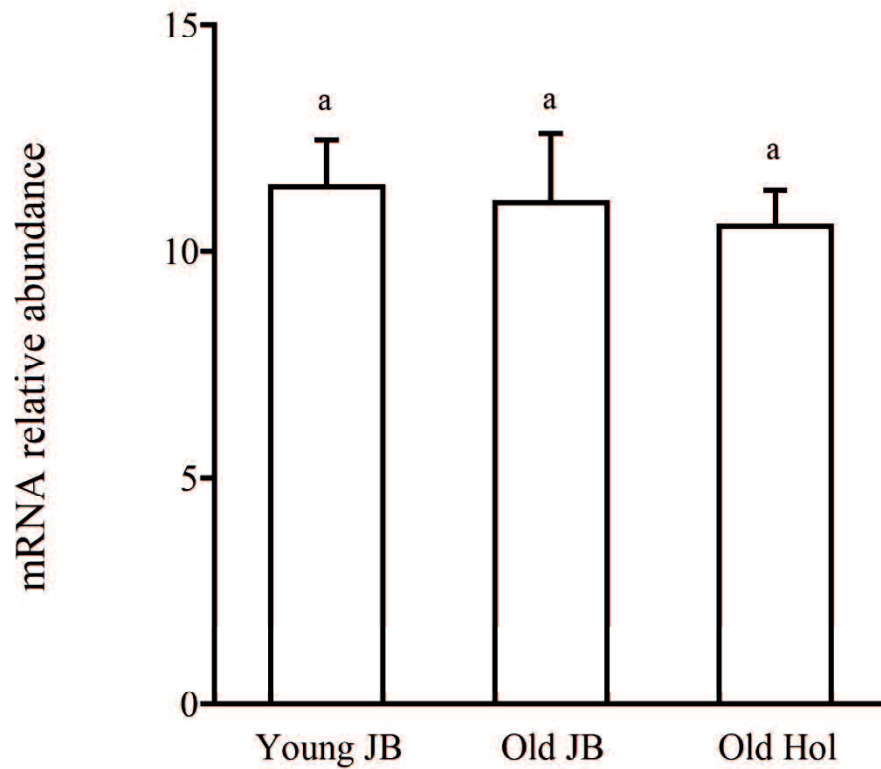


**Fig. 3.11.** Relative *AMHR2* mRNA levels (mean ± SEM) in bovine AP tissues obtained from healthy young Japanese heifers (young JB), old Japanese black cows (old JB), and old Holsteins cows (old Hol), as determined by real-time PCR. Data were normalized to the geometric means of *GAPDH* and *RANBP10* levels. The same letters indicate no significant differences ( $P>0.05$ ) across phases.

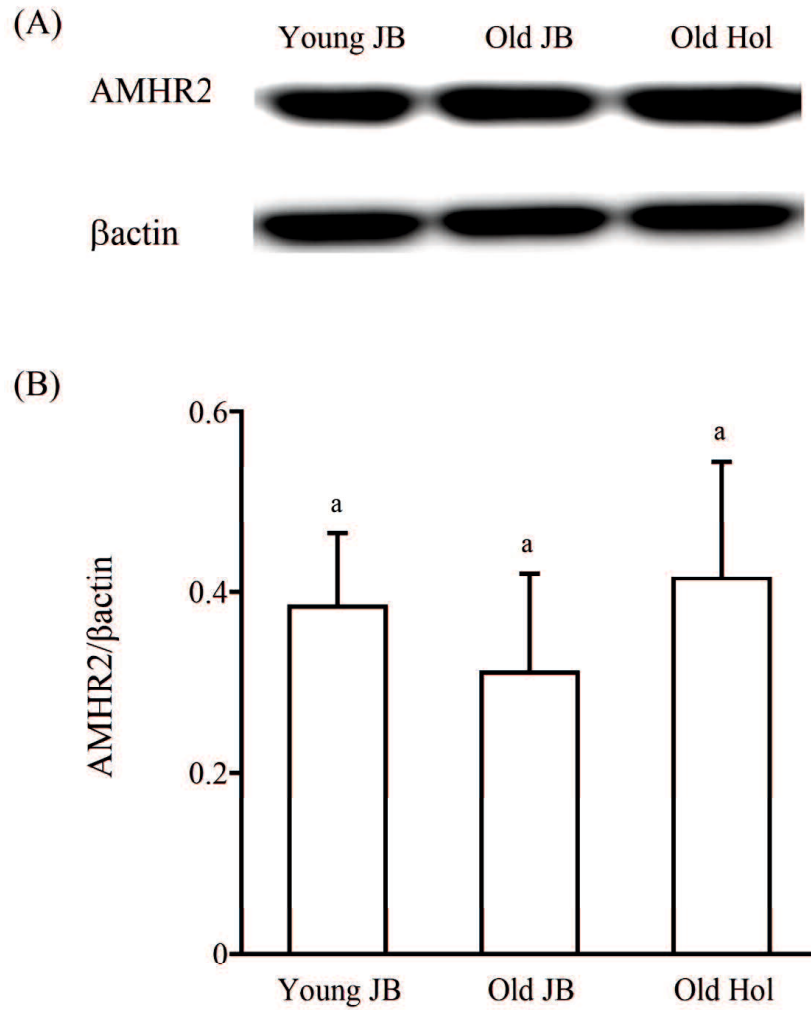


**Fig. 3.12.** (A) Representative AMHR2 (as full length monomer form) and  $\beta$ -actin protein expression in bovine AP tissues obtained from young JB, old JB, and old Hol. (B) Protein expression level of AMHR2 normalized to that of  $\beta$ -actin in bovine AP tissues obtained from young JB, old JB, and old Hol. Letters (a vs. b) indicate significant differences ( $P < 0.05$ ) between groups.

### 3.4. Discussion

This study is reporting that AP cells express AMHR2 in ruminants and that AMH significantly affects LH and FSH secretion from AP cells. Fluorescent immunohistochemistry using the anti-AMHR2 antibody showed the strong signal located on the surface of granulosa cells in small antral follicles, where *AMHR2* mRNA is expressed (Poole *et al.* 2016). Therefore, the anti-bovine AMHR2 is the first developed tool that can be used for immunohistochemistry in bovine samples.

In this study, treatment with 10–1000 pg/ml of AMH stimulated FSH secretion in the absence of GnRH. This agrees with *in vivo* experiments on rats, where AMH stimulates the secretion and expression of FSH (Garrel *et al.* 2016). These data suggested that AMH might bind with AMHR2 to increase FSH secretion from gonadotrophs in ruminants as well. Garrel *et al.* (2016) recently reported that AMH increases both FSH $\beta$  expression and phosphorylates SMAD 1/5/8 in L $\beta$ T2 cells, but such increases are blocked by GnRH. In this study, 1–10 pg/ml AMH did not change GnRH-stimulated FSH secretion; however, 100–1000 pg/ml AMH suppressed GnRH-stimulated FSH secretion. Therefore, further studies are required to clarify the molecular mechanisms controlling FSH secretion from ruminant gonadotrophs by AMH and GnRH, especially whether the SMAD 1/5/8 pathways have important roles.

Multiparous (third parity or higher) Japanese Black cows have significantly higher blood AMH concentrations (100 pg/ml level) than primiparous cows (1–10 pg/ml level) throughout the postpartum period (Koizumi and Kadokawa 2017). The multiparous Japanese Black cows have larger number of days from parturition to postpartum first ovulation than the primiparous cows (Koizumi *et al.* 2016). Therefore, the suppressing effect of 100–1000 pg/ml of AMH on GnRH-stimulated FSH secretion

may have an important role in the follicular growth and delayed postpartum first ovulation in multiparous cows.

Intraperitoneal injection with AMH increases FSH concentration in blood collected 18 h later, but only in pre-pubertal female rats (Garrel *et al.* 2016). In contrast, this study shows the significant effect of AMH on FSH secretion from the AP of post-pubertal heifers *in vitro*. Therefore, further studies are required to clarify whether there are any differences in AMH effects on FSH secretion among species.

The pituitary gland is located outside the blood-brain barrier unlike the hypothalamus (Nussey and Whitehead 2001); therefore, the AMHR2 on gonadotrophs may bind AMH secreted from preantral and small antral follicles. My data suggested that AMH, like the other TGF- $\beta$  family members such as inhibin and activin (Kushnir *et al.* 2017), can affect FSH secretion from gonadotrophs. However, little is known about the changes occurring in the blood AMH concentration during the estrous cycle in ruminants (Pfeiffer *et al.* 2014; Koizumi and Kadokawa 2017). The blood AMH concentration is influenced by age and parity (Koizumi and Kadokawa 2017); however, the concentration may not show a considerable change during the estrous cycle in ruminants *in vivo* (Pfeiffer *et al.* 2014; Koizumi and Kadokawa 2017; El-Sheikh Ali *et al.* 2013). Therefore, caution must be exercised when concluding that AMH contributes largely in controlling LH and FSH secretion from gonadotrophs *in vivo*.

My results suggested that preantral and small antral follicles may control gonadotropin secretion from the AP in post-pubertal heifers. Conversely, FSH suppresses AMH secretion from bovine granulosa cells (Rico *et al.* 2011). Therefore, there may be feedback mechanisms between gonadotrophs and granulosa cells in preantral and small antral follicles. AMH locally decreases the sensitivity of FSH in follicles in multiple species including the mouse and sheep (Durlinger *et al.* 2001;

Campbell *et al.* 2012; Visser and Themmen 2014). Recently, Ilha *et al.* (2016) reported that AMH mRNA levels decrease in both dominant and subordinate follicles during follicular deviation in cows. Thus, both dominant and subordinate follicles become more sensitive to FSH and can be recruited to enter the pool of follicles which may then become dominant (Visser and Themmen 2014). Therefore, AMH may have an important role in both the ovary and gonadotrophs during follicular selection in monovulatory species.

Gonadotrophs are a heterogeneous cell population comprising LH and FSH monohormonal and bihormonal subsets in rats, equines, and bovines (Townsend *et al.* 2004; Pals *et al.* 2008; Kadokawa *et al.* 2014). The fluorescent immunohistochemistry showed the AMHR2 expression in LH $\beta$ -positive cells as well as FSH $\beta$ -positive cells. In this study, 100 pg/ml and 1000 pg/ml of AMH stimulated LH secretion weakly. Therefore, AMH may control also LH secretion, but weakly. Intraperitoneal injection with AMH increases FSH concentration in blood collected 18 h later in rats; however, AMH injection does not significantly increase LH concentration in the same blood samples (Garrel *et al.* 2016). Therefore, the effect of AMH on LH secretion *in vivo* may not become significant.

It is well known that GPCR proteins can form functionally active homomers and heteromers with different receptors (Ritter and Hall 2009). I obtained the strong positive overlap coefficient between AMHR2 and GnRHR on the cell-surface. This overlap coefficient was greater than that reported between GnRHR and flotillin-1 in cultured L $\beta$ T2 cells (0.50; Wehmeyer *et al.* 2014) and similar to that we previously found between GnRHR and GPR61 (0.71; Pandey *et al.* 2017a) and GPR153 (0.75; Pandey *et al.* 2018) in bovine gonadotrophs. Heterodimerization among paralogs of GnRHRs of a protochordate results in the modulation of ligand-binding affinity, signal

transduction, and internalization (Satake *et al.* 2013). Thus, it is possible that AMHR2 forms a heteromer, affecting ligand-binding affinity, signal transduction, and internalization of GnRHR, and thus the synthesis and secretion of LH and FSH in AP of vertebrates. Furthermore, a study (Hossain *et al.* 2016) suggested that GPR61 form heteromers with other GPCRs. Therefore, further studies are required to clarify whether GnRHR form heteromers with GPR61, GPR153, and AMHR2.

In this study, I observed multiple, not single, bands of AMHR2 in western blotting, which has been reported previously. For example, Faure *et al.* (1996) reported three bands (82, 73, and 63 kDa) of dimers, full-length monomers, and cleaved monomers. Hirschhorn *et al.* (2015) reported more bands (~58 kDa, ~69 kDa, and ~71 kDa) of dimers, full-length monomers, and cleaved monomers. AMHR2 is present as dimers, full-length monomers, and cleaved monomers in bovine ovaries and APs. Treatment with *N*-glycosidase F shows a further two bands (68 kDa and 61 kDa) by cutting down by approximately 5 and 2 kDa, because AMHR2 is *O*-glycosylated (Faure *et al.* 1996). The full-length monomers in APs appeared as a doublet, whereas those in the ovary appeared as a single band in this study. Therefore, this study suggests that bovine AMHR2 is glycosylated, and the difference in the number of full-length monomers between the AP and ovary might be because of the glycosylation differences.

The anti-AMHR2 antibody revealed similar bands in the two tissues in the western blot. However, AP tissue showed weaker bands than ovarian tissue did. Nevertheless,  $\beta$ -actin bands showed weaker staining in both tissue types. This suggests that the AP cell lanes were loaded with a lower amount of proteins than expected. A second difference between AP and ovarian cells was the absence of the dimeric AMHR2 band in AP cells. However, this might be the consequence of the lower protein amount used

in the AP cell western blot. In fact, the high molecular weight band was detectable in the ovarian tissue extract only at the highest dose (i.e., 16 µg/lane).

This study found that approximately 20% of AMHR2-positive cells were non-gonadotrophs. At the time of this study, no reports published on AMHR2 in non-gonadotrophs. An AMHR2 polymorphism (482 A>G) was associated with lower prolactin levels in women with polycystic ovary syndrome (Georgopoulos *et al.* 2013). Therefore, lactotrophs may express AMHR2 to play an important role in polycystic ovary syndrome, which is a possibility that bears further consideration in future investigations.

My data showed no significant changes in AMHR2 at the mRNA and protein levels in APs during the estrous cycle. The 5'-flanking region of the bovine *AMHR2* gene does not contain ERE, half ERE, or PRE sequences. Therefore, AMHR2 expression in APs, is unlikely to change during the estrous cycle. I found no significant differences of AMHR2 expression in AP among the old Holsteins and young and old Japanese Black females. Further studies are required to conclude the contribution of AMH and AMHR2 in infertility after aging.

In conclusion, AMHR2 is expressed in the gonadotrophs of post-pubertal heifers to control gonadotropin secretion.

## **CHAPTER IV**

**(Study II)**

**Bovine gonadotrophs express anti-Müllerian hormone (AMH):  
comparison of AMH mRNA and protein expression levels between  
old Holsteins and young and old Japanese Black females**

## Abstract

AMH is secreted from ovaries and stimulates gonadotrophin secretion from bovine gonadotroph cells. Other important hormones for endocrinological gonadotroph regulation (e.g. gonadotrophin-releasing hormone, inhibin and activin) have paracrine and autocrine roles. Therefore, in this study, AMH expression in bovine gonadotroph cells and the relationships between AMH expression in the bovine AP and oestrous stage, age and breed were evaluated. *AMH* mRNA expression was detected in APs of postpubertal heifers (26 months old) by reverse transcription-polymerase chain reaction. Based on western blotting using an antibody to mature C-terminal AMH, AMH protein expression was detected in APs. Immunofluorescence microscopy utilising the same antibody indicated that AMH is expressed in gonadotrophs. The expression of AMH mRNA and protein in APs did not differ between oestrous phases ( $P > 0.1$ ). We compared expression levels between old Holsteins ( $79.2 \pm 10.3$  months old) and young ( $25.9 \pm 0.6$  months old) and old Japanese Black females ( $89.7 \pm 20.3$  months old). The APs of old Holsteins exhibited lower *AMH* mRNA levels ( $P < 0.05$ ) but higher AMH protein levels than those of young Japanese Black females ( $P < 0.05$ ). In conclusion, bovine gonadotrophs express AMH and this AMH expression may be breed-dependent.

#### 4.1. Introduction

In the previous study I discovered that the main AMH receptor; AMHR2, is colocalised with GnRHR on the surface of gonadotrophs. AMH activates the synthesis and secretion of gonadotrophins, e.g. LH and FSH, in gonadotrophs of rodents and bovines (Bédécarrats *et al.* 2003; Garrel *et al.* 2016; Kereilwe *et al.* 2018). Therefore, AMH has important roles in controlling gonadotrophin secretion.

GnRH secreted from the hypothalamus is a well-known endocrine mechanism to control gonadotrophin synthesis and secretion in gonadotrophs. However, GnRH is also expressed in gonadotrophs themselves, with paracrine or autocrine roles in the control of gonadotrophin synthesis and secretion (Pagesy *et al.* 1992; Miller *et al.* 1996). Inhibin and activin, other members of the TGF- $\beta$  superfamily, are secreted by the ovaries and affect gonadotrophs. It is important to note that gonadotrophs synthesise and secrete both inhibin and activin, with paracrine and autocrine effects on gonadotrophin synthesis and secretion (Popovics *et al.* 2011). The coordination of the endocrine, paracrine and autocrine control of these hormones is likely to be important for normal reproductive functions (de Kretser *et al.* 2002).

Old age is associated with decreased fertility in beef cows (Osoro and Wright 1992); however, little is known about the exact mechanisms underlying this association in domestic animals. Studies of AMH are promising for understanding these mechanisms. Blood AMH concentrations are highest in pubertal girls and decrease gradually from the age of 25 years until the postmenopausal period (Dewailly *et al.* 2014). In contrast, old Japanese Black cows have higher blood AMH concentrations than postpubertal heifers and young cows (Koizumi and Kadokawa 2017). These data suggest that age may be a determinant of blood AMH concentration.

AMH expression in gonadotrophs has not been evaluated in any species. However, AMH is expressed in the APs of both male and female tilapia (Poonlaphdecha *et al.* 2011). Therefore, I evaluated the hypothesis that AMH is expressed in bovine gonadotrophs in AP tissues. Ribeiro *et al.* (2014) reported a difference in blood AMH concentrations among dairy cow breeds. Infertility in Holsteins is an important issue in dairy industries worldwide (Kadokawa and Martin 2006; Adamczyk *et al.* 2017; Gernand and König 2017). Therefore, I also evaluated the relationship between AMH expression in APs and various physiological factors, i.e. stage of the oestrous cycle, age and breed.

## 4.2. Materials and methods

### 4.2.1. Antibodies used in this study

Human AMH is secreted as a homodimeric precursor consisting of two identical monomers (560 amino acids; NCBI accession number AAA98805.1; Mamsen *et al.* 2015). Each monomer consists of two domains: (1) a mature C-terminal region, which becomes bioactive after proteolytic cleavage and binds to AMHR2 and (2) a pro-region, which is important for AMH synthesis and extracellular transport. The human AMH precursor is cleaved at amino acid 451 (arginine) between the two domains. The pro-region has another cleavage site at amino acid 229 (arginine), giving rise to three potential cleavage products: pro-mid-mature, mid-mature and mature (Mamsen *et al.* 2015). The bovine AMH precursor monomer (575 amino acids; NCBI accession number NP\_776315.1) has 91% sequence similarity to the human protein (evaluated using Genetyx Version 11; Genetyx). The bovine AMH precursor contains an arginine cleavage site between the two domains at amino acid 466. However, the bovine AMH precursor does not contain arginine at the residue corresponding to amino acid 229 of the human pro-region of AMH. A rabbit polyclonal anti-AMH antibody (ARP54312\_P050; Aviva Systems Biology) that recognises the mature C-terminal form of human AMH (corresponding to amino acids 468–517; SVDLRAERSVLIPETYQANNCQGVCGWPQSDRNPRYGNHVVLLLKMQARG) was used. This sequence has 98% homology to amino acids 483–532 of the mature C-terminal form of bovine AMH but no homology to other bovine proteins, as determined using protein BLAST. Details of the other antibodies used in this study are described in chapter III

#### 4.2.2. AP and ovary sample collection for RT-PCR, western blotting and IHC

Samples were collected in the same manner as detailed in chapter III. The same procedure as described in chapter III were followed for protein extraction and western blotting against AMH.

RNA extraction, synthesis of cDNA and realtime PCR were carried out as described in chapter III using the primer for *AMH*. In order to determine the expression of *AMH* mRNA in the AP, PCR was conducted using a primer pair designed by Primer3 based on the reference sequence of bovine *AMH* (NCBI reference sequence of bovine AMH is NM\_173890). The expected PCR product size of *AMH* using the primer pair is 328 bp (nucleotides 1486–1813; forward primer: 5'-GTCATCCCCGAGACATACC-3'-; reverse primer: 5'-TTCCCGTGTTTAATGGGGCA-3'-). The primers used for real time PCR are listed in Table 4.1.

Immunofluorescence was similar to described in chapter III except that rabbit polyclonal anti-AMH was used. Immunocytochemical analysis of cells was same as described in chapter III using the rabbit polyclonal anti-AMH. The obtained data were analyzed using the same methods as described in chapter III (study I).

**Table 4.1.** Name, accession number and details of the primers used for real-time PCRs

Gene name	Accession number	Primer	Sequence 5'-3'	Size (bp)
<i>GAPDH</i>	NM_001034034	Forward	TGGTGAAGGTCGGAGTGAAC	91
		Reverse	ATGGCGACGATGTCCAATTT	
<i>RANBP10</i>	NM_001098125	Forward	CCCAGTCCTACCAGCCTACT	133
		Reverse	CCCCCAGAGTTGAATGACCC	
<i>AMH</i>	NM_173890 Exon 3 4	Forward	GGGTTAGCCCTTACCCTGC	121
		Reverse	GTAACAGGGCTGGGGTCTTT	

#### 4.2.3. Analysis of the AMH gene 5'- flanking region

The 5000-nucleotide sequence of the 5' flanking region of the *AMH* gene (Chromosome 7: 22 691 978–22 696 977) was obtained using the online Ensembl ([www.ensembl.org](http://www.ensembl.org)) and BLAT Search Genome program (<http://genome.ucsc.edu>) (Cow Jun. 2014, Bos\_taurus\_UMD\_3.1.1/bosTau8). The sequence was analysed using Genetyx software Version 13 (Genetyx) for the presence of consensus response element sequences for oestrogen i.e. ERE (5'-GGTCANNNTGACC-3'; Gruber *et al.* 2004) and half ERE (GGTCA, TGACC or TGACTION; Liu *et al.* 1995), as well as for progesterone i.e. PRE (5'-G/A G G/T AC A/G TGGTGTCT-3'; Geserick *et al.* 2005).

### **4.3. Results**

#### **4.3.1. Expression of *AMH* mRNA in APs of post-pubertal heifers**

PCR products of the expected size (328 bp), indicating *AMH*, were obtained by agarose gel electrophoresis (Fig. 4.1). Homology searching in the gene databases for the obtained sequence of amplified products revealed that the best match alignment was bovine *AMH* (NM\_173890.1), which had a query coverage of 100%, an e-value of 0.0, and a maximum alignment identity of 99%. There was no other bovine gene found to have a homology for the obtained sequences of amplified products, which lead to the conclusion that the sequences of the amplified products were identical with the sequence of bovine *AMH*.

#### **4.3.2. AMH protein expression in APs**

Western blotting confirmed the presence of AMH in both the AP and ovary samples, with differences in intensity between sample types (Fig. 4.2A). Weaker bands for the AMH precursor (70 kDa) were detected in the AP samples than in the ovary samples. Stronger bands for the mature C-terminal form were observed for the AP samples than the ovary samples, and there was a difference in molecular weights between AP (20 kDa) and ovary (25 kDa) samples. Fig. 4.2B shows representative  $\beta$ -actin bands for both tissue types.

#### **4.3.3. Immunofluorescence analysis of AMH expression in bovine small follicles and AP tissues**

Figure 4.3 shows immunofluorescence signals in the granulosa cells of small follicles in the ovary tissues of post-pubertal heifers.

Also the expression of GnRHR, AMH, LH $\beta$ , and FSH $\beta$  in bovine AP tissues was investigated by immunohistochemistry. AMH was localized in the majority of LH $\beta$ -positive (Fig. 4.4A) and FSH $\beta$ -positive (Fig. 4.4B) cells. In AP samples, there were  $53.2 \pm 2.1$  GnRHR-positive cells,  $43.2 \pm 2.5$  AMH-positive cells, and  $30.2 \pm 1.6$  double-positive cells;  $57.0\% \pm 3.4\%$  of GnRHR-positive cells were AMH-positive, whereas  $82.0\% \pm 5.5\%$  of AMH-positive cells were GnRHR-positive.

#### **4.3.4. Relationship between AMH in APs and the estrous phase**

I used real-time PCR and western blotting to evaluate the relationship between the estrous phase and AMH expression at the mRNA and protein levels in APs. There were no differences among phases of the estrous cycle in AMH expression at the mRNA ( $P > 0.05$ ; Fig. 4.5) or protein levels ( $P > 0.05$ ; Fig. 4.6).

#### **4.3.5. AMH expression in APs of Holstein cows, Japanese black heifers, and Japanese black cows**

Real-time PCR and western blotting were used to analyze AMH expression at the mRNA and protein levels in the AP. The levels of *AMH* mRNA were lower in the old Hol group than in young JB group ( $P < 0.05$ ; Fig. 4.7). The old JB group had tendency to express lower levels *AMH* mRNA than those in the young JB group ( $P = 0.10$ ). AMH protein levels were greater in the old Hol group than in the old JB and young JB groups ( $P < 0.05$ ; Fig. 4.8). There was no difference in AMH levels between the young JB and old JB groups ( $P > 0.10$ ).

#### **4.3.6. ERE, and PRE in the 5'-flanking region of bovine AMH gene**

The 5'-flanking region of the bovine *AMH* gene was analyzed for EREs, PREs, and similar sequences. There were no ERE, no half ERE, nor PRE sequences.

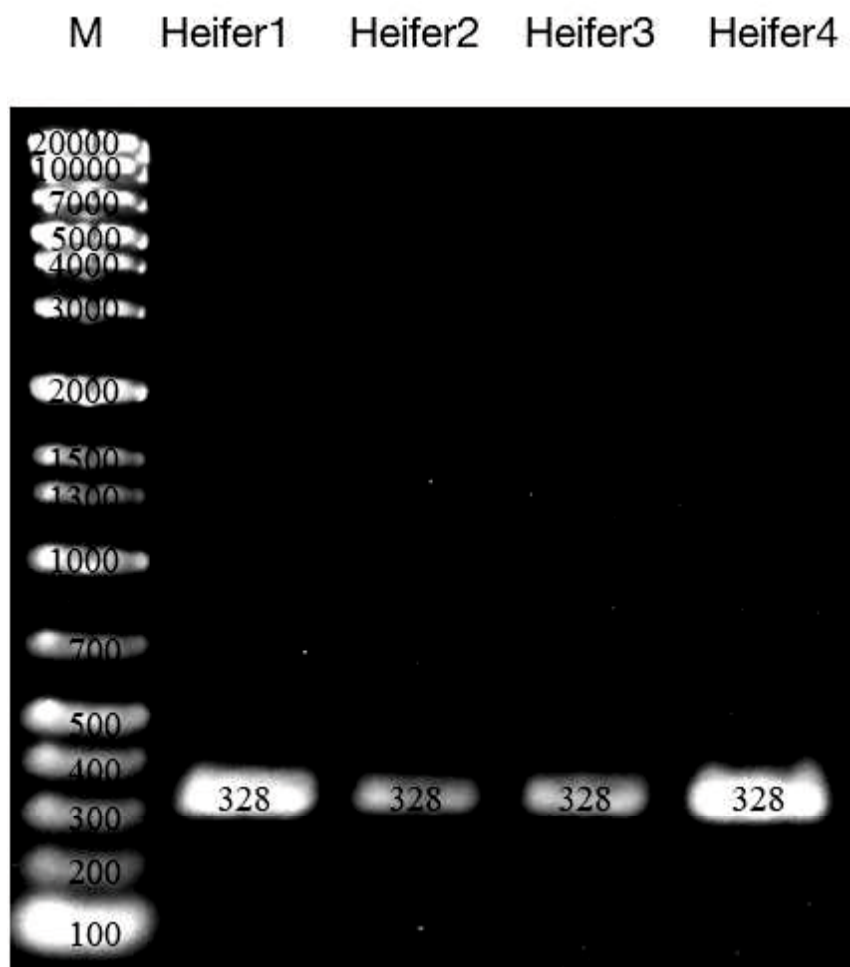


**Fig. 4.1.** Expression of *AMH* mRNA, as detected by RT-PCR. Electrophoresis of PCR-amplified DNA products using the primer pair for bovine *AMH* and cDNA derived from the AP of post-pubertal heifers. The lanes labeled Heifers 1 to 4 demonstrate that the DNA products were of the expected size, i.e., 328 bp. Lane M showed the band sizes of the DNA marker.

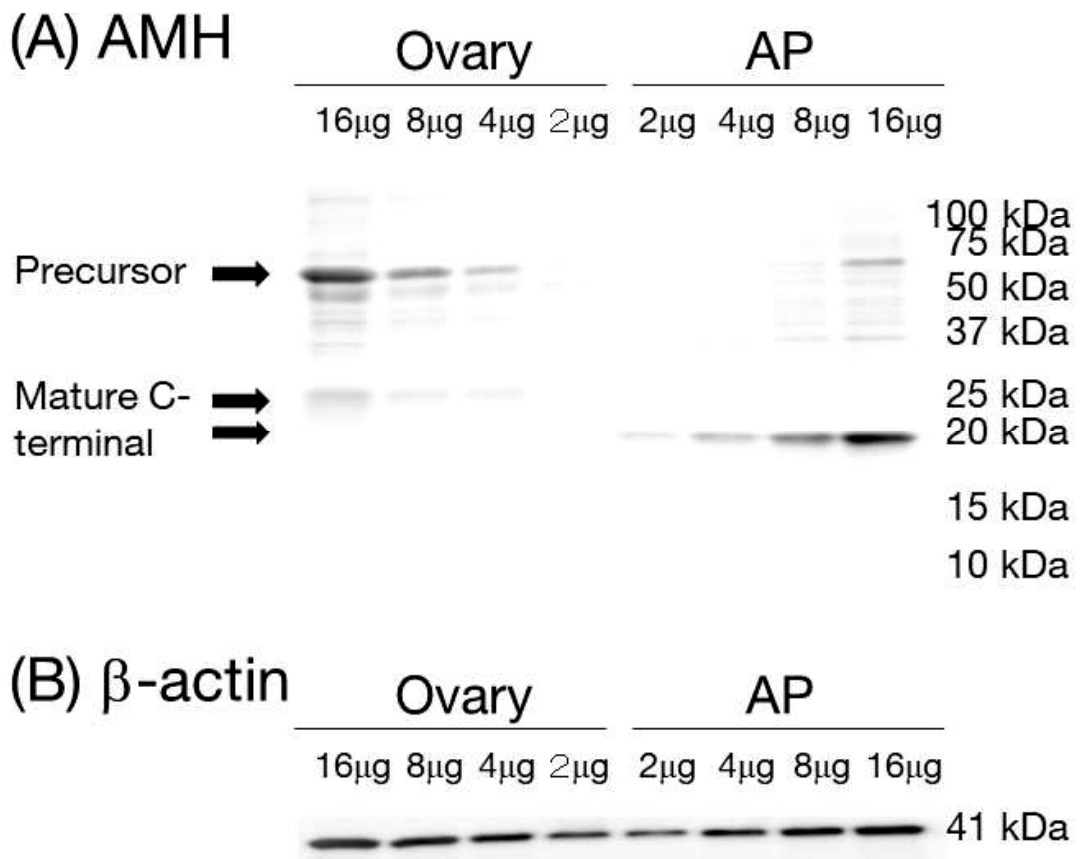


**Fig. 4.2.** Western blotting results using extracts (2, 4, 8, or 16 µg of total protein) from the APs or ovaries of post-pubertal heifers and an anti-AMH rabbit antibody (A) or anti-β-actin mouse antibody (B).

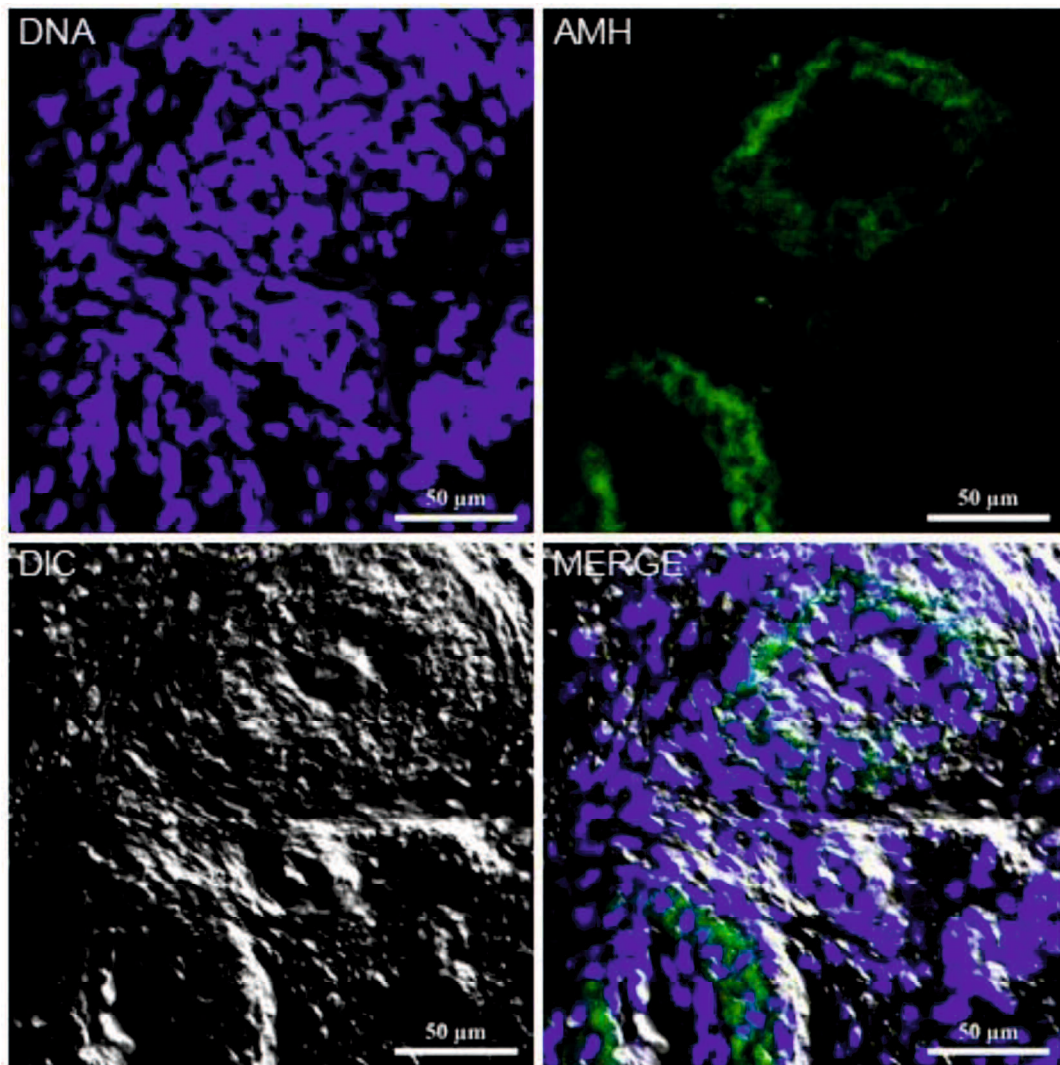


**Fig. 4.3.** Fluorescence immunohistochemical analysis of AMH on small antral follicles in ovaries of post-pubertal heifers. Images were captured by laser confocal microscopy for AMH (green) with counter-staining by DAPI (dark blue, indicating DNA) and differential interference contrast (DIC). Scale bars represent 50 µm.

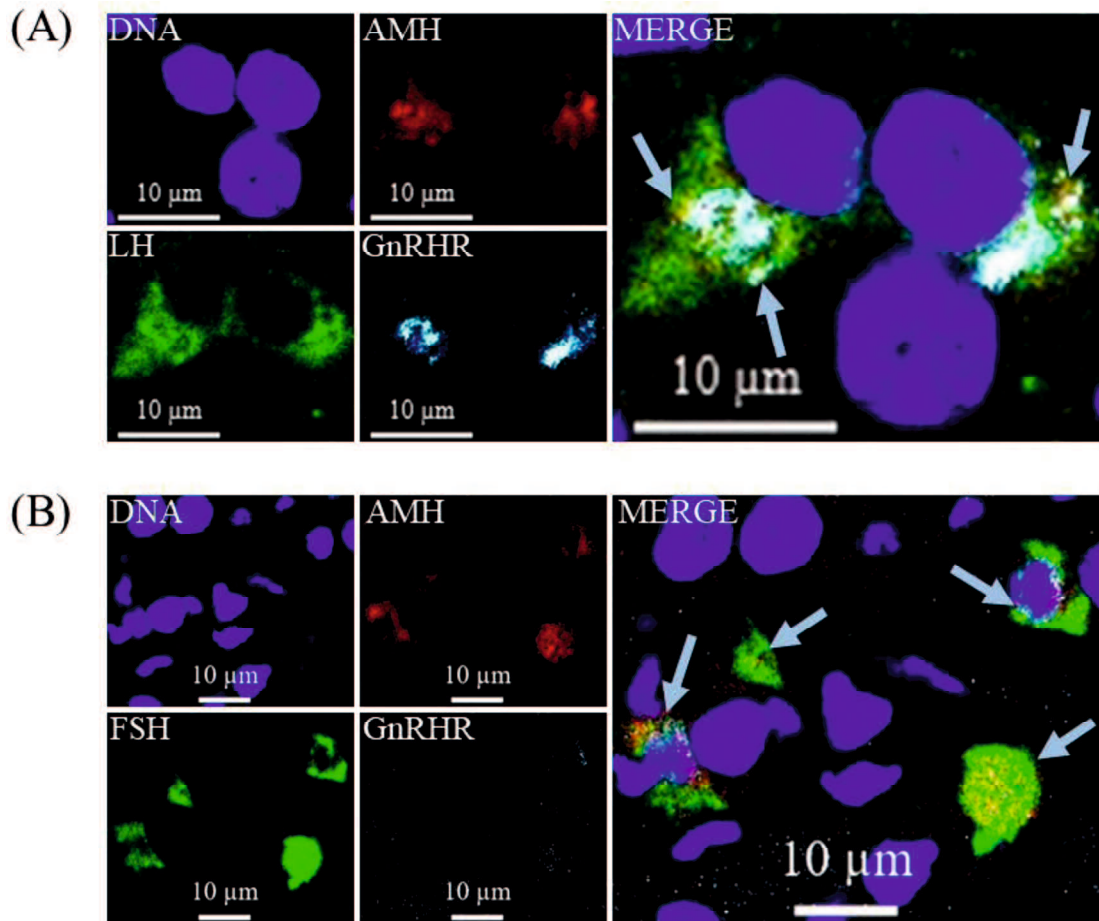


**Fig. 4.4.** Triple-fluorescence immunohistochemistry of AP tissues in post-pubertal heifers for the detection of GnRHR, AMH, and LH (A) or FSH (B). Images were captured by laser confocal microscopy for GnRHR (cyan), AMH (red), and LH or FSH (green) with counter-staining by DAPI for DNA (dark blue). Yellow indicates the colocalization of AMH and LH/FSH, indicated by blue arrows. Scale bars represent 10 μm.

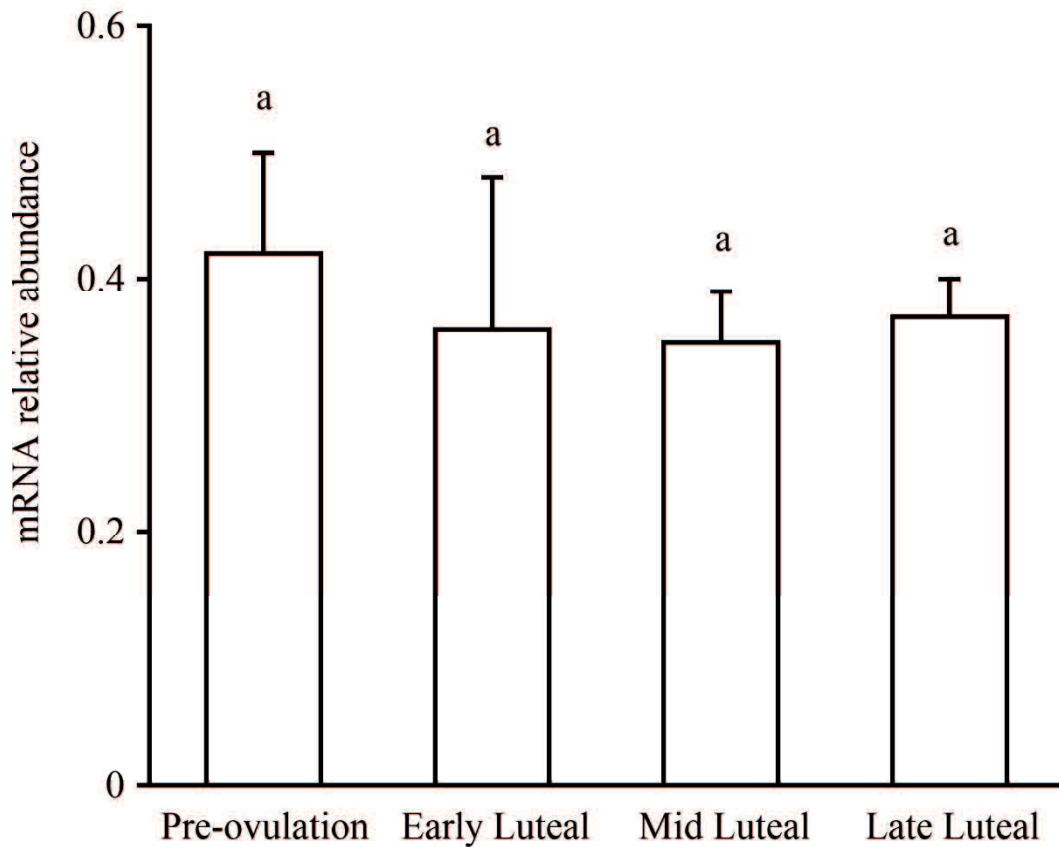


**Fig. 4.5.** Relative *AMH* mRNA levels (mean  $\pm$  SEM) in bovine APs during pre-ovulation [day 19 to 21 (day 0 = day of estrus)], early luteal (day 2 to 5), mid-luteal (day 8 to 12), or late luteal (day 15 to 17) phases, as determined by real-time PCR. Data were normalized to the geometric means of *GAPDH* and *RANBP10* levels. The same letters indicate no significant differences ( $P > 0.05$ ) across phases.

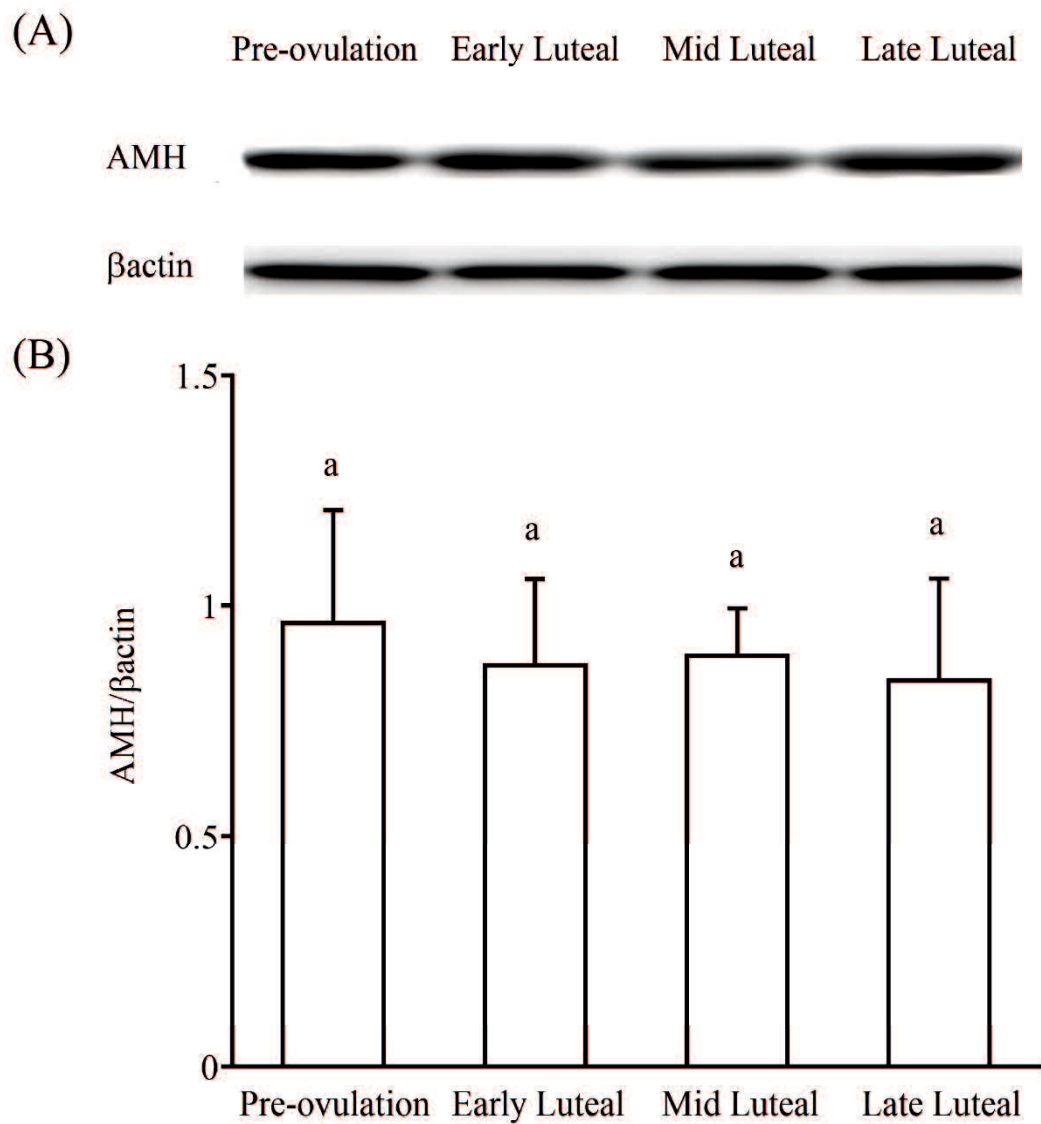


**Fig. 4.6.** (A) Representative AMH (as mature C-terminal form) and  $\beta$ -actin protein expression in bovine AP tissues obtained during the pre-ovulation, early luteal, mid luteal, or late luteal phases of estrous, as detected by western blotting. (B) AMH protein expression level of AMH normalized to that of  $\beta$ -actin in healthy post-pubertal heifer AP tissues obtained during pre-ovulation (n =5), early luteal (n =5), mid-luteal (n =6), and late luteal (n = 5) phases. The same letters indicate no significant differences ( $P > 0.05$ ) across phases.

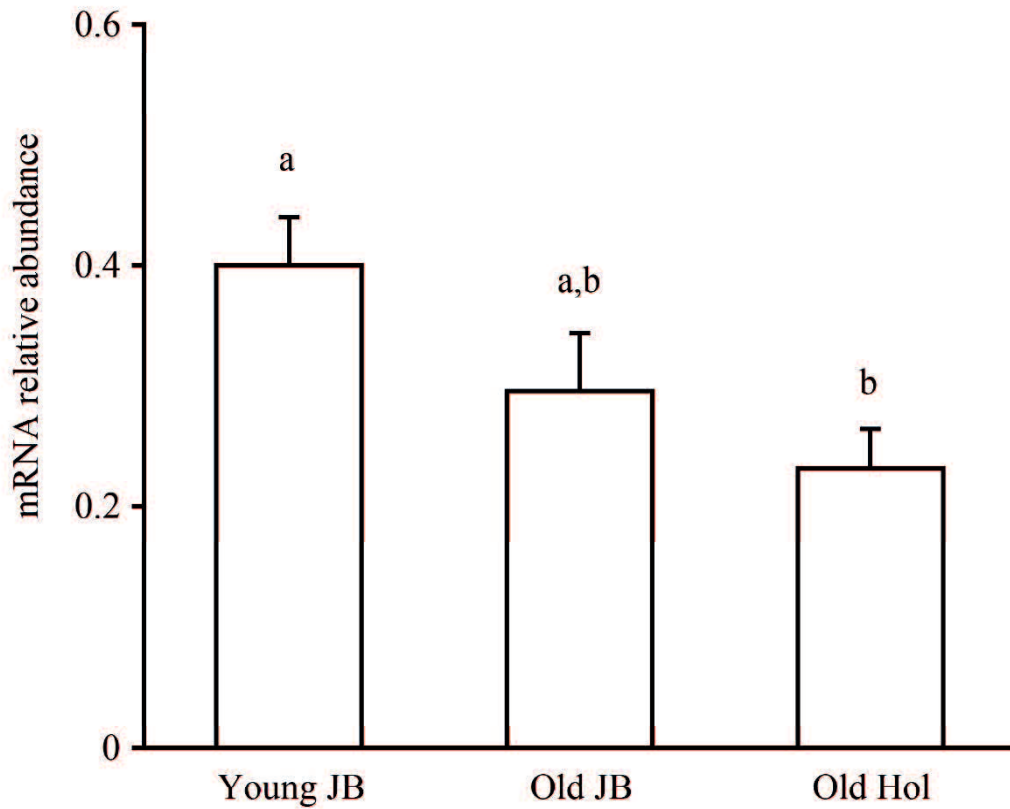


**Fig. 4.7.** Relative *AMH mRNA* levels (mean ± SEM) in bovine AP tissues obtained from healthy young Japanese heifers (young JB), old Japanese black cows (old JB), and old Holsteins cows (old Hol), as determined by real-time PCR. Data were normalized to the geometric means of *GAPDH* and *RANBP10* levels. Letters (a vs. b) indicate significant differences ( $P < 0.05$ ) among groups.

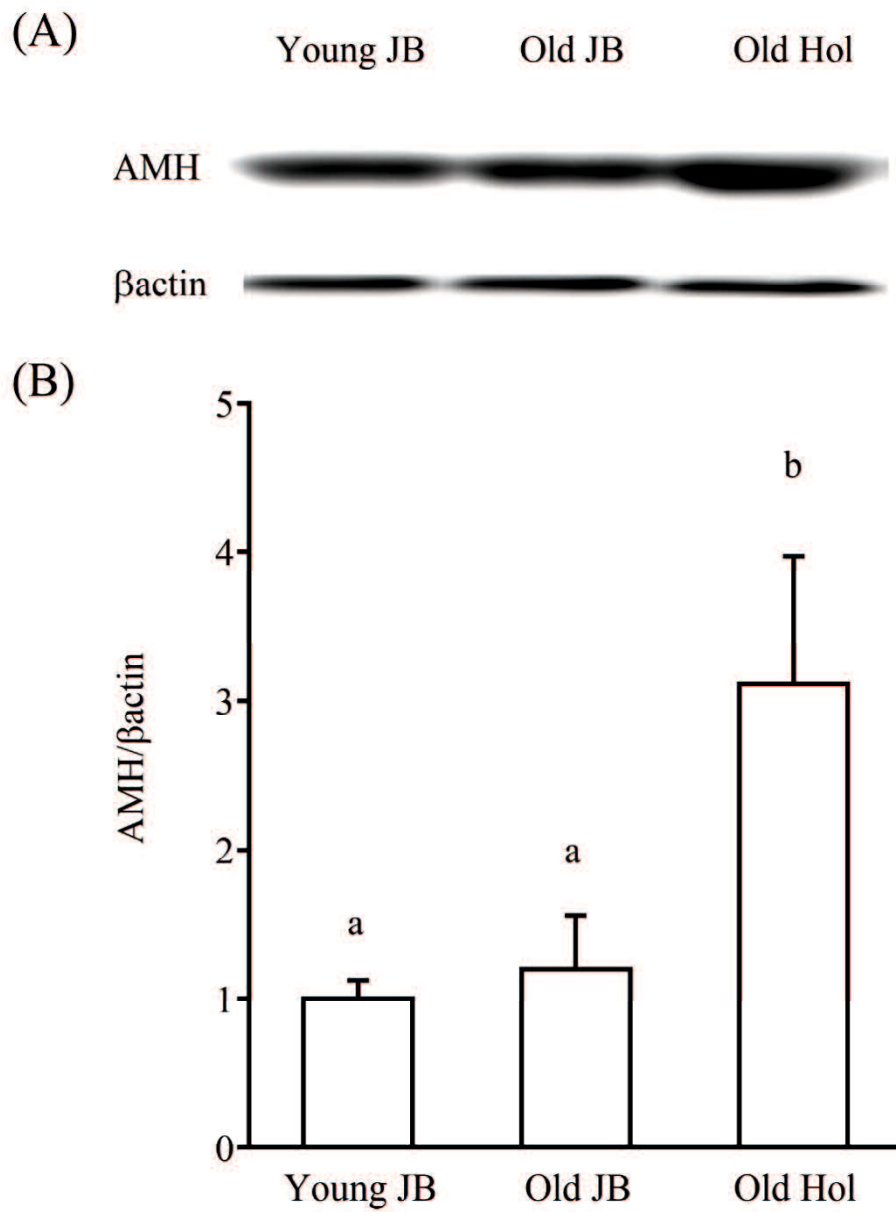


**Fig. 4.8.** (A) Representative AMH (in the mature C-terminal form) and  $\beta$ -actin protein expression in bovine AP tissues obtained from young JB, old JB, and old Hol. (B) Protein expression level of AMH normalized to that of  $\beta$ -actin in bovine AP tissues obtained from young JB, old JB, and old Hol. Letters (a vs. b) indicate significant differences ( $P < 0.05$ ) between groups.

#### 4.4. Discussion

The APs of tilapia express AMH but the specific cells expressing AMH are unclear (Poonlaphdecha *et al.* 2011). In this study I evaluated whether gonadotrophs expressing AMH. AMH activates the synthesis and secretion of gonadotropins from the gonadotrophs of rodents and bovines (Bédécarrats *et al.* 2003; Garrel *et al.* 2016; Kereilwe *et al.*, 2018). Therefore, the coordination of the endocrine, paracrine, and autocrine control of AMH may be important for normal reproductive functions, similar to GnRH, inhibin, and activin (Pagesy *et al.* 1992; Miller *et al.* 1996; Popovics *et al.* 2011).

Immunohistochemistry using an anti-AMH antibody has shown a strong signal in the granulosa cells of small antral follicles, which express *AMH* mRNA (Campbell *et al.* 2012), consistent with AMH expression in granulosa cells of ruminants (Rocha *et al.* 2016). Additionally, the band patterns observed by western blotting were similar to those of a previous study of AMH (Mamsen *et al.* 2015). Therefore, the anti-AMH antibody can be used for immunohistochemical analyses of bovine samples. Gonadotrophs are a heterogeneous cell population including LH and FSH monohormonal and bihormonal subsets in rats, equines, and bovines (Townsend *et al.* 2004; Pals *et al.* 2008; Kadokawa *et al.* 2014). My results showed that both LH $\beta$ -positive cells and FSH $\beta$ -positive cells express AMH, suggesting that AMH secreted from the three types of gonadotrophs have paracrine or autocrine roles.

Western blotting showed differences in band strength or size between APs and ovaries. The APs exhibited weaker bands for the AMH precursor (70 kDa) than those for ovary samples, suggesting that APs store less AMH precursor than ovaries. The band size for the mature C-terminal form was smaller for APs (20 kDa) than for ovaries (25 kDa). I did not observe a 25-kDa band in the AP lane or a 20-kDa band in the ovary

lane, even after longer exposure periods (data not shown). A potential explanation for the band size difference for the mature C-terminal form may be a difference in *O*-glycosylation among organs (Medzihradzky *et al.* 2015; Skaar *et al.* 2011).

AMH expressed by gonadotroph has not been evaluated previously in any species; accordingly, it was impossible to compare my data with the results of previous studies. The data showed that AMH expression at the mRNA and protein levels in APs differ between the young JB and old Hol groups. Jerseys have higher blood AMH concentrations than those of Holsteins (Ribeiro *et al.* 2014). Therefore, the difference in AMH expression in APs may be explained by a difference among breeds or any factor related to breed. The APs of the old Hol group expressed lower levels of *AMH* mRNA than those of the young JB group. In contrast, the APs of the old Hol group exhibited higher AMH protein levels than those of the young and old JB groups. However, the results for the effects of breed and age on AMH expression in APs should be interpreted with caution because we could not obtain APs from young Holsteins. Further studies are required to clarify whether AMH secretion from APs is decreased in old Hol and results in higher AMH protein levels within APs.

Koizumi and Kadokawa (2017) reported that old Japanese Black cows have significantly higher blood AMH concentrations (100 pg/mL) than those of young Japanese Black cows (1–10 pg/mL) throughout the postpartum period. However, I observed a small difference in AMH expression at the mRNA and protein levels in APs between the young and old JB groups in this study. Therefore, AMH secreted by the ovary, rather than AMH secreted by the AP, may explain the difference in blood AMH concentrations between young and old cows.

Previous studies have not detected significant changes in the blood AMH concentration during the estrous cycle in ruminants (Pfeiffer *et al.* 2014; Koizumi and

Kadokawa 2017; El-Sheikh Ali *et al.* 2013). My data also showed no significant changes in AMH at the mRNA and protein levels in APs during the estrous cycle. The 5'-flanking region of the bovine *AMH* gene does not contain ERE, half ERE, or PRE sequences. Therefore, AMH expression in APs, similar to the blood AMH concentration, is unlikely to change during the estrous cycle. In conclusion, bovine gonadotrophs express AMH, and the AMH expression may be breed-dependent. Further studies are needed to determine the precise effects of age and breed on AMH expression.

## **CHAPTER V**

**(Study III)**

**Anti-Müllerian hormone and its receptor is colocalized in  
the majority of gonadotropin-releasing-hormone cell bodies  
and fibers in heifer brains**

## Abstract

Circulating concentrations of AMH can indicate fertility in various animals, but the physiological mechanisms underlying the effect of AMH on fertility remain unknown. We recently discovered that AMH has extragonadal functions via its main receptor, AMHR2. Specifically, AMH stimulates the secretion of luteinizing hormone and follicle stimulating hormone from bovine gonadotrophs. Moreover, gonadotrophs themselves express AMH to exert paracrine/autocrine functions, and AMH can activate GnRH neurons in mice. This study aimed to evaluate whether AMH and AMHR2 are detected in areas of the brain relevant to neuroendocrine control of reproduction: the POA, ARC and ME and in particular within GnRH neurons. Reverse transcription-polymerase chain reaction detected both *AMH* and *AMHR2* mRNA in tissues containing POA as well as in those containing both ARC and ME, collected from post-pubertal heifers. Western blotting detected AMH and AMHR2 protein in the collected tissues. Triple fluorescence immunohistochemistry revealed that the majority of cell bodies or fibers of GnRH neurons were AMHR2-positive and AMH-positive, although some were negative. Immunohistochemistry revealed that 75 to 85% of cell bodies and fibers of GnRH neurons were positive for both AMH and AMHR2 in the POA, ARC, and both the internal and external zones of ME. The cell bodies of GnRH neurons were situated around other AMH-positive cell bodies or fibers of GnRH and non-GNRH neurons. The findings thus indicate that AMH and AMHR2 are detected in the majority of cell bodies or fibers of GnRH neurons in POA, ARC, or ME of heifer brains. These data support the need for further study as to how AMH and AMHR2 act within the hypothalamus to influence GnRH and gonadotropin secretion.

## 5.1. Introduction

The HPG axis drives reproduction and some of the most important components of the axis are the GnRH neurons (Herbison 2016; Nestor *et al.* 2018). GnRH neurons originate in the POA and ARC and project to the ME, the interface between the neural and peripheral endocrine systems, and secrete GnRH into the pituitary portal blood vessels (Clarke *et al.* 1987; Jansen *et al.* 1997). The secreted GnRH binds to the GnRH receptors on the lipid raft portion of the plasma membrane of gonadotrophs to stimulate the secretion of LH and FSH (Kadokawa *et al.* 2014). It is thus important to clarify mechanisms controlling GnRH neurons in the hypothalamus.

Plasma AMH concentrations can predict the fertility of adult female goats, ewes, cows, and women (Monniaux *et al.* 2012; Meczekalski *et al.* 2016; Mossa *et al.* 2017). Recent studies have revealed that AMH exerts extragonadal functions in the gonadotrophs of the anterior pituitaries. The main AMH receptor, AMHR2, colocalizes with GnRH receptors on the lipid raft of gonadotrophs (Kereilwe *et al.* 2018). Furthermore, AMH activates AMHR2 and thereby stimulates the synthesis and secretion of LH and FSH in the gonadotrophs of bovines and rodents (Kereilwe *et al.* 2018; Bédécarrats *et al.* 2003; Garrel *et al.* 2016). However, it remains unknown whether AMH and AMHR2 play any significant roles in the hypothalamus.

Little is known concerning the relationship between AMH and the brain. While the brains of adult tilapia express AMH, the localization of AMH expression in the brain remains unclarified (Poonlaphdecha *et al.* 2011). Another recent study found that GnRH neurons contain AMHR2 in various regions of female human and rodent brains, including the POA, ARC, and ME (Cinimo *et al.* 2016). Furthermore, both *in vivo* and *in vitro* studies have demonstrated that AMH potently activates GnRH neurons, and

consequently GnRH-dependent LH secretion in adult female mice (Cinimo *et al.* 2016). However, it remains unknown as to whether female mammalian brains-express AMH. Therefore, this study evaluated whether AMH and AMHR2 are detected in the POA, ARC, and ME of heifers, and especially within GnRH neurons.

## **5.2. Materials and Methods**

### **5.2.1. Antibodies used in this study**

Antibodies used for AMHR2 and AMH in this study were similar to those used in chapter III (study I; AMHR2) and chapter IV (study II; AMH).

We also used an anti-GnRH mouse monoclonal antibody (clone number GnRH I HU11B: sc-32292, Santa Cruz Biotechnology, Inc.) raised against a synthetic GnRH I decapeptide by Urbanski (1991). This antibody was used for immunohistochemistry to visualize GnRH neurons in rat and monkey (Naugle and Gore 2014; Naugle *et al.* 2016).

### **5.2.2. Brain and ovary sample collection**

I obtained brain samples from healthy, post-pubertal (26 months of age) non-lactating Japanese Black heifers managed by farmers in western Japan. The farms had open free stall barns with free access to water. The heifers were fed twice daily with a total mixed ration according to the Japanese feeding standard (Ministry of Agriculture 2008).

The heifers were slaughtered for harvesting beef according to the regulation of Ministry of Agriculture, Forestry and Fisheries of Japan. The heifers were in periestrus – i.e., -3 d to +4 d from estrus – as determined by macroscopic examination of the ovaries and uterus (Miyamoto *et al.* 2000). I used the samples (n = 5) obtained from the periestrus period for the following three reasons. First, there is no difference in GnRH immunoreactivity in the bovine POA, ARC, and ME between the periestrus and diestrus phases, however, while kisspeptin immunoreactivity in the bovine POA and ME does not differ between the periestrus and diestrus phases, it is higher in the periestrus phase than in the diestrus phase in the ARC (Tanco *et al.* 2016). Second, the promoter regions

of bovine AMH and AMHR2 genes lack the consensus response element for estrogen and progesterone (Kereilwe *et al.* 2018; Kereilwe and Kadokawa 2019). Third, there are no changes in AMH and AMHR2 expression in the anterior pituitary gland (Kereilwe *et al.* 2018; Kereilwe and Kadokawa 2019) or in blood AMH concentrations during the estrous cycle (Koizumi and Kadokawa 2017). I followed a method established by previous studies to collect brain block samples from cows to perform immunohistochemistry (Tanco *et al.* 2016). Briefly, blocks were dissected with the following margins: rostrally-rostral border of the optic chiasm; caudally-rostral to the mammillary bodies; lateral to the optic chiasm; and 0.5 cm dorsal to the third ventricle. I then followed previously reported methods (Hassaneen *et al.* 2016) for splitting the block into two parts by cutting rostral to the ME, yielding an anterior part containing the POA (POA block) and a posterior part containing the ARC and ME (ARC&ME block). Each block was stored in 4% paraformaldehyde at 4° C for 24 h. The fixed blocks were placed in a 20% sucrose solution at 4° C for 72 h. They were then stored in 30% sucrose solution at 4° C until the block sank – at least 48 h. Serial coronal sections were cut into 50 µm thick sections using a cryostat (CM1900, Leica Microsystems Pty Ltd.).

I obtained POA and ARC&ME tissue samples based on the bovine brain atlas (Leshin *et al.* 1988; Okamura 2002) using methods detailed in previous studies as shown in Fig. 5.1. Previous papers showing an atlas of bovine brain sections were used as a guide (Okamura 2002; Leshin *et al.* 1988). Briefly, sections were cut while monitoring (from both anterior and lateral views) the shape of the third ventricle and ventral or dorsal edge line, and the position and size of the anterior commissure, optic chiasm, mammillothalamic tract, or fornix. The selected POA tissues contained both anterior commissure or optic chiasm, and POA was medial or lateral to the third

ventricle, similar to Fig 8, 9 , and 10 in Okamura (2002) and Fig 2E and 2F in Leshin *et al.* (1988). The selected ARC&ME tissues contained fornix and ARC adjacent to both the evident infundibular recess of third ventricle and the median eminence which attached to infundibulum, the same as Fig. 18, 19, and 20 of the atlas of Okamura (2002) and Fig2E, F of another atlas Leshin *et al.* (1988). Every sixth section of the tissue was subjected to triple immunostaining for GnRH, AMH, and AMHR2. At least four sections—from the rostral end of the OVLT to the rostral edge of the hypothalamic paraventricular nucleus were used for the POA. At least four sections from the rostral edge of the dorsomedial hypothalamic nucleus to the rostral edge of the mammillary bodies were used for the ME and ARC. As performed in a previous study (Hassaneen *et al.* 2016), the sections were then stored in 25 mM PBS containing 50% glycerol, 250 mM sucrose, and 3.2 mM MgCl<sub>2</sub>•6H<sub>2</sub>O at -20°C until used for immunohistochemistry.

POA and ARC&ME tissue samples were also collected from other periestrus heifers (n = 5) to perform RT-PCR or western blotting. Both POA and ARC&ME blocks were cut at their midlines to obtain left and right sides. Using the bovine brain atlas (Okamura 2002; Leshin *et al.* 1988) as a reference, the blocks were further cut using their exterior shapes and the third or lateral ventricles as landmarks. Finally, the size of each tissue sample containing POA was less than 1 cm along its lateral axis; 2 cm along the rostrocaudal axis; and 3 cm along the vertical axis. The size of each tissue containing the ARC&ME was less than 1 cm along its lateral axis; 2 cm along the rostrocaudal axis; and 1 cm along the vertical axis. The POA and ARC&ME tissues were immediately frozen in liquid nitrogen and stored at -80° C until RNA or protein extraction.

Granulosa cells in preantral and small antral follicles express *AMH* (Campbell *et al.* 2012) and *AMHR2* mRNA (Poole *et al.* 2016). Therefore, I also collected ovary

tissue samples from the same heifers to use as a positive-controls for AMH and AMHR2 in the RT-PCR (n = 5) and western blotting (n = 5) analyses.

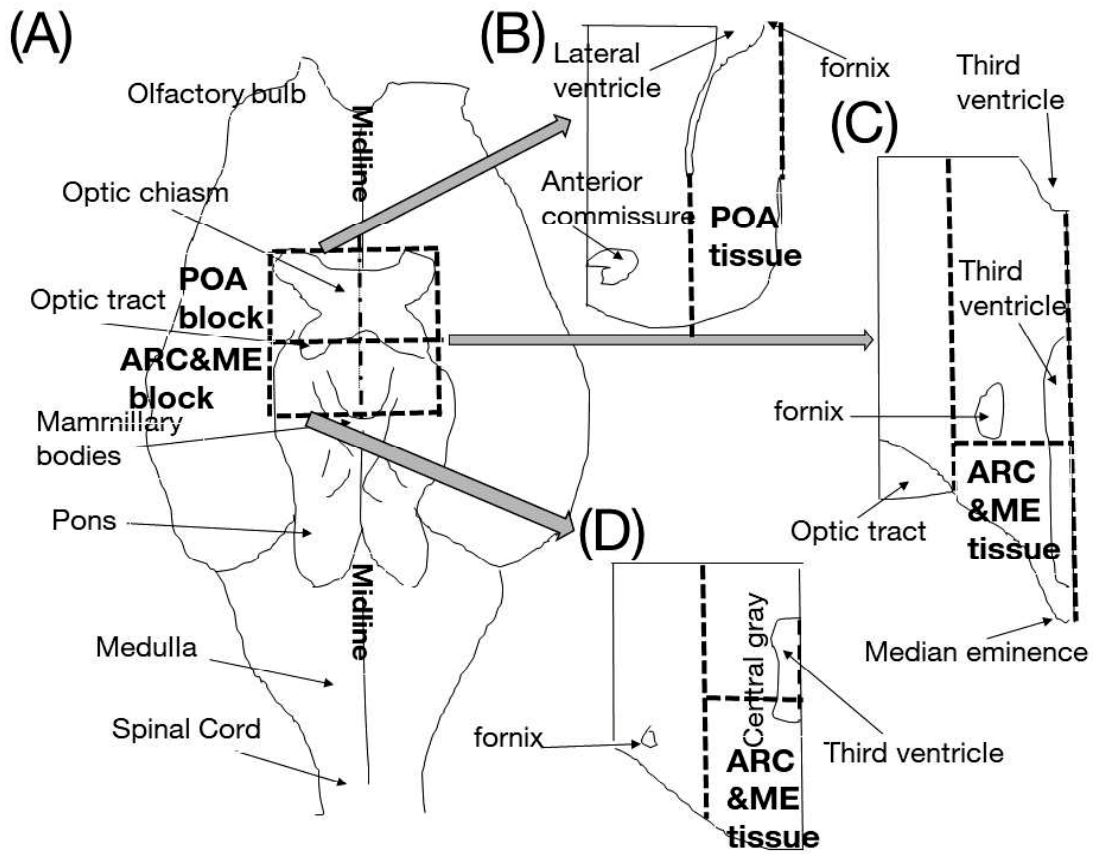


**Fig. 5.1.** Schematic illustration of brain tissue sampling from bovine brain to yield POA and ARC&ME blocks.

### **5.2.3. Western Blotting and RT-PCR for AMH or AMHR2 detection**

The western blotting and RT-PCR method described in chapter III was followed in this study to detect *AMH* or *AMHR2* mRNA in the POA tissue (n = 5) and ARC&ME tissue (n = 5). The expected PCR-product sizes of *AMH* and *AMHR2* using the primer pairs are 328 bp, and 320 bp, respectively. The primer pairs used in this study are listed in Table 5.1.

**Table 5.1.** Details concerning the primers used for PCR to detect mRNA of *AMH* and *AMHR2*.

Primer	5'-3'	Position	Product		
			size (bp)		
		Nucleotide	Exon		
<i>AMH</i>	up	GTCATCCCCGAGACATACC	1486-1505	5	328
	down	TTCCCGTGTTTAATGGGGCA	1794-1813	5	
<i>AMHR2</i>	up	AGATTTGCGACCTGACAGCAG	1272-1292	9-10	320
	down	CTTCCAGGCAGCAAAGTGAG	1572-1591	11	

#### **5.2.4. Fluorescent immunohistochemistry and confocal microscopy**

The frozen-stock POA or ARC&ME tissue was thawed and washed twice with PBS. Free-floating tissue sections were permeabilized with PBS containing 0.5% Tween 20 for 3 min. I then combined two quenching methods, glycine/hydrogen peroxide (Rosas-Arellano *et al.* 2016) and Vector True VIEW autofluorescence quenching kit (Vector Laboratories Inc.), because I observed tissue autofluorescence in a preliminary study. Briefly, the tissue was blocked with PBS containing 2% normal goat serum, 50 mM glycine, 0.05% Tween 20, 0.1% Triton X 100, and 0.1% BSA for 30 min (Rosas-Arellano *et al.* 2016). Subsequently Vector True VIEW autofluorescence quenching kit was employed following the manufacturer's protocol. After 5 min of incubation with the quencher kit, the sections were washed twice with PBS. The sections were then incubated with a cocktail of primary antibodies (anti-GnRH mouse, anti-AMH rabbit, and anti-AMHR2 chicken antibodies [all diluted as 1:1,000]) dissolved in PBS containing 10 mM glycine, 0.05% Tween 20, 0.1% Triton X 100, and 0.1% hydrogen peroxide at 4° C for 16 h. After the primary antibody incubation, the sections were washed twice with PBS and then incubated with a cocktail of fluorochrome-conjugated secondary antibodies (Alexa Fluor Alexa Fluor 488 goat anti-chicken IgG, Alexa Fluor 546 goat anti-mouse IgG, and Alexa Fluor 647 goat anti-rabbit IgG [all from Thermo Fisher Scientific and diluted to 1 µg/mL]) and 1 µg/mL of DAPI (Wako Pure Chemicals) for 4 h at room temperature. Each free-floating section was then transferred onto a slide glass (76 × 26 mm, Crest-adhesive glass slide, Matsunami-Glass) with the dorsal-ventral axis of the bovine brain section parallel to the long axis of slides. Cover glass (55 × 24 mm, Neo micro cover glass, Matsunami-Glass) was then attached using Vectashield hardset mounting medium (Vector Laboratories Inc.).

The sections were observed with a confocal microscope (LSM710; Carl Zeiss) equipped with a 405 nm diode laser, a 488 nm argon laser, a 533 nm HeNe laser, and a 633 nm HeNe laser. Images obtained by fluorescence microscopy were scanned with a 20× or 40× oil-immersion objective and recorded with a CCD camera system controlled by ZEN2012 black edition software (Carl Zeiss). GnRH, AMH, and AMHR2 localization were examined in confocal images of triple-immunolabeled specimens. To verify the specificity of the signals, I included several negative controls in which the primary antiserum had been omitted or pre-absorbed with 5 nM of the antigen peptide (Kereilwe *et al.* 2018; Kereilwe and Kadokawa 2019), or in which normal rabbit IgG (Wako Pure Chemicals) was used instead of the primary antibody.

The internal zone (iME; ventral to third ventricle) and the external zone of the ME (eME) were distinguished based on differences in fluorescence intensity. I defined various segments of neurons based on the following criteria: cell body is round or polygonal shape and diameter is more than 8 μm; axon is shown as a continuous line of immunopositive signal; varicosity is shown as a dotted line; bouton is shown as a single dot with a diameter more than 3 μm. In the POA, ARC, and iME, I decided on the presence of a fiber of neuron if the axon, or varicosity were observed in these areas; whereas the presence of a fiber of neuron was decided if axon, varicosity, or bouton were observed in the eME. GnRH neuron was specified if the neuron had a similar shape compared to the previous paper reporting bovine GnRH neuron (Leshin *et al.* 1988) and showed GnRH-positive signal (red color).

To evaluate colocalization, the GnRH signal was shown in red and either AMH or AMHR2 was shown in green. Therefore, yellow coloration in the images indicated colocalization of GnRH with AMH or AMHR2. The percentage of cell bodies or fibers of GnRH single-labeled neurons and the percentage of double/triple-labeled cell bodies

or fibers of neurons among all of the GnRH-positive cell bodies or fibers of neurons were determined in the POA, ARC, iME, or eME of five heifers. From each heifer, four sections containing the POA and four sections containing the anterior or intermediate part of the ARC, iME, and eME with a similar shape to those shown in Fig. 18 and 19 of the atlas (Okamura 2002) were analyzed.

Additionally, z-stacks of the optical sections of triple-labeled cell bodies in POA tissues or triple-labeled fibers in eME were captured using a confocal microscope system and transparent projection (i.e., the strongest and nearest colors to observer were shown). Images of the confocal microscope findings were generated using ZEN2012 black edition software (Carl Zeiss). To evaluate colocalization, the signals corresponding to AMHR2, GnRH, and AMH are depicted in green, red, and blue, respectively.

## 5.3 Results

### 5.3.1. Detection of AMH and AMHR2 mRNA in POA and ARC&ME tissues

The agarose gel electrophoresis yielded PCR products of the expected sizes, indicating that *AMH* (328 bp; Fig. 5.2A) and *AMHR2* (320 bp; Fig. 5.2B) were amplified from the POA and ARC&ME tissues. The same was found for the PCR products obtained from ovary tissues. Homology searching for the obtained sequences of amplified products in the gene databases revealed that the best match alignment was bovine *AMH* (NM\_173890.1) or bovine *AMHR2* (NM\_001205328.1). Both had a query coverage of 100%, an e-value of 0.0, and a maximum alignment identity of 99%. No other bovine gene was found to have homology with the obtained sequences of the amplified products, thus showing that the sequences of the amplified products were identical with the sequences of bovine *AMH* or *AMHR2*.

### 5.3.2. Detection of AMH and AMHR2 protein in POA and ARC&ME tissues

Western blotting confirmed the presence of AMH in the POA, ARC&ME, and ovary tissues, with differences in intensity among sample types (Fig. 5.3A). Unlike in the ovary samples, no bands for the AMH precursor (70 kDa) were detected in the POA or ARC&ME samples. Stronger bands for the mature C-terminal form were observed in the POA and ARC&ME samples than in the ovary samples, and differences in the number of bands were found between those of POA, ARC&ME (25 kDa and 20 kDa), and ovary (25 kDa only) samples. Figure 5.3A' shows representative  $\beta$ -actin bands for each sample.

Western blotting confirmed the presence of AMHR2 in POA, ARC&ME, and ovary tissues (Fig. 5.3B). While the anti-AMHR2 antibody revealed similar bands in

the three tissues, a few differences were noted. The full-length and cleaved monomers in the ovary appeared as a single band but appeared as a doublet in the POA. Figure 5.3B' shows representative  $\beta$ -actin bands for both tissue types.

### **5.3.3. Immunofluorescence analysis of AMH and AMHR2**

The triple fluorescence immunohistochemistry detected AMH, AMHR2, and GnRH in the POA and ARC&ME tissues. Figure 5.4 diagrammatically presents the distribution of GnRH-positive, AMH-positive or AMHR2-positive cell bodies and fibers. This drawn distribution represents a pattern typical to all heifers studied. The triple-positive (GnRH-positive, AMH-positive and AMHR2-positive) cell bodies and fibers (green in Fig. 5.4) were observed in distribution extending from the preoptic region to the hypothalamic area. GnRH neurons were shown as cell bodies with varicosities, or axons (CB1 and CB2 in Fig.5.5). The clusters of 2-10 cells were observed (Fig. 5.5 and 5.7).

In the preoptic region, the triple positive cell bodies were abundant in the anterior MPOA and anterior POA (Fig. 5.4A and B), but were less frequently observed in the posterior MPOA and POA (Fig. 5.4C). I observed that the majority of cell bodies and fibers of GnRH neurons were AMHR2-positive and AMH-positive (CB1, CB3-8, and CB10,11 in Fig.5.5). Figure 5.6. presents a transparent projection of the z-stack images of triple-stained cell bodies and fibers in the POA, with AMHR2, GnRH, and AMH depicted in green, red, and blue, respectively. The three colors were mixed in almost all areas. However, I also observed AMHR2-negative, AMH-negative cell bodies or fibers of GnRH neurons (CB2), as less frequently in the anterior MPOA and POA (red cross in Fig. 5.4A). Less frequently GnRH-negative AMHR2 cell bodies (CB9) were observed. The AMHR2-positive and AMH-positive cell bodies of GnRH neurons were

observed in close proximity (within 5  $\mu\text{m}$ ) to cell bodies of another GnRH neuron, as shown in CB2 and CB3, CB6 and CB7, and CB10 and CB11.

In the anterior ARC, we observed that all of the GnRH cell bodies were AMHR2-positive and AMH-positive (CB1-5 in Fig.5.7), although the triple positive cell bodies were only occasionally observed (Fig. 5.4D, 5.4E), and not in the posterior ARC (Fig. 5.4F). I observed that majority of GnRH fibers were AMHR2-positive and AMH-positive (Fig. 5.7A, 5.7C, 5.7D), although AMHR2-positive AMH-negative GnRH fibers (Fig.5.6B) were observed. The triple-positive cell bodies or fibers of neurons were observed in close proximity (within 5  $\mu\text{m}$ ) as shown in CB1 and CB2, and CB4 and CB5.

In the iME, I observed that the majority of fibers of GnRH neurons were AMHR2-positive and AMH-positive (low magnification of Fig. 5.8A, B, and Fig. 5.9A, yellow Vs in Enlarged 1, 2, 3), AMHR2-negative, AMH-negative varicosities of GnRH neurons (red Vs in Enlarged 2, 3) were observed. These fibers were observed in close proximity (within 5  $\mu\text{m}$ ), as shown (Enlarged 2, 3).

In the eME, it was observed that the majority of fibers of GnRH neurons were AMHR2-positive and AMH-positive (yellow arrows in Enlarged 1 and 2 in Fig. 5.9); I also observed AMHR2-negative, AMH-negative fibers of GnRH neurons (red arrows in Enlarged 2), and GnRH-negative fibers of AMH neurons (blue arrows in Enlarged 2). Figure 5.10. presents a transparent projection of the z-stack images of triple-stained fibers (Fig. 5.10A) and the terminal (Fig. 5.10B) in eME. AMHR2, GnRH, and AMH signals are depicted in green, red, and blue, respectively. These colors were mixed in almost all parts of the fibers, whereas, most areas of the terminal exhibited only GnRH and AMH staining.

Table 5.2 and Table 5.5 show the number of examined GnRH-positive, AMHR2-positive, or AMH-positive cell bodies and fibers in the POA, ARC, iME, or eME. As shown in Tables 5.3, 5.4 and 5.6, 75 to 85% of cell bodies and fibers of GnRH neurons are positive for both AMH and AMHR2 in the POA, ARC, and both the internal and external zones of ME.

**Table 5.2** Mean  $\pm$  SEM of the number of examined GnRH-positive, AMHR2-positive, or AMH-positive cell bodies (round or polygonal shape, diameter is more than 8  $\mu$ m) and fibers (axon shown as continuous line of immunopositive signal, or varicosity shown as dotted line) in the preoptic area.

	<b>POA cell body</b>		<b>POA fiber</b>	
	Mean	SEM	Mean	SEM
<b>GnRH+</b>	27.0	0.5	31.0	0.5
<b>AMHR2+</b>	30.6	0.4	30.6	0.5
<b>AMH+</b>	30.0	1.1	31.6	0.8

**Table 5.3** Mean  $\pm$  SEM of the percentage of GnRH cells that co-localize AMHR2 or AMH, the percentage of AMHR2 or AMH cells that co-localize GnRH in the POA

	<b>POA cell body</b>	
	Mean	SEM
<b>GnRH cells co-localize AMHR2</b>	87.5	1.4
<b>GnRH cells co-localize AMH</b>	78.7	1.8
<b>GnRH cells co-localize both AMHR2 and AMH</b>	78.7	1.8
<b>AMHR2 cells co-localize GnRH</b>	77.1	0.3
<b>AMH cells co-localize GnRH</b>	70.9	1.9

**Table 5.4** Mean  $\pm$  SEM of the percentage of GnRH fibers that co-localize AMHR2 or AMH, the percentage of AMHR2 or AMH fibers that co-localize GnRH in the POA.

	<b>POA fibers</b>	
	Mean	SEM
<b>GnRH fibers co-localize AMHR2</b>	82.8	3.0
<b>GnRH fibers co-localize AMH</b>	76.9	2.8
<b>GnRH fibers co-localize both AMHR2 and AMH</b>	76.9	2.8
<b>AMHR2 fibers co-localize GnRH</b>	83.6	0.3
<b>AMH fibers co-localize GnRH</b>	75.5	2.4

**Table 5.5** Mean  $\pm$  SEM of the number of examined GnRH-positive, AMHR2-positive, or AMH-positive fibers in the ARC or iME or eME.

	ARC		iME		eME	
	Mean	SEM	Mean	SEM	Mean	SEM
<b>GnRH+</b>	21.6	0.7	22.8	0.4	56.4	0.9
<b>AMHR2+</b>	21.6	0.8	24.4	0.8	54.0	1.9
<b>AMH+</b>	20.2	0.7	22.4	1.2	53.4	1.4

**Table 5.6** Mean  $\pm$  SEM of the percentage of GnRH fibers that co-localize AMHR2 or AMH, the percentage of AMHR2 or AMH fibers that co-localize GnRH in the ARC, iME, or eME.

	ARC		iME		eME	
	Mean	SEM	Mean	SEM	Mean	SEM
<b>GnRH fibers co-localize AMHR2</b>	84.2	1.9	83.3	1.7	86.2	3.5
<b>GnRH fibers co-localize AMH</b>	76.7	1.8	74.6	0.8	84.7	3.3
<b>GnRH fibers co-localize both AMHR2 and AMH</b>	76.7	1.8	74.6	0.8	84.7	3.3
<b>AMHR2 fibers co-localize GnRH</b>	84.3	2.1	78.3	3.7	89.9	1.7
<b>AMH fibers co-localize GnRH</b>	82.1	2.1	76.6	3.5	89.4	2.4

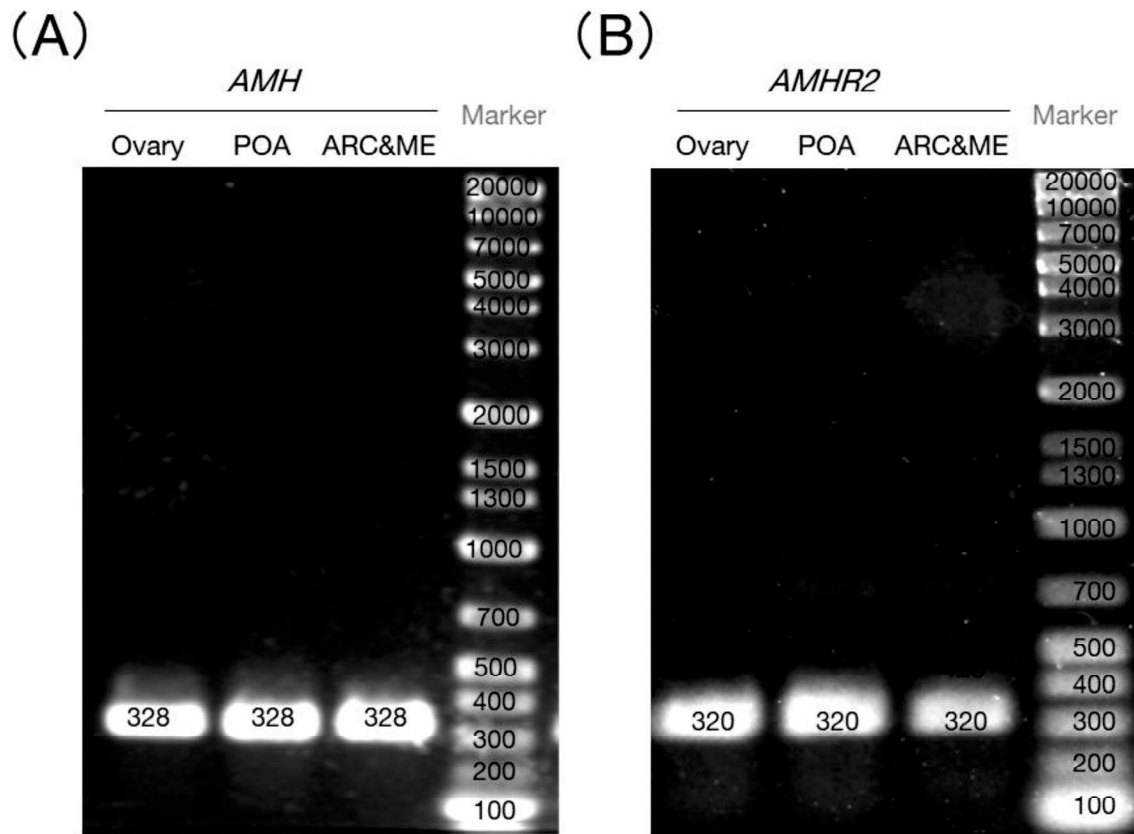


**Fig. 5.2.** Detection of *AMH* mRNA (A) and *AMHR2* mRNA (B) by RT-PCR. Electrophoresis of PCR-amplified DNA products using primers for bovine *AMH* or *AMHR2* and cDNA derived from the ovary, tissues containing the POA tissue or ARC&ME tissue of post-pubertal heifers. The lanes labeled as AMH or AMHR2 demonstrate that the sizes of the obtained DNA products met expectations: 328 or 320 bp, respectively. The Marker lane indicates the DNA marker.

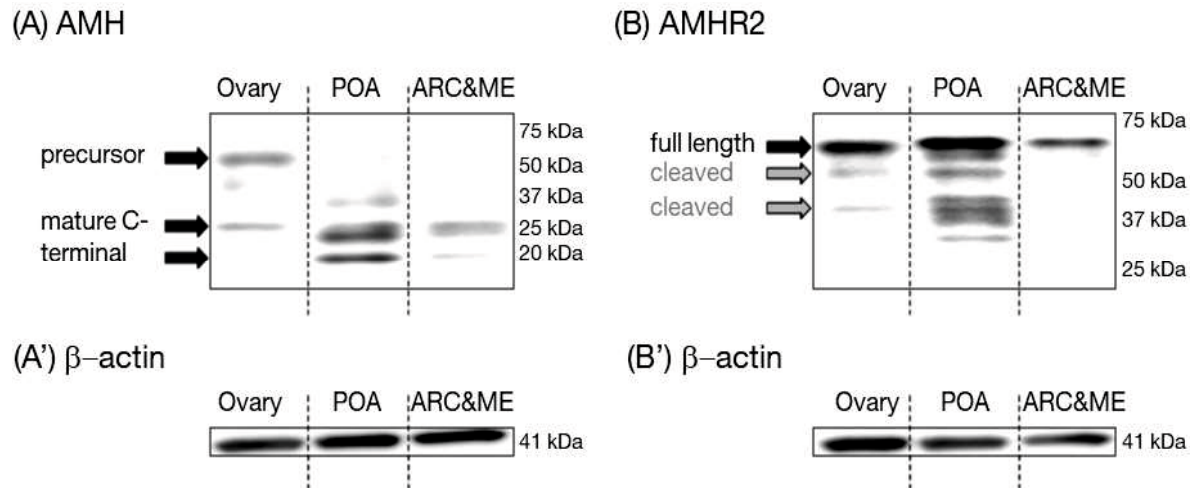


**Fig. 5.3.** Results of western blotting using extracts from the ovary, POA, or ARC&ME tissue of post-pubertal heifers and anti-AMH antibody (A), anti-AMHR2 antibody (B), or anti- $\beta$ -actin antibody (A' and B'). Bovine AMH bands were defined based on size as either precursors or mature C-terminal proteins. Bovine AMHR2 bands were defined based on size as either full-length or cleaved monomers.

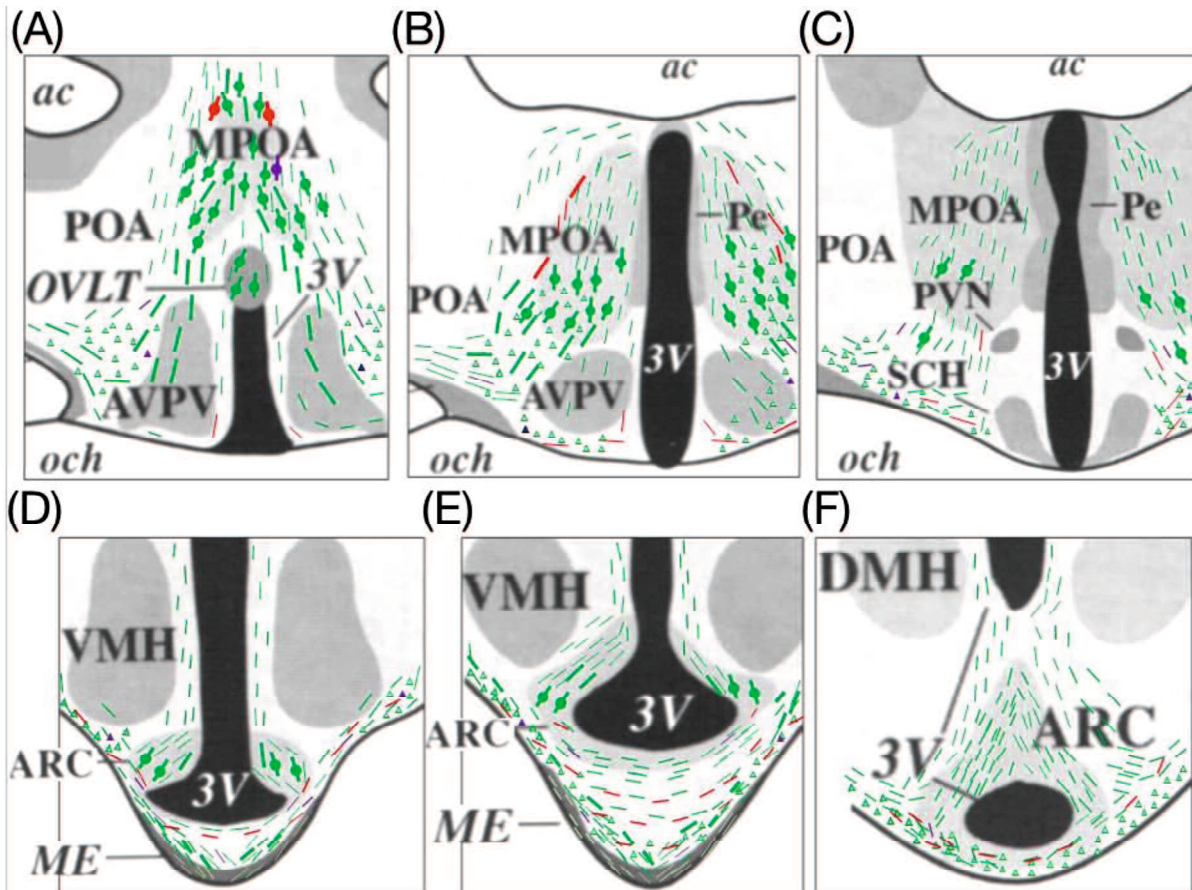


**Fig. 5.4.** Immunocytochemical distribution of GnRH, AMH and AMHR2 in coronal sections containing POA (A, B, C), or ARC and ME (D, E, F) drawn on the corresponding region of the bovine brain atlas (Okamura 2002). The crosses, lines, and triangles indicate cell body, and longitudinal and cross-section of fibers, respectively. The green ones indicate GnRH-positive, AMH-positive and AMHR2-positive (triple positive). The red ones indicate GnRH-positive AMH-negative and AMHR2-negative. The purple ones indicate lack of colocalization of AMH and GnRH.

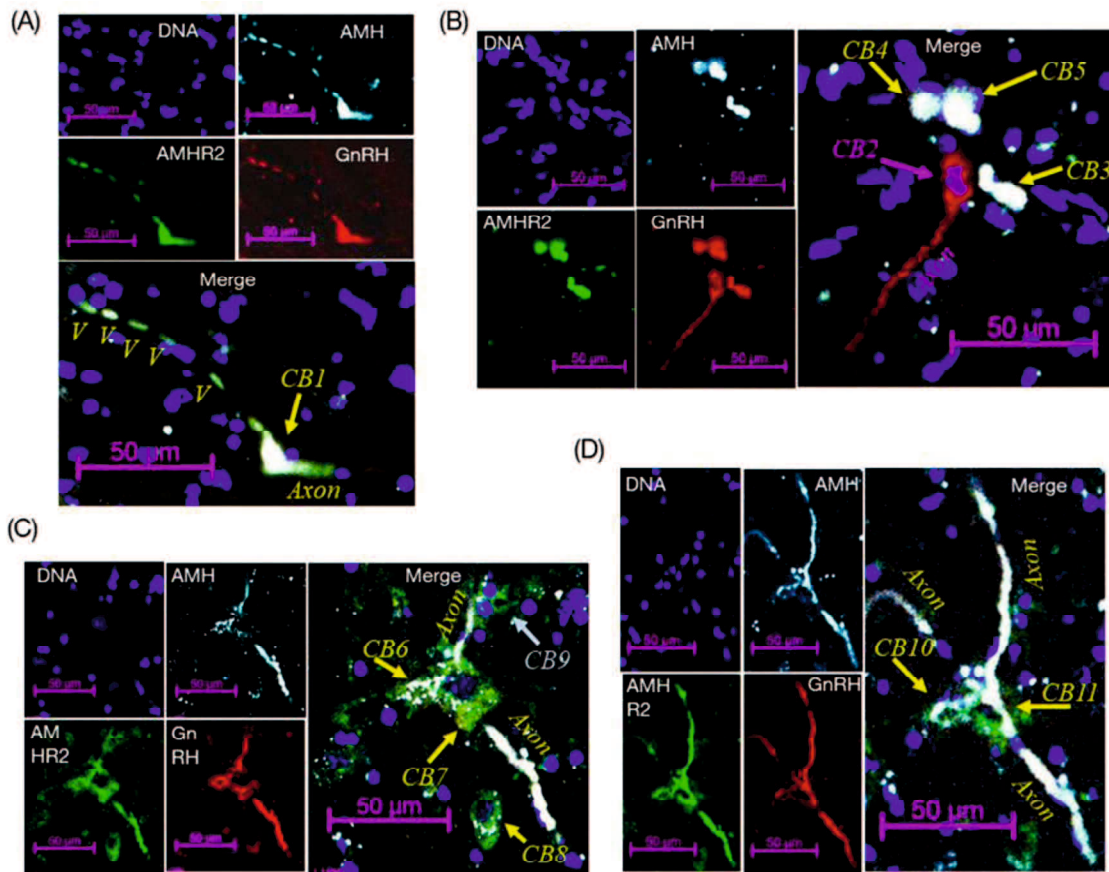


**Fig. 5.5.** Triple-fluorescence photomicrographs of AMH, AMHR2, and GnRH in the POA (A, B, C, D) of post-pubertal heifers. Images were captured with laser confocal microscopy for AMH (light blue), AMHR2 (green), and GnRH (red). In the merged photos, CB, Axon, V indicate cell body, axon, and varicosity of neuron. The yellow arrows, CB, Axon, and V indicate the colocalization of AMH, AMHR2, and GnRH. Light blue ones indicate lack of colocalization of AMH and GnRH. Red ones indicate lack of colocalization of GnRH and AMH or AMHR2. Scale bars are 50  $\mu$ m.

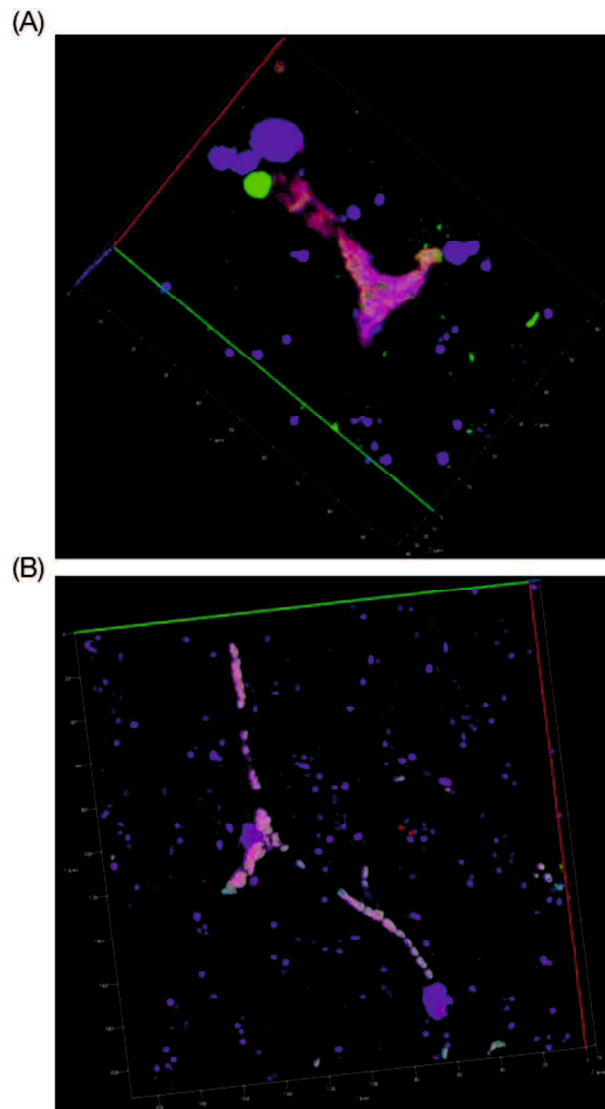


**Fig. 5.6.** Transparent projection of the z-stack images of triple-stained cell bodies and fibers in the POA (A, B) of post-pubertal heifers. The images were captured using a laser confocal microscope. AMH, AMHR2, and GnRH are depicted in blue, green, and red, respectively. Note that the color indicating DNA has been excluded because the large number of cell nuclei containing DNA would have masked the main objects.

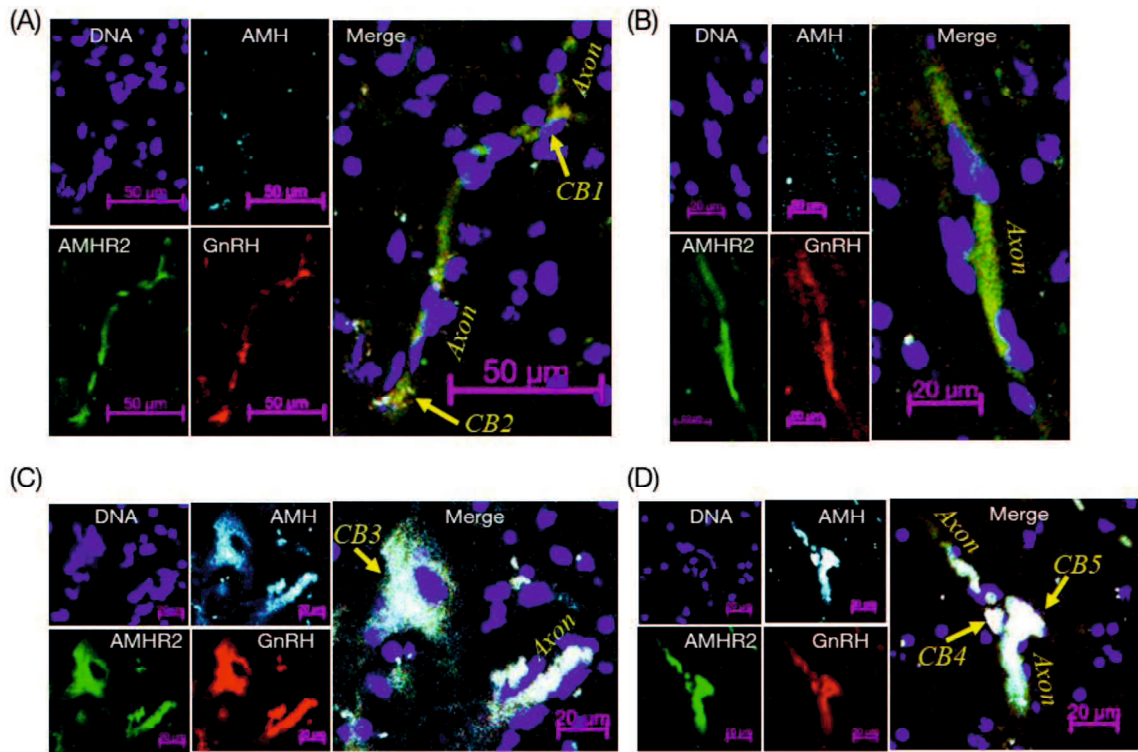


**Fig. 5.7.** Triple-fluorescence photomicrographs of ARC (A, B, C, D) tissue obtained from post-pubertal heifers. Images were captured with laser confocal microscopy for AMH (light blue), AMHR2 (green), and GnRH (red). In the merged photos, the yellow arrows CB, and Axon indicate the colocalization of AMH, AMHR2, and GnRH. Scale bars are 50  $\mu\text{m}$  (A) or 20  $\mu\text{m}$  (B, C, D).

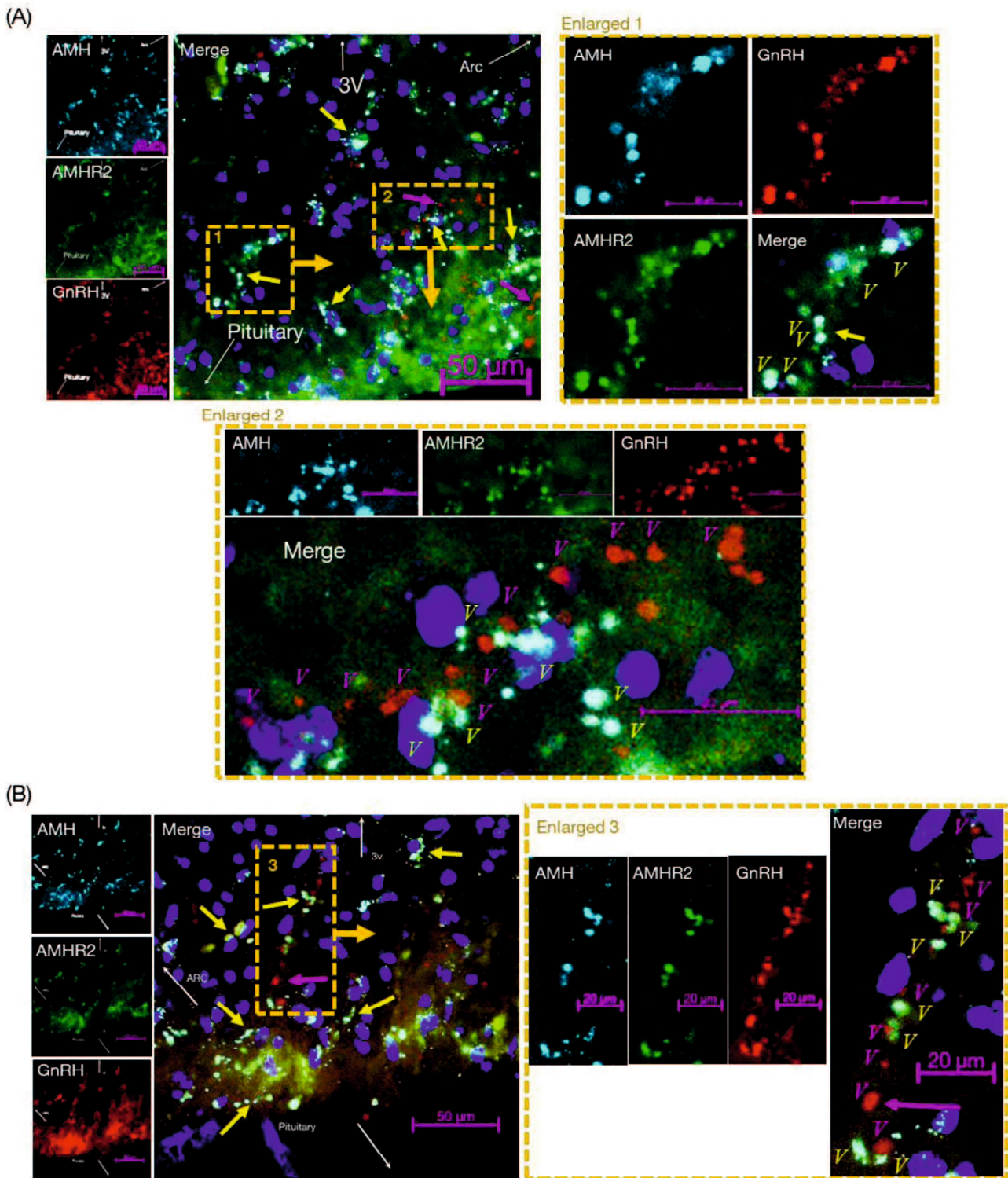


**Fig. 5.8.** Triple-fluorescence photomicrographs of ME (A, B) tissue obtained from post-pubertal heifers. Images were captured with laser confocal microscopy for AMH (light blue), AMHR2 (green), and GnRH (red). The orange rectangle within the low

magnification image indicates the position of high magnification. In the merged photos, the yellow arrows and V indicate the colocalization of AMH, AMHR2, and GnRH; the red arrows and V indicate the lack of colocalization of GnRH and AMH or AMHR2. Scale bars are 50  $\mu\text{m}$  in the low-magnification photos of (A, B), and 20  $\mu\text{m}$  in the high magnification photos of (A,B). White arrows labeled as 3V, Arc, or Pituitary indicate the direction of the third ventricle, arcuate nucleus, and pituitary, respectively.

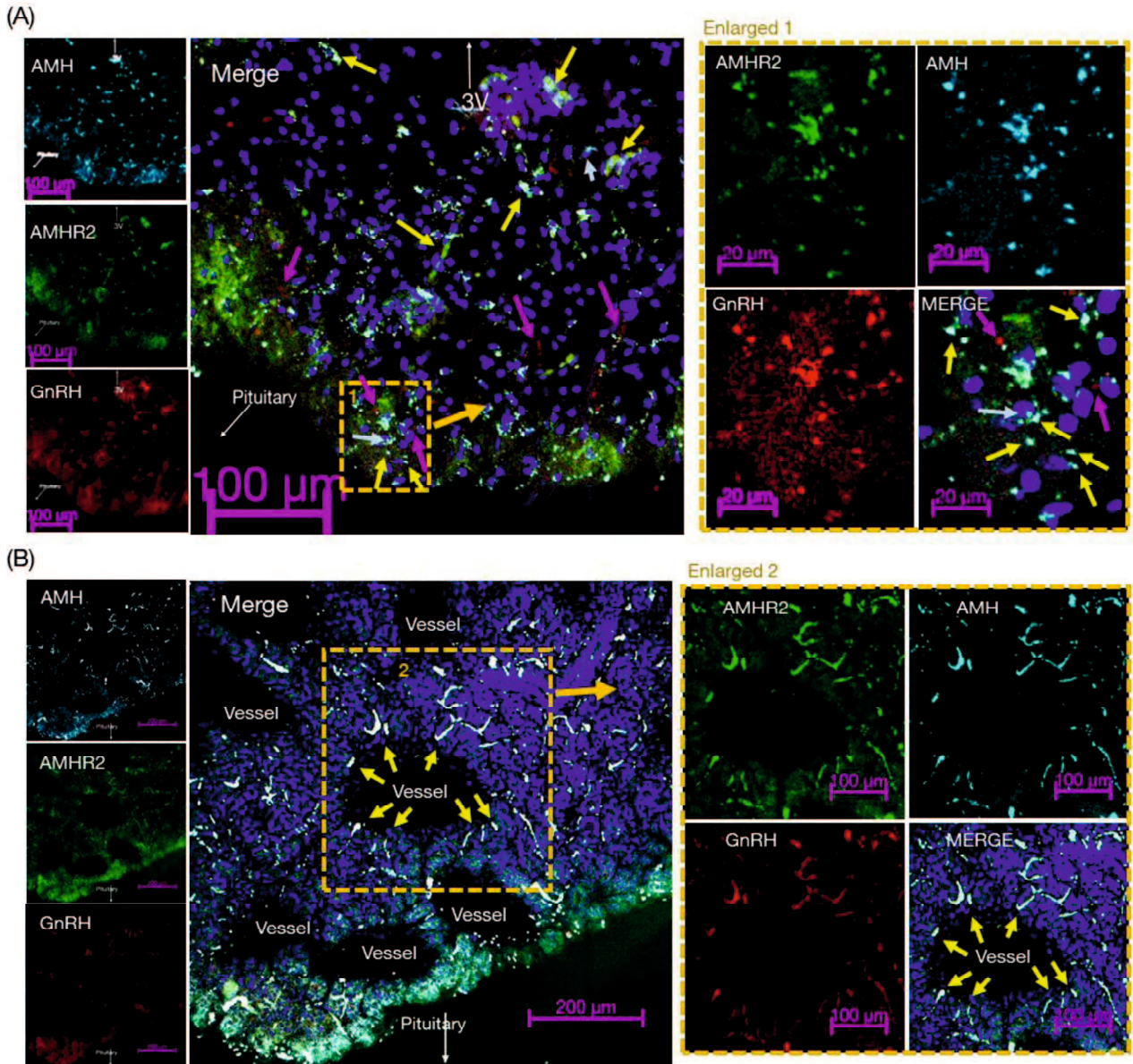


**Fig. 5.9.** Triple-fluorescence photomicrographs of other parts of ME (A, B) tissue obtained from post-pubertal heifers. Images were captured with laser confocal microscopy for AMH (light blue), AMHR2 (green), and GnRH (red). The orange rectangle within the low magnification image indicates the position of high magnification. Vessel indicate the position of vessel. In the merged photos, the yellow arrows indicate the colocalization of AMH, AMHR2, and GnRH; the light blue arrows indicate the lack of colocalization of AMH and GnRH; the red arrows and V indicate the lack of colocalization of GnRH and AMH or AMHR2. Scale bars are 100 μm in the

low-magnification photos of (A) and high-magnification photos of (B), 20  $\mu\text{m}$  in the high magnification photos of (A), and 200  $\mu\text{m}$  in the low-magnification photos of (B). White arrows labeled as 3V, or Pituitary indicate the direction of the third ventricle, and pituitary, respectively.

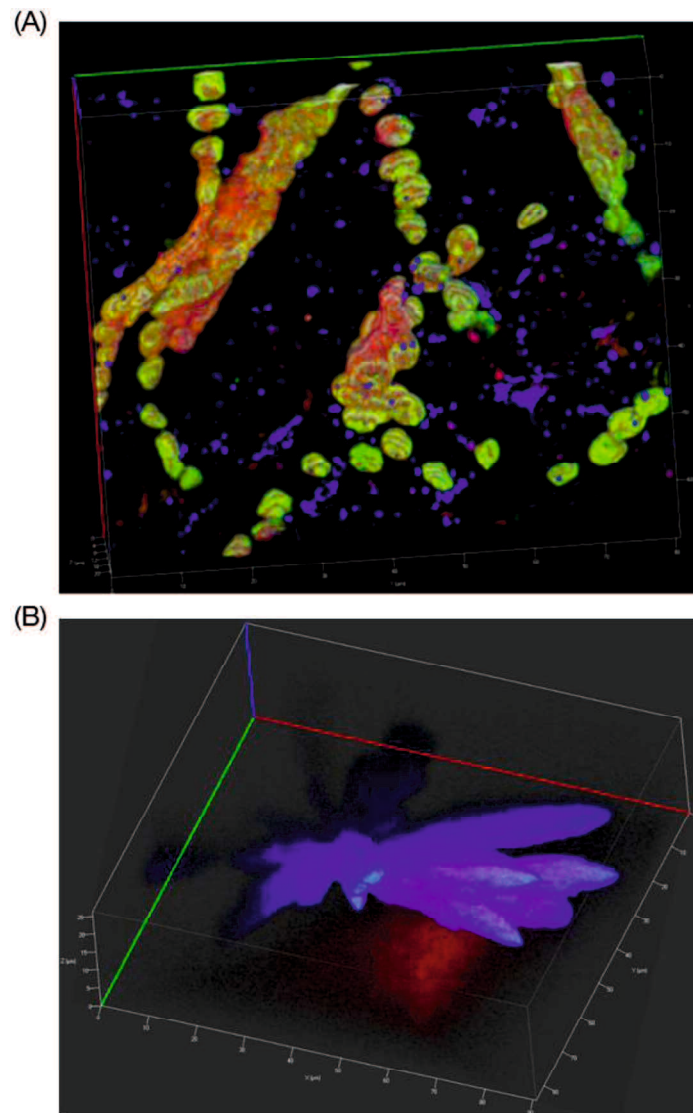


**Fig. 5.10.** Transparent projection of the z-stack images of triple-stained fibers (A) and terminal (B) in the eME of post-pubertal heifers. The images were captured using a laser confocal microscope. AMH, AMHR2, and GnRH are depicted in blue, green, and red, respectively. Note that the color indicative of DNA has been excluded because the large number of cell nuclei containing DNA would have masked the main objects.

#### 5.4. Discussion

This study detected AMH and AMHR2 in the bovine POA, ARC, and ME. This study is reporting AMH in the brains of mammals and AMHR2 in the brains of ruminants. The discovered AMH and AMHR2 in the POA, ARC, and ME warrant further exploration because their localization have significant implications for reproduction.

In the POA, ARC and ME, majority of cell bodies or fibers of GnRH neurons were AMHR2-positive and AMH-positive. Little is known of the relationship between AMH and GnRH neurons. However, Cimino *et al.* (2016) reported that (1) more than 50% of mouse and human GnRH neurons express AMHR2, and (2) AMH directly activates 50 to 64% of GnRH neurons in a dose-dependent manner in mice. The great majority of GnRH neurons (86%) form multiple close appositions with dendrites of other GnRH neurons, probably for GnRH neuron synchronization via the dendro-dendritic communication (Campbell *et al.* 2009). Therefore, AMH and AMHR2 in GnRH neurons might indeed be relevant to the regulation of GnRH secretion by direct actions on GnRH neurons. Further studies are required to clarify the importance of AMH and AMHR2 in the regulation of GnRH neurons.

GnRH neurons in the POA and ARC project to the ME and secrete GnRH into the pituitary portal blood vessels (Clarke *et al.* 1987; Jansen *et al.* 1997). Cimino *et al.* (2016) observed AMHR2 in the eME in mice and women. In addition, the present study found AMH signals in the bovine eME. Intracerebroventricular injection of AMH induces a LH surge within 15 min in mice (Cimino *et al.* 2016). AMHR2 is expressed in bovine gonadotrophs, and AMH can stimulate LH and FSH secretion from the

cultured bovine gonadotrophs (Kereilwe *et al.* 2018). Therefore, AMH may be secreted into the pituitary portal blood to stimulate LH and FSH secretion from gonadotrophs.

There is one caveat to this study that should be considered: both the POA and ARC&ME specimens also contained other brain areas and nuclei because it was impossible to obtain precisely cut samples under these experimental conditions. However, western blotting conducted in the present study showed differences in band strength and/or size between brains and ovaries. Unlike findings obtained from ovary samples, the POA and ARC&ME exhibited no bands that indicated the presence of the AMH precursor (70 kDa), suggesting that cells in POA and ARC&ME store fewer AMH precursors than do ovaries. Two bands for the mature C-terminal form were observed in the POA and ARC&ME, whereas only a single band was observed in the ovary (25 kDa). The band-size variances in the mature C-terminal band may be ascribed to differences in O-glycosylation among organs (Medzihradzky *et al.* 2015; Skaar *et al.* 2011). Western blotting also revealed multiple, not single, bands of AMHR2, which has been reported previously. This may be explained by AMHR2 presenting as a dimer, full-length monomer, and cleaved monomers, and by AMHR2 having O-glycosylation (Faure *et al.* 1996; Di Clemente *et al.* 2010). I observed that full-length and cleaved monomers in the POA appeared as doublets, whereas those in the ovary appeared as single bands. Therefore, this study suggests that bovine AMHR2 is glycosylated and that the difference in the number of full-length monomers between the POA and ovary samples might be attributed to differences in glycosylation.

AMHR2 positive non-GnRH cells were observed in the POA, ARC, and ME. I could not find any related published data with which to compare these findings. Therefore, further studies are required to characterize this type of neuron, specifically, whether AMHR2 is expressed in kisspeptin, neurokinin B, dynorphin neurons of the

ARC (Nestor *et al.* 2018). AMH signals were observed in non-GnRH cells in the eME. The localization of AMH in the eME has not been previously examined in any species. Approximately 20% of AMHR2-positive cells are non-gonadotrophs in the bovine anterior pituitary (Kereilwe *et al.* 2018), and such cells may be lactotrophs (Georgopoulos *et al.* 2013). Further studies are required to evaluate the relationship between AMH in the eME and non-gonadotroph anterior pituitary cells.

In conclusion, AMH and AMHR2 are detected in the majority of GnRH neurons in POA, ARC, and ME of heifer brains. These data support the need for further study as to how AMH and AMHR2 act within the hypothalamus to influence GnRH and gonadotropin secretion.

**CHAPTER VI**

**(Study IV)**

**Decreased anti-Müllerian hormone and anti-Müllerian hormone receptor type 2  
in Hypothalami of Old Cows**

## Abstract

Cow fertility decreases with age, but the hypothalamic pathomechanisms are not understood. AMH stimulates GnRH neurons via AMHR2, and most GnRH neurons in the POA, ARC and ME express AMH and AMHR2. Therefore, I hypothesized that both protein amounts would differ in the anterior hypothalamus (containing the POA) and posterior hypothalamus (containing the ARC and ME) between young post-pubertal heifers and old cows. Western blot analysis showed lower ( $P < 0.05$ ) expressions of AMH and AMHR2 in the posterior hypothalamus, but not in the anterior hypothalamus, of old Japanese Black and old Holstein cows compared to young Japanese Black heifers. Therefore, AMH and AMHR2 were decreased in the posterior hypothalami of old cows.

## 6.1. Introduction

Fertility decreases during aging in human and bovine females (Osoro and Wright 1992; Scheffer *et al.* 2018), but the exact pathophysiological mechanisms in the hypothalamus are not clarified yet. Plasma AMH concentrations can predict the fertility of adult female goats, ewes, cows, and women (Meczekalski *et al.* 2016; Monniaux *et al.* 2012). In the chapters III and IV, I discovered the extragonadal functions of AMH mediated by AMHR2. AMHR2 colocalizes with GnRHR on the lipid rafts of gonadotrophs and AMH stimulates the secretion of LH and FSH from bovine gonadotrophs. Moreover, GnRH neurons in the areas of the brain relevant to neuroendocrine control of reproduction [in the POA, ARC and ME] in humans and rodents were reported to express AMHR2 (Cimino *et al.* 2016). Additionally, in chapter V, I reported that 75-85% of cell bodies and fibers of GnRH neurons are positive for both AMH and AMHR2 in the POA, ARC, and the internal and external zones of the ME. Furthermore, AMH strongly activates GnRH neurons in adult female mice both *in vivo* and *in vitro* (Cimino *et al.* 2016), and AMHR2-deficient mice showed abnormal development and function of GnRH neurons, which resulted in reduced fertility (Malone *et al.* 2019). These data suggest that AMH and AMHR2 have important roles in the brain areas controlling reproductive functions. Therefore, in this study, I hypothesized that the levels of AMH and AMHR2 in the anterior hypothalamus (containing the POA; hereby referred to as POA tissue) as well as the posterior hypothalamus (containing the ARC and ME; hereby referred to as ARC&ME tissue) would differ between young post-pubertal heifers and old cows.

## **6.2. Materials and methods**

Sample collection and western blotting were performed as described in the chapters III, IV and V. The antibodies used in this study are the same one used in chapter III and IV. Statistical analysis was also done as described in the previous chapters.

### 6.3. Results

Figures 6.1A, 6.2A, 6.3A, and 6.4A show representative immunoreactive protein bands for AMH (25 kDa), AMHR2 (70 kDa), and  $\beta$ -actin (41 kDa) in the POA and ARC&ME tissues of Japanese black young heifers (young JB), old Japanese black cows (old JB) and old Holstein cows (old Hol) groups. AMH and AMHR2 protein levels in POA tissue were not different (Fig. 6.1B and Fig. 6.3B) between young and old groups. In contrast, AMH and AMHR2 protein levels in ARC&ME tissue in the Japanese black young heifers group were higher than those in the old Japanese black cows and old Holstein cows groups ( $P < 0.05$ ; Figs. 6.2B and 6.4B).

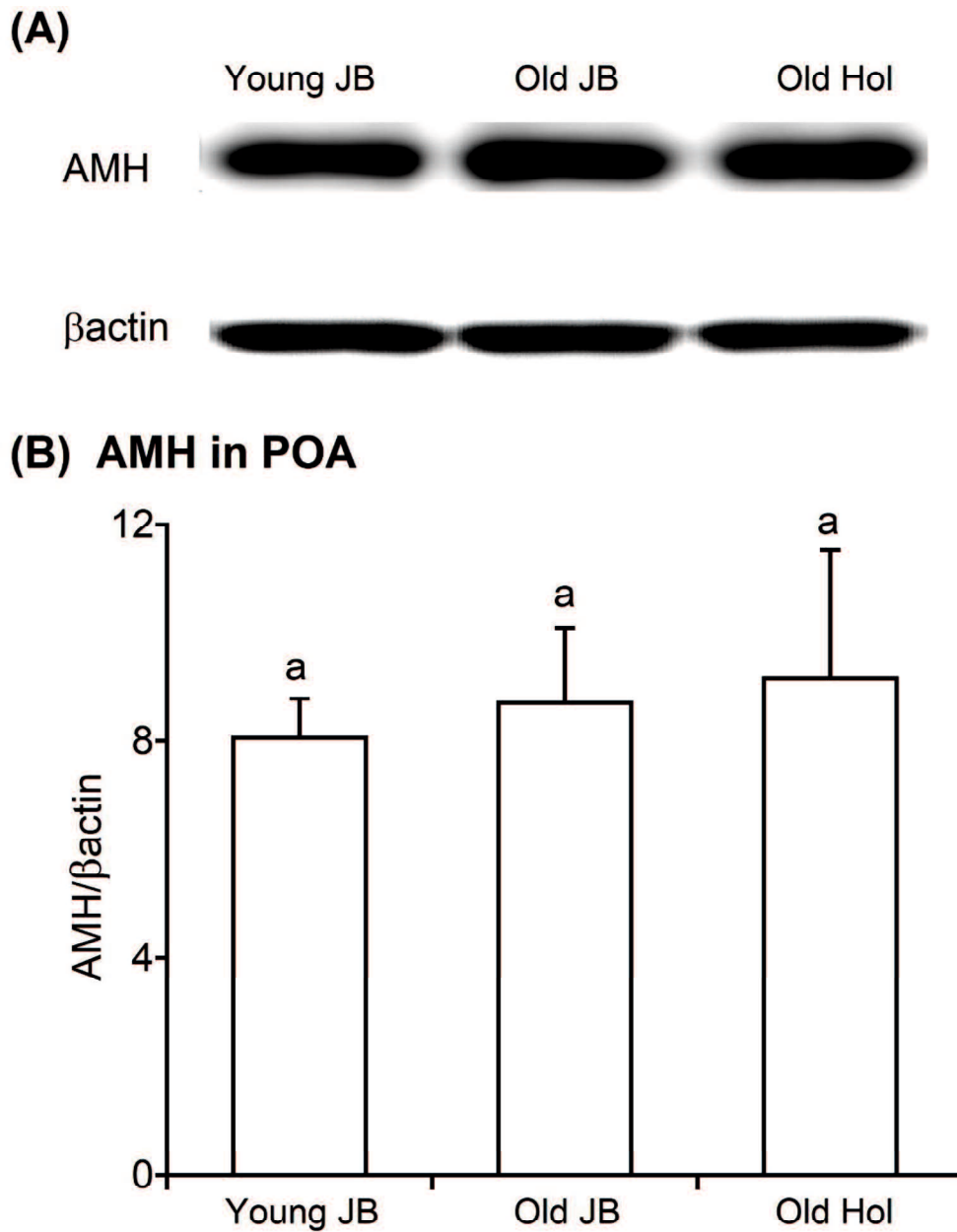


**Fig. 6.1.** Representative AMH (in mature C-terminal form) and  $\beta$ -actin immunoreactive protein bands in POA tissues (A) obtained from Japanese black young heifers (young JB), old Japanese black cows (old JB) and old Holstein cows (old Hol). Comparison of AMH protein expression normalized to that of  $\beta$ -actin ( $n=5$  per group) in POA (B). Same letters indicate no significant differences ( $P>0.05$ ) among groups.

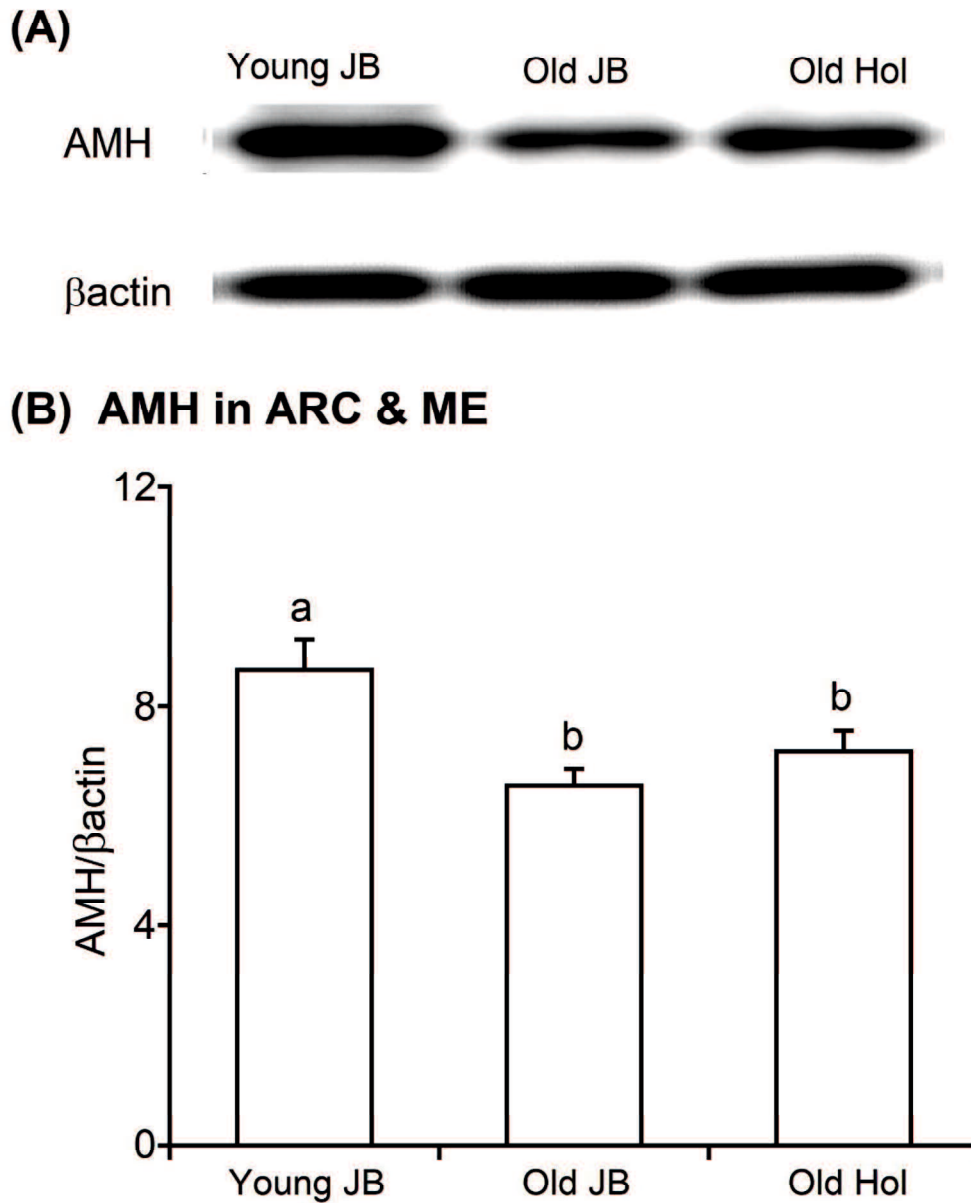
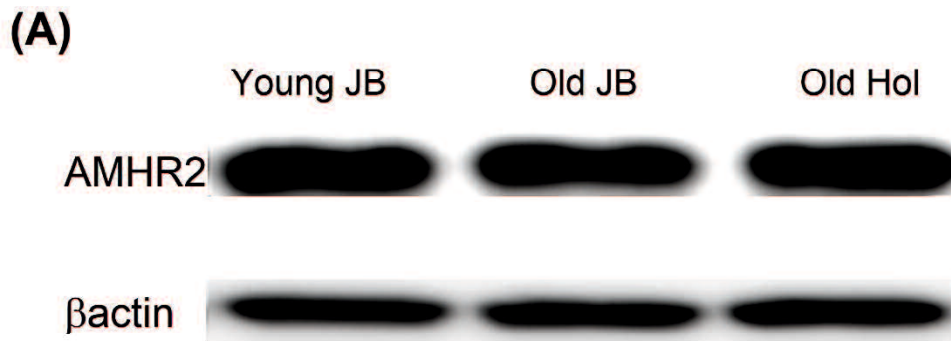


**Fig. 6.2.** Representative AMH (in mature C-terminal form) and  $\beta$ -actin immunoreactive protein bands in ARC&ME tissues (A) obtained from young JB, old JB, and old Hol. Comparison of AMH protein expression normalized to that of  $\beta$ -actin ( $n=5$  per group) in ARC&ME (B). Letters (a vs. b) indicate significant differences ( $P<0.05$ ) between groups.



**(B) AMHR2 in POA**

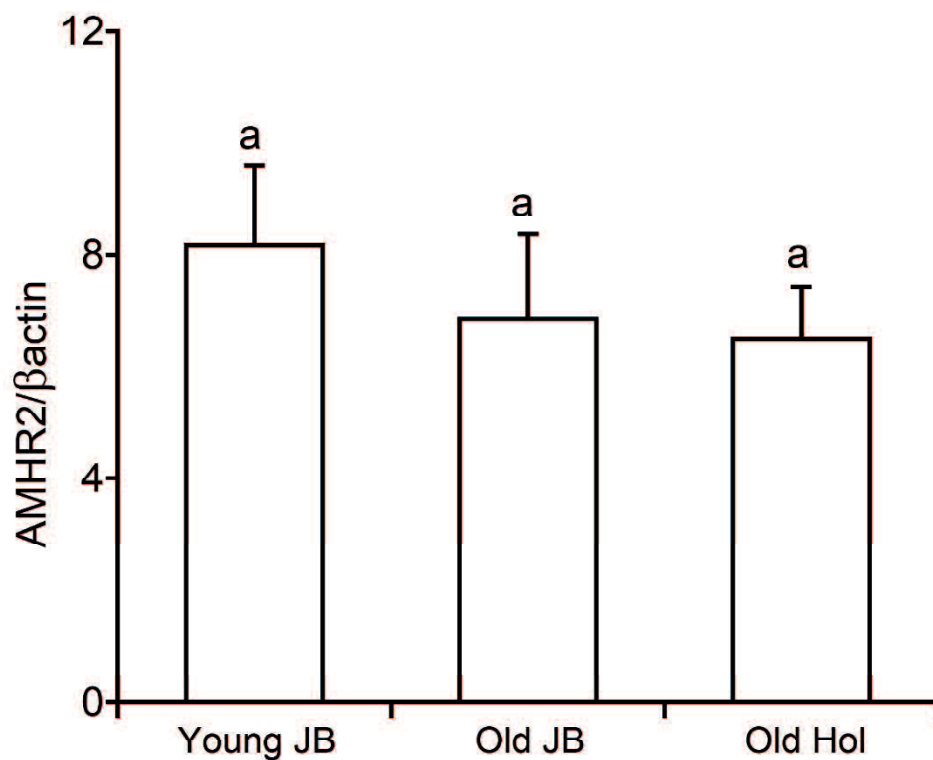
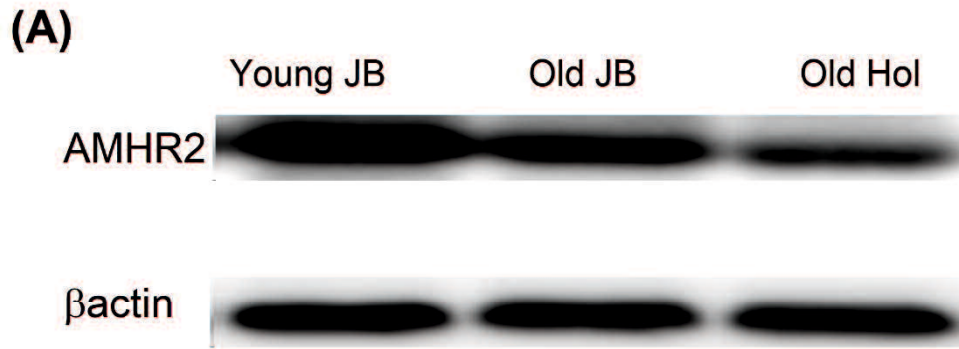


**Fig. 6.3.** Representative AMHR2 (in full length monomer form) and  $\beta$ -actin immunoreactive protein bands in POA tissues (A) obtained from young JB, old JB, and old Hol. Comparison of AMHR2 protein expression normalized to that of  $\beta$ -actin ( $n=5$  per group) in POA (B). Same letters indicate no significant differences ( $P > 0.05$ ) among groups.



**(B) AMHR2 in ARC & ME**

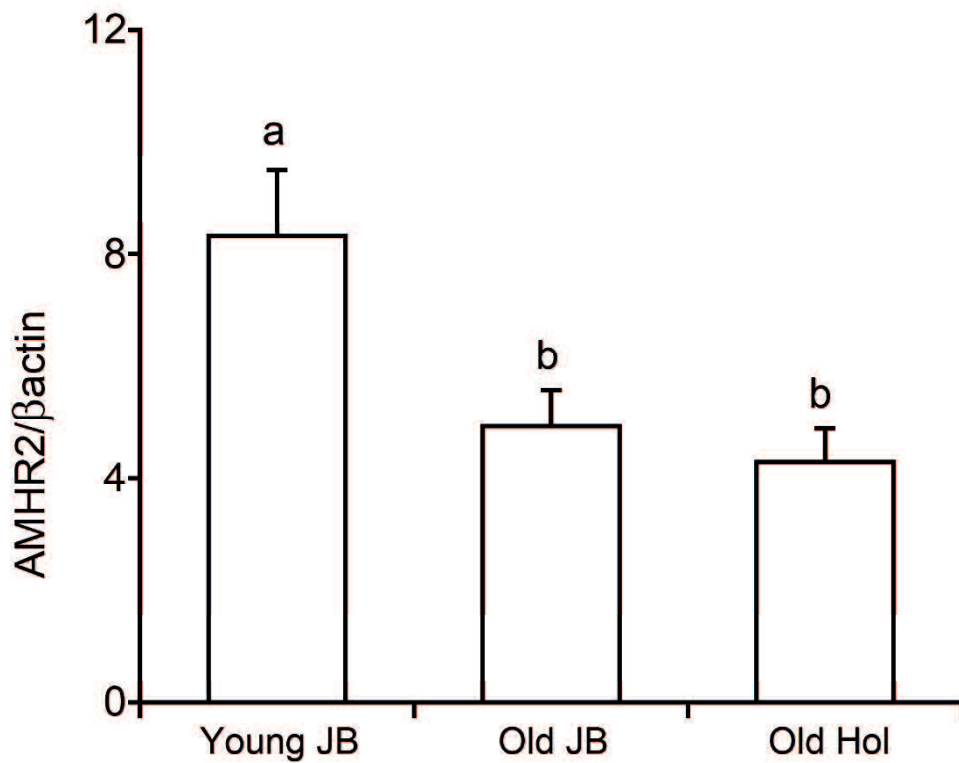


**Fig. 6.4.** Representative AMHR2 (in full length monomer form) and  $\beta$ -actin immunoreactive protein bands in ARC&ME tissues (A) obtained from young JB, old JB, and old Hol. Comparison of AMHR2 protein expression normalized to that of  $\beta$ -actin ( $n=5$  per group) in ARC&ME (B). Letters (a vs. b) indicate significant differences ( $P<0.05$ ) between groups.

#### 6.4. APPENDIX

We could not perform RT-qPCR for evaluating differences in *AMH* and *AMHR2* mRNA expression, because there were no appropriate steadily expressed housekeeping genes in the brain until recent (Bond *et al.* 2002). Recently, two stably expressed housekeeping genes, *YWHAZ* and *SDHA*, have been detected in ovine hypothalamus (Ciechanowska, *et al.* 2018). Also we confirmed individual differences of *YWHAZ* and *SDHA* were small in our RNA-seq data in bovine hypothalamus (unpublished). Therefore, we tried to do RT-qPCR for evaluating differences in *AMH* and *AMHR2* mRNA expression in hypothalamus to compare between young and old JB, although we could not obtain old Hol samaples.

Sample collection, RNA extraction, synthesis of cDNA and realtime PCR were carried out as described in the previous chapters using the same primers for *AMHR2* and *AMH* as in chapter III and IV respectively. In this study I used tyrosine 3-monooxygenase/tryptophan 5-monooxygenase activation protein zeta (*YWHAZ*; NCBI reference sequence, NM\_174814.2) and succinate dehydrogenase complex flavoprotein subunit A (*SDHA*; NCBI reference sequence, NM\_174178.2). Details of primers are provided online in Table 6.1.

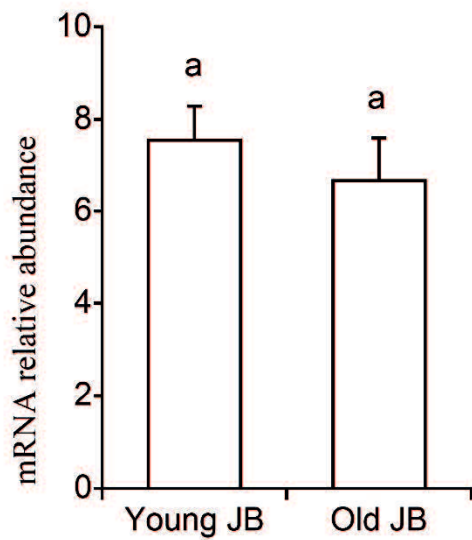
The expression of *AMH* and *AMHR2* was normalised against the geometric mean of the expression of two house-keeping genes *YWHAZ* and *SDHA*. The two housekeeping genes were reported for ewe's hypothalamus (Ciechanowska *et al.* 2018) and presented 100% homology with the respective bovine genes.

*AMH* and *AMHR2* mRNA levels in POA tissue were not different between young and old JB (Fig. 6.5A and 6.6A). In contrast, *AMH* and *AMHR2* mRNA levels in ARC&ME tissue in the JB young heifers group were higher than those in the old JB cows ( $P<0.05$ ; Fig. 6.5B and 6.6B).

**Table 6.1** Name, accession number, and details of the primers used for RT-qPCRs

Gene name	Accession number	Primer	Sequence 5'-3'	Size (bp)
<i>YWHAZ</i>	NM_174814.2	Forward	AGACGGAAGGTGCTGAGAAA	123
	Exon 2 3	Reverse	CGTTGGGGATCAAGAACTTT	
<i>SDHA</i>	NM_174178.2	Forward	CATCCACTACATGACGGAGCA	90
	Exon 5 5	Reverse	ATCTTGCCATCTTCAGTTCTGCTA	
<i>AMH</i>	NM_173890	Forward	GGGTTAGCCCTTACCCTGC	121
	Exon 3 4	Reverse	GTAACAGGGCTGGGGTCTTT	
<i>AMHR2</i>	NM_001205328	Forward	TGGGAGATTATGAGTCGCTGC	52
	Exon 9 10	Reverse	GTGGTGGTCTGCTGTCAGGT	

**(A) AMH in POA**



**(B) AMH in ARC & ME**

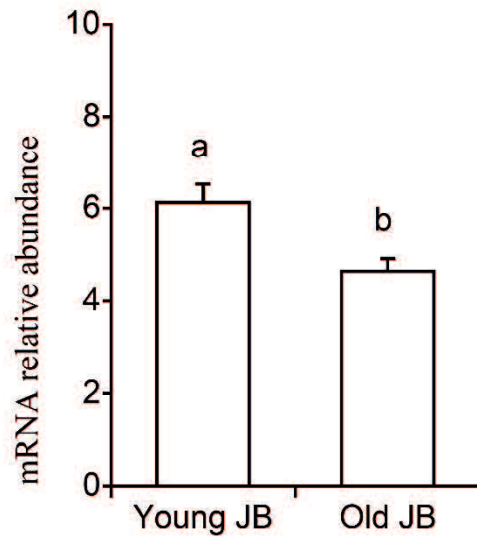
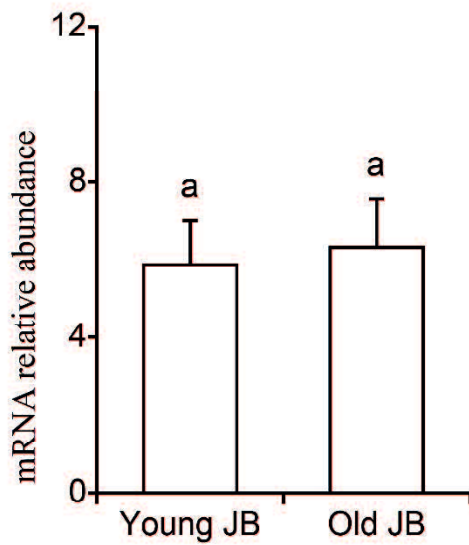


**Fig. 6.5.** Relative *AMH* mRNA levels (mean ± SEM) in bovine POA and ARC & ME tissues obtained from young and old JB, as determined by RT-qPCR. Data were normalized to the geometric means of *YWHAZ* and *SDHA* levels. Letters (a vs b) indicate significant differences ( $P < 0.05$ ) among groups.

**(A) AMHR2 in POA**



**(B) AMHR2 in ARC & ME**

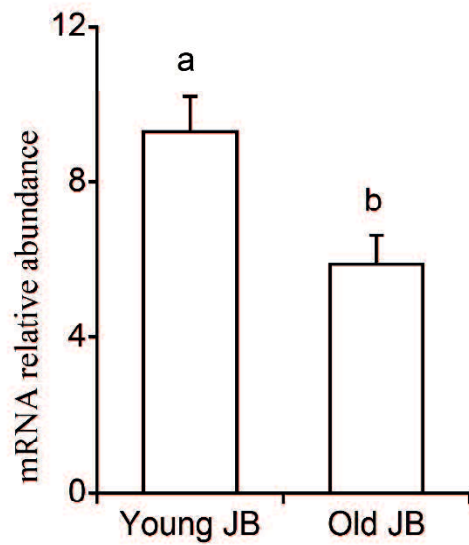


**Fig. 6.6.** Relative *AMHR2* mRNA levels (mean ± SEM) in bovine POA and ARC&ME tissues obtained from young and old JB, as determined by RT-qPCR. Data were normalized to the geometric means of *YWHAZ* and *SDHA* levels. Letters (a vs b) indicate significant differences ( $P < 0.05$ ) among groups.

## 6.5. Discussion

The present study revealed a correlative relationship between aging and a decrease in AMH and AMHR2 protein in the ARC&ME tissues of the posterior hypothalamus. However, further studies are necessary to investigate a potential causal relationship between this decrease in AMH and AMHR2 protein and aging.

I also analyzed AMH and AMHR2 by immunofluorescence in the POA, ARC, and ME in young and old hypothalami (data not shown); however, no differences were detected since the immunofluorescence method was qualitative and not quantitative. Possible mechanisms include decreased axonal transport from GnRH neurons in the POA, or decreased expression of AMH and AMHR2 in GnRH neurons in the POA.

Previous studies have demonstrated the importance of AMH and AMHR2 in GnRH-positive neurons in hypothalamic function. Approximately 85% of hypothalamic GnRH neuronal fibers are positive for both AMH and AMHR2, including those in the external zones of the ME (Kereilwe and Kadokawa 2020). The ME is the interface between the neural and peripheral endocrine systems through which GnRH is secreted into the pituitary portal blood vessels (Jansen *et al.* 1997). Using three-dimensional immunofluorescence, chapter V study suggested that bovine GnRH neurons secrete AMH as well as GnRH into the pituitary portal blood, which may lead to AMH stimulation of LH and FSH secretion from gonadotrophs in the pituitary. However, it should be noted that less than 30% of AMH- and AMHR2-positive neurons are non-GnRH neurons in the POA, ARC, and ME (Kereilwe and Kadokawa 2020). To date, there is no published data on AMH or AMHR2 in non-GnRH neurons, or specifically on whether kisspeptin neurons express these proteins. Therefore, further studies are necessary to investigate a potential causal relationship between this decrease in AMH and AMHR2 protein and aging.

Kermath *et al.* (2014) compared neuroendocrine gene expressions in three hypothalamic regions— the ARC, ME, and AVPV nucleus located close to the POA (Okamura 2002). Interestingly, Kermath *et al.* (2014) also reported that the majority of the aging-related changes occurred in the ARC and ME, whereas there were few in the AVPV nucleus, and the overall pattern was a decrease with aging. Their results suggest important roles of the ARC and ME during reproductive senescence. The majority of the GnRH neurons in the bovine hypothalamus express both AMH and AMHR2 (Kereilwe and Kadokawa 2020). AMH strongly activates GnRH neurons in adult female mice both *in vivo* and *in vitro* (Cimino *et al.* 2016). Combined with the results of Kermath *et al.* (2014), my data suggests important roles of the ARC and ME in reproductive senescence.

In conclusion, both AMH and AMHR2 were decreased in the posterior hypothalamus containing ARC and ME in old cows, suggesting an important correlation between aging and both proteins. However, this study did not demonstrate a causal relationship. Therefore, further studies are required to clarify the roles of the AMH-AMHR2 system in GnRH neurons during aging.

## **CHAPTER VII**

### **General Discussion and Conclusion**

## 7.1. General discussion

I hypothesized that preantral and small antral follicles may secrete AMH to control gonadotropin secretion from ruminant gonadotrophs, and the study I discovered that mRNA and protein of AMHR2 are expressed in APs. Also the immunofluorescence microscopy visualized colocalization of AMHR2 with GnRHR on the plasma membrane of gonadotrophs. Furthermore, AMH controlled LH and FSH secretion from the cultured bovine AP cells. Therefore, the study I support the hypothesis that the endocrine feedback roles of AMH secreted from ovaries to control gonadotropin secretion. The preantral and small antral follicles are not silent majority in ovaries.

In addition to the AMH's endocrine roles, the study II discovered that bovine gonadotrophs express AMH. This data suggested that AMH is similar with other important hormones (e.g. GnRH, inhibin, and activin), and the gonadotroph, targeted by hypothalamus or ovaries, itself, synthesizes and secretes the important hormone, for paracrine and autocrine roles. Furthermore, this data suggested that the combination of endocrine effect and paracrine and autocrine effects finely tune gonadotrophs.

Depending on the discoveries of AMH and AMHR2 in gonadotrophs, I challenged to discover of AMH and AMHR2 in GnRH neurons, then, the obtained data supported this hypothesis. My findings thus indicate that AMH and AMHR2 are detected in the majority of cell bodies or fibers of GnRH neurons in POA, ARC, or ME of heifer brains. The data support the hypothesis that AMH and AMHR2 affect reproduction at the level of hypothalamus and AP.

Cow fertility decreases with age, but the hypothalamic and pituitary pathomechanisms are not understood. I challenged to estimate contribution of AMHR2 and AMH in AP for infertility after aging. I compared expression levels of AMH and AMHR2 between old Holsteins and young and old Japanese Black females. In the study

I, the APs of old Holsteins exhibited similar AMHR2 expression levels compared to those of young Japanese Black females. In contrast, in the study II, the APs of old Holsteins exhibited lower AMH mRNA levels but higher AMH protein levels than those of young Japanese Black females, suggesting weaker AMH secretion of old Holstein AP compared to young Japanese Black. The difference in AMH expression in APs may be explained by a difference among breeds or any factor related to breed. However, the results for the effects of breed and age on AMH expression in APs should be interpreted with caution because I could not obtain APs from young Holsteins.

In the study IV, lower expressions of AMH and AMHR2 in the posterior hypothalamus (containing the ARC and ME), but not in the anterior hypothalamus (containing the POA), of old Japanese Black and old Holstein cows compared to young heifers. A previous study found that GnRH neurons contain AMHR2 in various regions of female human and rodent brains, including the POA, ARC, and ME (Cinimo *et al.* 2016). Furthermore, both *in vivo* and *in vitro* studies have demonstrated that AMH potently activates GnRH neurons, and consequently GnRH-dependent LH secretion in adult female mice (Cinimo *et al.* 2016). Therefore the study IV suggested the suppressed AMH stimulation in ARC for pulsatile GnRH secretion, and decreased AMH secretion into pituitary portal blood in ME leading to the infertility in aged cows.

## **7.2. Conclusion**

In conclusion, this thesis discovered the AMH and AMHR2 in bovine AP and GnRH neurons, also this thesis discovered the possibility that these systems may have important roles in age-related infertility.

## References

- Adamczyk, K., Makulska, J., Jagusiak, W., and Weglarz, A. (2017). Associations between strain, herd size, age at first calving, culling reason and lifetime performance characteristics in Holstein–Friesian cows. *Animal* **11**, 327–334.
- Agriculture, Forestry and Fisheries Research Council Secretariat. (2008). Nutrition requirement. In: Ministry of Agriculture, Forestry and Fisheries, eds. Japanese Feeding Standard for Beef Cattle. pp 31-48. (Tokyo, Japan: Central Association of Livestock Industry)
- Belville, C., Van, Vlijmen, H., Ehrenfels, C., Pepinsky, B., Rezaie, A. R., Picard, J. Y., Josso, N., di Clemente, N., and Cate, R. L. (2004). Mutations of the anti-mullerian hormone gene in patients with persistent mullerian duct syndrome: biosynthesis, secretion, and processing of the abnormal proteins and analysis using a three-dimensional model. *Mol. Endocrinol.* **18**, 708-721.
- Ben-Shlomo, A., and Melmed. S. (2011). Hypothalamic Regulation of Anterior Pituitary Function. In: The Pituitary, 3rd ed. (Melmed, S. ed.). pp. 21-46. (Academic Press, San Diego.)
- Bhide, P., and Homburg, R. (2016). Anti-Müllerian hormone and polycystic ovary syndrome. *Best. Pract. Res. Clin. Obstet. Gynaecol.* **37**, 38-45.
- Bond, B. C., Virley, D. J., Cairns, N. J., Hunter, A. J., Moore, G. B., Moss, S. J., Mudge, A. W., Walsh, F. S., Jazin, E., and Preece, P. (2002). The quantification of gene expression in an animal model of brain ischaemia using TaqMan real-time RT-PCR. *Brain. Res. Mol. Brain Res.* **106**, 101–116.
- Borromeo, V., Amsterdam, A., Berrini, A., Gaggioli, D., Dantes, A., and Secchi, C. (2004). Characterization of biologically active bovine pituitary FSH purified by immunoaffinity chromatography using a monoclonal antibody. *Gen. Comp. Endocrinol.* **139**, 179-189. doi: 10.1016/j.ygcen.2004.09.005

- Bryner, R. W., Garcia-Winder, M., Lewis, P. E., Inskoop, E. K., and Butcher, R. L. (1990). Changes in hormonal profiles during the estrous cycle in old lactating beef cows. *Domest. Anim. Endocrinol.* **7**, 181-189.
- Bédécarrats, G. Y., O'Neill, F. H., Norwitz, E. R., Kaiser, U. B., and Teixeira, J. (2003). Regulation of gonadotropin gene expression by Mullerian inhibiting substance. *Proc. Natl. Acad. Sci. U. S. A.* **100**, 9348-9353.
- Campbell, B. K., Clinton, M., and Webb, R. (2012). The role of anti-Mullerian hormone (AMH) during follicle development in a monovulatory species (sheep). *Endocrinology* **153**, 4533-4543.
- Campbell, R. E., Gaidamaka, G., Han, S. K., and Herbison, A. E. (2009). Dendro-dendritic bundling and shared synapses between gonadotropin-releasing hormone neurons. *Proc. Natl. Acad. Sci. U. S. A.* **106**, 10835-10840.
- Chenoweth, P. J. (1994). Aspects of reproduction in female *Bos indicus* cattle: a review. *Aust. Vet. J.* **71**, 422-426.
- Childs, G. V. (1997). Cytochemical studies of multifunctional gonadotropes. *Microsc. Res. Tech.* **39**, 114–130.
- Ciechanowska, M., Kowalczyk, M., Lapot, M., Malewski, T., Antkowiak, B., Brytan, M., Winnicka, I., and Przekop, F. (2018). Effect of corticotropin releasing hormone and corticotropin releasing hormone nist on biosynthesis of gonadotropin releasing hormone and gonadotropin releasing hormone receptor in the hypothalamic-pituitary unit of follicular-phase ewes and contribution of kisspeptin. *J. Physiol. Pharmacol.* **69**, 451–461.
- Cimino, I., Casoni, F., Liu, X., Messina, A., Parkash, J., Jamin, S. P., Catteau-Jonard, S., Collier, F., Baroncini, M., Dewailly, D., Pigny, P., Prescott, M., Campbell, R., Herbison, A. E., Prevot, V., and Giacobini, P. (2016). Novel role for anti-

- Müllerian hormone in the regulation of GnRH neuron excitability and hormone secretion. *Nat. Commun.* **7**, 10055.
- Clarke, I. J., Cummins, J. T., Karsch, F. J., Seeburg, P. H., and Nikolics, K. (1987). GnRH-associated peptide (GAP) is cosecreted with GnRH into the hypophyseal portal blood of ovariectomized sheep. *Biochem. Biophys. Res. Commun.* **143**, 665-671.
- de Kretser, D. M., Hedger, M. P., Loveland, K. L., and Phillips, D. J. (2002). Inhibins, activins and follistatin in reproduction. *Hum. Reprod. Update* **8**, 529–541.
- Dewailly, D., Andersen, C. Y., Balen, A., Broekmans, F., Dilaver, N., Fanchin, R., Griesinger, G., Kelsey, T. W., La Marca, A., Lambalk, C., Mason, H., Nelson, S. M., Visser, J. A., Wallace, W. H., and Anderson, R. A. (2014). The physiology and clinical utility of anti-Müllerian hormone in women. *Hum. Reprod. Update* **20**, 370-385.
- di Clemente, N., Jamin, S. P., Lugovskoy, A., Carmillo, P., Ehrenfels, C., Picard, J. Y., and Cate, R. L. (2010). Processing of anti-Müllerian hormone regulates receptor activation by a mechanism distinct from TGF- $\beta$ . *Mol. Endocrinol.* **24**, 2193–2206.
- Durlinger, A. L., Gruijters, M. J., Kramer, P., Karels, B., Kumar, T. R., Matzuk, M. M., Rose, U. M., de Jong, F. H., Uilenbroek, J. T., Grootegoed, J. A., and Themmen, A. P. (2001). Anti-Müllerian hormone attenuates the effects of FSH on follicle development in the mouse ovary. *Endocrinology* **142**, 4891-4899.
- El-Sheikh Ali, H., Kitahara, G., Nibe, K., Yamaguchi, R., Horii, Y., Zaabel, S., and Osawa, T. (2013). Plasma anti-Müllerian hormone as a biomarker for bovine granulosa-theca cell tumors: Comparison with immunoreactive inhibin and ovarian steroid concentrations. *Theriogenology* **80**, 940-949.

- Erickson, B. H., Reynolds, R. A., and Murphree, R. L. (1976). Ovarian characteristics and reproductive performance of the aged cow. *Biol. Reprod.* **15**, 555-560.
- Faure, E., Gouédard, L., Imbeaud, S., Cate, R., Picard, J. Y., Josso, N., and di Clemente, N. (1996). Mutant isoforms of the anti-Müllerian hormone type II receptor are not expressed at the cell membrane. *J. Biol. Chem.* **271**, 30571-30575.
- Garrel, G., Racine, C., L'Hôte, D., Denoyelle, C., Guigon, C. J., di Clemente, N., and Cohen-Tannoudji, J. (2016). Anti-Müllerian hormone: a new actor of sexual dimorphism in pituitary gonadotrope activity before puberty. *Sci. Rep.* **6**, 23790.
- Georgopoulos, N. A., Karagiannidou, E., Koika, V., Roupas, N. D., Armeni, A., Marioli, D., Papadakis, E., Welt, C. K., and Panidis, D. (2013). Increased frequency of the anti-mullerian-inhibiting hormone receptor 2 (AMHR2) 482 A>G polymorphism in women with polycystic ovary syndrome: relationship to luteinizing hormone levels. *J. Clin. Endocrinol. Metab.* **98**, E1866-E1870.
- Gernand, E., and König, S. (2017). Genetic relationships among female fertility disorders, female fertility traits and productivity of Holstein dairy cows in the early lactation period. *J. Anim. Breed. Genet.* **134**, 353–363.
- Geserick, C., Meyer, H. A., and Haendler, B. (2005). The role of DNA response elements as allosteric modulators of steroid receptor function. *Mol. Cell. Endocrinol.* **236**, 1–7.
- Gruber, C. J., Gruber, D. M., Gruber, I. M., Wieser, F., and Huber, J. C. (2004). Anatomy of the estrogen response element. *Trends Endocrinol. Metab.* **15**, 73–78.

- Hashizume, T., Horiuchi, M., Tate, N., Nonaka, S., Kojima, M., Hosoda, H., and Kangawa, K. (2003). Effects of ghrelin on growth hormone secretion from cultured adenohypophysial cells in cattle. *Endocr. J.* **50**, 289-295.
- Hashizume, T., Onodera, Y., Shida, R., Isobe, E., Suzuki, S., Sawai, K., Kasuya, E., and Nagy, G. M. (2009). Characteristics of prolactin-releasing response to salsolinol (SAL) and thyrotropin-releasing hormone (TRH) in ruminants. *Domest. Anim. Endocrinol.* **36**, 99-104.
- Hassaneen, A., Naniwa, Y., Suetomi, Y., Matsuyama, S., Kimura, K., Ieda, N., Inoue, N., Uenoyama, Y., Tsukamura, H., Maeda, K. I., Matsuda, F., and Ohkura, S. (2016). Immunohistochemical characterization of the arcuate kisspeptin/neurokinin B/dynorphin (KNDy) and preoptic kisspeptin neuronal populations in the hypothalamus during the estrous cycle in heifers. *J. Reprod. Dev.* **62**, 471-477.
- Head, B. P., Patel, H. H., and Insel, P. A. (2014). Interaction of membrane/lipid rafts with the cytoskeleton: impact on signaling and function: membrane/lipid rafts, mediators of cytoskeletal arrangement and cell signaling. *Biochim. Biophys. Acta.* **1838**, 532-545.
- Herbison, A. E. (2016). Control of puberty onset and fertility by gonadotropin-releasing hormone neurons. *Nat. Rev. Endocrinol.* **12**, 452-466.
- Hernandez-Medrano, J. H., Campbell, B. K., and Webb, R. (2012). Nutritional influences on folliculogenesis. *Reprod. Dom. Anim.* **4**, 274-282.
- Hirokawa, T., Boon-Chieng, S., and Mitaku, S. (1998). SOSUI: classification and secondary structure prediction system for membrane proteins. *Bioinformatics* **14**, 378-379.

- Hirschhorn, T., di Clemente, N., Amsalem, A. R., Pepinsky, R. B., Picard, J. Y., Smorodinsky, N. I., Cate, R. L., and Ehrlich, M. (2015). Constitutive negative regulation in the processing of the anti-Müllerian hormone receptor II. *J. Cell Sci.* **128**, 1352-1364.
- Hopp, T. P., and Woods, K. R. (1981). Prediction of protein antigenic determinants from amino acid sequences. *Proc. Natl. Acad. Sci. U. S. A.* **78**, 3824-3828.
- Hossain, M. S., Mineno, K., and Katafuchi, T. (2016). Neuronal orphan G-protein coupled receptor proteins mediate plasmalogens-induced activation of ERK and Akt signaling. *PLoS One* **11**, e0150846.
- Ilha, G. F., Rovani, M. T., Gasperin, B.G., Ferreira, R., de Macedo, M. P., Neto, O. A., Duggavathi, R., Bordignon, V., and Goncalves, P. B. (2016). Regulation of anti-Mullerian hormone and its receptor expression around follicle deviation in cattle. *Reprod. Domest. Anim.* **51**,188-194.
- Iqbal, J., Latchoumanin, O., Sari, I. P., Lang, R. J., Coleman, H. A., Parkington, H. C., and Clarke, I. J. (2009). Estradiol-17beta inhibits gonadotropin-releasing hormone-induced Ca<sup>2+</sup> in gonadotropes to regulate negative feedback on luteinizing hormone release. *Endocrinology* **150**, 4213-4220.
- Ireland, J. L., Scheetz, D., Jimenez-Krassel, F., Themmen, A. P., Ward, F., Lonergan, P., Smith, G. W., Perez, G. I., Evans, A. C., and Ireland, J. J. (2008). Antral follicle count reliably predicts number of morphologically healthy oocytes and follicles in ovaries of young adult cattle. *Biol. Reprod.* **79**, 1219-1225.
- Jansen, H. T., Hileman, S. M., Lubbers, L. S., Kuehl, D. E., Jackson, G. L., and Lehman, M. N. (1997). Identification and distribution of neuroendocrine gonadotropin-releasing hormone neurons in the ewe. *Biol. Reprod.* **56**, 655-662.

- Kadokawa, H., Takusari, N., Yamada, Y., Takahashi, H., and Kariya, T. (1998). GnRH inducing LH release, nutrition and plasma cortisol in high producing dairy cows postpartum. *J. Reprod. Dev.* **44**, 197-203.
- Kadokawa, H., and Yamada, Y. (1999). Enhancing effect of acute fasting on ethanol suppression of pulsatile luteinizing hormone release via an estrogen-dependent mechanism in Holstein heifers. *Theriogenology* **51**, 673-680.
- Kadokawa, H., and Yamada, Y. (2000). Effects of a long-lasting opioid receptor antagonist (naltrexone) on pulsatile LH release in early postpartum Holstein dairy cows. *Theriogenology* **54**, 75-81.
- Kadokawa, H., Blache, D., and Martin, G. B. (2006). Plasma leptin concentrations correlate with luteinizing hormone secretion in early postpartum Holstein cows. *J. Dairy Sci.* **89**, 3020-3027.
- Kadokawa, H., and Martin, G. B. (2006). A new perspective on management of reproduction in dairy cows: the need for detailed metabolic information, an improved selection index and extended lactation. *J. Reprod. Dev.* **52**, 161-168.
- Kadokawa, H. (2007). Seasonal differences in the parameters of luteinizing hormone release to exogenous gonadotropin releasing hormone in prepubertal Holstein heifers in Sapporo. *J. Reprod. Dev.* **53**, 121-125.
- Kadokawa, H., Matsui, M., Hayashi, K., Matsunaga, N., Kawashima, C., Shimizu, T., Kida, K., and Miyamoto, A. (2008a). Peripheral administration of kisspeptin-10 increases plasma concentrations of GH as well as LH in prepubertal Holstein heifers. *J. Endocrinol.* **196**, 331-334.
- Kadokawa, H., Suzuki, S., and Hashizume, T. (2008b). Kisspeptin-10 stimulates the secretion of growth hormone and prolactin directly from cultured bovine anterior pituitary cells. *Anim. Reprod. Sci.* **105**, 404-408.

- Kadokawa, H., Pandey, K., Nahar, A., Nakamura, U., and Rudolf, F. O. (2014). Gonadotropin-releasing hormone (GnRH) receptors of cattle aggregate on the surface of gonadotrophs and are increased by elevated GnRH concentrations. *Anim. Reprod. Sci.* **150**, 84-95.
- Kadokawa, H. (2020). Discovery of new receptors regulating luteinizing hormone and follicle-stimulating hormone secretion by bovine gonadotrophs to explore a new paradigm for mechanisms regulating reproduction. *J. Reprod. Dev.* **66**, 291-297.
- Kaiser, U. B. (2011). Gonadotropin Hormones. In 'The Pituitary'. (Ed S. Melmed). pp. 205-260. (Elsevier Inc: Philadelphia, USA)
- Kamomae, H. (2012). Reproductive disturbance. In 'Veterinary Theriogenology'. (Eds T. Nakao, S. Tsumagari and S. Katagiri.). pp. 283–340. (Buneidou Press: Tokyo, Japan.) [In Japanese]
- Kereilwe, O., Pandey, K., Borromeo, V., and Kadokawa, H. (2018). Anti-Müllerian hormone receptor type 2 is expressed in gonadotrophs of postpubertal heifers to control gonadotrophin secretion. *Reprod. Fertil. Dev.* **30**, 1192–1203.
- Kereilwe, O., and Kadokawa, H. (2019). Bovine gonadotrophs express anti-Müllerian hormone (AMH): comparison of AMH mRNA and protein expression levels between old Holsteins and young and old Japanese Black females. *Reprod. Fertil. Dev.* **31**, 810-819.
- Kereilwe, O., and Kadokawa, H. (2020). Anti-Müllerian hormone and its receptor are detected in most gonadotropin-releasing-hormone cell bodies and fibers in heifer brains. *Domest. Anim. Endocrinol.* **72**, 106432.
- Kermath, B. A., Riha, P. D., Woller, M. J., Wolfe, A., and Gore, A. C. (2014). Hypothalamic molecular changes underlying natural reproductive senescence in the female rat. *Endocrinology* **155**: 3597-3609.

- Ko, J. H., and Kim, S. N. (2018). A literature review of women's sex hormone changes by acupuncture treatment: analysis of human and animal studies. *Evid. Based Complement. Alternat. Med.* 3752723.
- Koizumi, M., Nahar, A., Yamabe, R., and Kadokawa, H. (2016). Positive correlations of age and parity with plasma concentration of macrophage migration inhibitory factor in Japanese black cows. *J. Reprod. Dev.* **62**, 257-263.
- Koizumi, M., and Kadokawa, H. (2017). Positive correlations of age and parity with plasma anti-Müllerian hormone concentrations in Japanese Black cows. *J. Reprod. Dev.* **63**, 205-209.
- Kushnir, V. A., Seifer, D. B., Barad, D. H., Sen, A., and Gleicher, N. (2017). Potential therapeutic applications of human anti-Müllerian hormone (AMH) analogues in reproductive medicine. *J. Assist. Reprod. Genet.* **34**, 1105-1113.
- Larco, D. O., Semsarzadeh, N. N., Cho-Clark, M., Mani, S. K., and Wu, T. J. (2013). The novel actions of the metabolite GnRH-(1-5) are mediated by a G protein-coupled receptor. *Front. Endocrinol. (Lausanne)* **4**, 83.
- Leshin, L. S., Rund, L. A., Crim, J. W., and Kiser, T. E. (1988). Immunocytochemical localization of luteinizing hormone-releasing hormone and proopiomelanocortin neurons within the preoptic area and hypothalamus of the bovine brain. *Biol. Reprod.* **39**, 963-975.
- Liu, D., Xiong, F., and Hew, C. L. (1995). Functional analysis of estrogen-responsive elements in chinook salmon (*Oncorhynchus tshawytscha*) gonadotropin II beta subunit gene. *Endocrinology* **136**, 3486-3493.
- Malhi, P. S., Adams, G. P., Pierson, R. A., and Singh, J. (2006). Bovine model of reproductive aging: response to ovarian synchronization and superstimulation. *Theriogenology* **66**, 1257-1266.

- Malone, S. A., Papadakis, G. E., Messina, A., Mimouni, N. E. H., Trova, S., Imbernon, M., Allet, C., Cimino, I., Acierno, J., Cassatella, D., Xu, C., Quinton, R., Szinnai, G., Pigny, P., Alonso-Cotchico, L., Masgrau, L., Maréchal, J. D., Prevot, V., Pitteloud, N., and Giacobini, P. (2019). Defective AMH signaling disrupts GnRH neuron development and function and contributes to hypogonadotropic hypogonadism. *eLife* **8**: pii: e47198.
- Mamsen, L. S., Petersen, T. S., Jeppesen, J. V., Møllgard, K., Grøndahl, M. L., Larsen, A., Ernst, E., Oxvig, C., Kumar, A., Kalra, B., and Andersen, C. Y. (2015). Proteolytic processing of anti-Müllerian hormone differs between human fetal testes and adult ovaries. *Mol. Hum. Reprod.* **21**, 571–582.
- Manders, E. M. M., Verbeek, F. J., and Aten, J. A. (1993). Measurement of co-localization of objects in dual-colour confocal images. *J. Microscopy* **169**, 375-382.
- Martin, T. L., Fogwell, R. L., and Ireland, J. J. (1991). Concentrations of inhibins and steroids in follicular fluid during development of dominant follicles in heifers. *Biol. Reprod.* **44**, 693-700.
- Matteri, R. L., Roser, J. F., Baldwin, D. M., Lipovetsky, V., and Papkoff, H. (1987). Characterization of a monoclonal antibody which detects luteinizing hormone from diverse mammalian species. *Domest. Anim. Endocrinol.* **4**, 157-165.
- Meczekalski, B., Czyzyk, A., Kunicki, M., Podfigurna-Stopa, A., Plociennik, L., Jakiel, G., Maciejewska-Jeske, M., and Lukaszuk, K. (2016). Fertility in women of late reproductive age: the role of serum anti-Müllerian hormone (AMH) levels in its assessment. *J. Endocrinol. Invest.* **39**, 1259-1265.
- Medzihradzky, K. F., Kaasik, K., and Chalkley, R. J. (2015). Tissue-specific glycosylation at the glycopeptide level. *Mol. Cell. Proteomics* **14**, 2103–2110.

- Miller, G. M., Alexander, J. M., and Klibanski, A. (1996). Gonadotropin-releasing hormone messenger RNA expression in gonadotroph tumors and normal human pituitary. *J. Clin. Endocrinol. Metab.* **81**, 80–83.
- Miyamoto, Y., Skarzynski, D. J., and Okuda, K. (2000). Is tumor necrosis factor alpha a trigger for the initiation of endometrial prostaglandin F (2alpha) release at luteolysis in cattle? *Biol. Reprod.* **62**, 1109-1115.
- Monniaux, D., Baril, G., Laine, A. L., Jarrier, P., Poulin, N., Cognié, J., and Fabre, S. (2011). Anti-Mullerian hormone as a predictive endocrine marker for embryo production in the goat. *Reproduction* **142**, 845-854.
- Monniaux, D., Drouilhet, L., Rico, C., Estienne, A., Jarrier, P., Touzé, J. L., Sapa, J., Phocas, F., Dupont, J., Dalbiès-Tran, R., and Fabre, S. (2012). Regulation of anti-Müllerian hormone production in domestic animals. *Reprod. Fertil. Dev.* **25**, 1-16.
- Mossa, F., Jimenez-Krassel, F., Scheetz, D., Weber-Nielsen, M., Evans, A. C. O., and Ireland, J. J. (2017). Anti-Müllerian Hormone (AMH) and fertility management in agricultural species. *Reproduction* **154**, R1-R11.
- Nakamura, U., Rudolf, F.O., Pandey, K., and Kadokawa, H. (2015). The non-steroidal mycoestrogen zeranol suppresses luteinizing hormone secretion from the anterior pituitary of cattle via the estradiol receptor GPR30 in a rapid, non-genomic manner. *Anim. Reprod. Sci.* **156**, 118-127.
- Naugle, M. M., and Gore, A. C. (2014). GnRH neurons of young and aged female rhesus monkeys co-express GPER but are unaffected by long-term hormone replacement. *Neuroendocrinology* **100**, 334-346.
- Naugle, M. M., Lozano, S. A., Guarraci, F. A., Lindsey, L. F., Kim, J. E., Morrison, J. H., Janssen, W. G., Yin, W., and Gore, A. C. (2016). Age and long-term

- hormone treatment effects on the ultrastructural morphology of the median eminence of female rhesus macaques. *Neuroendocrinology* **103**, 650-664.
- Navratil, A. M., Song, H., Hernandez, J. B., Cherrington, B. D., Santos, S. J., Low, J. M., Do, M. H., and Lawson, M. A. (2009). Insulin augments gonadotropin releasing hormone induction of translation in LbetaT2 cells. *Mol. Cell. Endocrinol.* **311**, 47-54.
- Nestor, C. C., Bedenbaugh, M. N., Hileman, S. M., Coolen, L. M., Lehman, M. N., and Goodman, R. L. (2018). Regulation of GnRH pulsatility in ewes. *Reproduction* **156**, R83-R99.
- Nett, T. M., Cermak, D., Braden, T., Manns, J., and Niswender, G. (1987). Pituitary receptors for GnRH and estradiol, and pituitary content of gonadotropins in beef cows. I. Changes during the estrous cycle. *Domest. Anim. Endocrinol.* **4**, 123-132.
- Nussey, S. S., and Whitehead, S. A. (2001). The pituitary gland. In 'Endocrinology: an integrated approach.' (Eds. S. S. Nussey and S. A. Whitehead). pp. 283-334. (BIOS scientific publishers, Oxford, UK.)
- Okamura, H. (2002). Brain atlas of cattle (in Japanese) In: A Foundational Research for Elucidation and Estimation of Agriculture, pp. 41-72. (Forestry and Fisheries Research Council.)
- Osoro, K., and Wright, I. A. (1992). The effect of body condition, live weight, breed, age, calf performance, and calving date on reproductive performance of spring-calving beef cows. *J. Anim. Sci.* **70**: 1661-1666.
- Pagesy, P., Li, J. Y., Berthet, M., and Peillon, F. (1992). Evidence of gonadotropin-releasing hormone mRNA in the rat anterior pituitary. *Mol. Endocrinol.* **6**, 523–528.

- Pals, K., Roudbaraki, M., and Deneff, C. (2008). Growth hormone-releasing hormone and glucocorticoids determine the balance between luteinising hormone (LH) beta- and LH beta/follicle-stimulating hormone beta-positive gonadotrophs and somatotrophs in the 14-day-old rat pituitary tissue in aggregate cell culture. *J. Neuroendocrinol.* **20**, 535-548.
- Pandey, K., Nahar, A., and Kadokawa, H. (2016). Method for isolating pure bovine gonadotrophs from anterior pituitary using magnetic nanoparticles and anti-gonadotropin-releasing hormone receptor antibody. *J. Vet. Med. Sci.* **78**, 1699-1702.
- Pandey, K., Kereilwe, O., Borromeo, V., and Kadokawa, H. (2017a). Heifers express G-protein coupled receptor 61 in anterior pituitary gonadotrophs in stage-dependent manner. *Anim. Reprod. Sci.* **181**, 93-102.
- Pandey, K., Mizukami, Y., Watanabe, K., Sakaguti, S., and Kadokawa, H. (2017b). Deep sequencing of the transcriptome in the anterior pituitary of heifers before and after ovulation. *J. Vet. Med. Sci.* **79**, 1003-1012.
- Pandey, K., Kereilwe, O., and Kadokawa, H. (2018). Heifers express G-protein coupled receptor 153 in anterior pituitary gonadotrophs in stage-dependent manner. *Anim. Sci. J.* **89**, 60–71.
- Pfeiffer, K. E., Jury, L. J., and Larson, J. E. (2014). Determination of anti-Müllerian hormone at estrus during a synchronized and a natural bovine estrous cycle. *Domest. Anim. Endocrinol.* **46**, 58-64.
- Pierre, A., Racine, C., Rey, R. A., Fanchin, R., Taieb, J., Cohen-Tannoudji, J., Carmillo, P., Pepinsky, R. B., Cate, R. L., and di Clemente, N. (2016). Most cleaved anti-Müllerian hormone binds its receptor in human follicular fluid but little is competent in serum. *J. Clin. Endocrinol. Metab.* **101**, 4618–4627.

- Poole, D. H., Ocón-Grove, O. M., and Johnson, A. L. (2016). Anti-Müllerian hormone (AMH) receptor type II expression and AMH activity in bovine granulosa cells. *Theriogenology* **86**, 1353-1360.
- Poonlaphdecha, S., Pepey, E., Huang, S. H., Canonne, M., Soler, L., Mortaji, S., Morand, S., Pfennig, F., Melard, C., Baroiller, J. F., and D’Cotta, H. (2011). Elevated AMH gene expression in the brain of male tilapia (*Oreochromis niloticus*) during testis differentiation. *Sex. Dev.* **5**, 33–47.
- Popovics, P., Rekasi, Z., Stewart, A. J., and Kovacs, M. (2011). Regulation of pituitary inhibin/activin subunits and follistatin gene expression by GnRH in female rats. *J. Endocrinol.* **210**, 71–79.
- Rekawiecki, R., Rutkowska, J., and Kotwica, J. (2012). Identification of optimal housekeeping genes for examination of gene expression in bovine corpus luteum. *Reprod. Biol.* **12**, 362–367.
- Ribeiro, E. S., Bisinotto, R. S., Lima, F. S., Greco, L. F., Morrison, A., Kumar, A., Thatcher, W. W., and Santos, J. E. (2014). Plasma anti-Müllerian hormone in adult dairy cows and associations with fertility. *J. Dairy Sci.* **97**, 6888-6900.
- Rico, C., Médigue, C., Fabre, S., Jarrier, P., Bontoux, M., Clément, F., and Monniaux, D. (2011). Regulation of anti-Müllerian hormone production in the cow: a multiscale study at endocrine, ovarian, follicular, and granulosa cell levels. *Biol. Reprod.* **84**, 560-571.
- Ritter, S. L., and Hall, R. A. (2009). Fine-tuning of GPCR activity by receptor-interacting proteins. *Nat. Rev. Mol. Cell. Biol.* **10**, 819–830.
- Rocha, R. M., Lima, L. F., Carvalho, A. A., Chaves R. N., Bernuci, M. P., Rosa-e-Silva, A. C., Rodrigues, A. P., Campello, C. C., and Figueiredo, J. R. (2016). Immunolocalization of the anti-Müllerian hormone (AMH) in caprine follicles

- and the effects of AMH on in vitro culture of caprine pre-antral follicles enclosed in ovarian tissue. *Reprod. Domest. Anim.* **51**, 212-219.
- Rosas-Arellano, A., Villalobos-González, J. B., Palma-Tirado, L., Beltrán, F. A., Cárabez-Trejo, A., Missirlis, F., and Castro, M. A. (2016). A simple solution for antibody signal enhancement in immunofluorescence and triple immunogold assays. *Histochem. Cell Biol.* **146**, 421-430.
- Rudolf, F. O., and Kadokawa, H. (2014). Effects of STX, a novel estrogen membrane receptor agonist, on GnRH-induced luteinizing hormone secretion from cultured bovine anterior pituitary cells. *J. Vet. Med. Sci.* **76**, 1623–1625.
- Sakalar, C., Mazumder, S., Johnson, J. M., Altuntas, C. Z., Jaini, R., Aguilar, R., Naga Prasad, S. V., Connolly, D. C., and Tuohy, V. K. (2015). Regulation of murine ovarian epithelial carcinoma by vaccination against the cytoplasmic domain of anti-Müllerian hormone receptor II. *J. Immunol. Res.* **2015**, 630287.
- Satake, H., Matsubara, S., Aoyama, M., Kawada, T., and Sakai, T. (2013). GPCR heterodimerization in the reproductive system: functional regulation and implication for biodiversity. *Front. Endocrinol. (Lausanne)* **4**, 1-8.
- Scheffer, J. A. B., Scheffer, B., Scheffer, R., Florencio, F., Grynberg, M., and Lozano, D. M. (2018). Are age and anti-Müllerian hormone good predictors of ovarian reserve and response in women undergoing IVF? *JBRA Assist. Reprod.* **22**: 215-220.
- Seifer, D. B., and Merhi, Z. (2014). Is AMH a regulator of follicular atresia? *Assist. Reprod. Genet.* **31**, 1403-1407.
- Sheldon, I. M., and Dobson, H. (2004). Postpartum uterine health in cattle. *Anim. Reprod. Sci.* **82–83**, 295–306.

- Simons, K., and Tooter, D., (2000). Lipid rafts and signal transduction. *Nat. Rev. Mol. Cell Biol.* **1**, 31-39.
- Skaar, K. S., Nobrega, R. H., Magaraki, A., Olsen, L. C., Schulz, R. W., and Male, R. (2011). Proteolytically activated, recombinant anti Müllerian hormone inhibits androgen secretion, proliferation, and differentiation of spermatogonia in adult zebrafish testis organ cultures. *Endocrinology* **152**, 3527–3540.
- Suzuki, S., Kadokawa, H., and Hashizume, T. (2008). Direct kisspeptin-10 stimulation on luteinizing hormone secretion from bovine and porcine anterior pituitary cells. *Anim. Reprod. Sci.* **103**, 360-365.
- Tanco, V. M., Whitlock, B. K., Jones, M. A., Wilborn, R. R., Brandebourg, T. D., and Foradori, C. D. (2016). Distribution and regulation of gonadotropin-releasing hormone, kisspeptin, RF-amide related peptide-3, and dynorphin in the bovine hypothalamus. *PeerJ* **4**, e1833.
- Townsend, J., Sneddon, C. L., and Tortonese, D. J. (2004). Gonadotroph heterogeneity, density and distribution, and gonadotroph-lactotroph associations in the pars distalis of the male equine pituitary gland. *J. Neuroendocrinol.* **16**, 432-440.
- Tsutsumi, R., and Webster, N. J. (2009). GnRH pulsatility, the pituitary response and reproductive dysfunction. *Endocr. J.* **56**, 729-737.
- Urbanski, H. F. (1991). Monoclonal antibodies to luteinizing hormone-releasing hormone: production, characterization, and immunocytochemical application. *Biol. Reprod.* **44**, 681-686.
- Visser, J. A., and Themmen, A. P. (2014). Role of anti-Müllerian hormone and bone morphogenetic proteins in the regulation of FSH sensitivity. *Mol. Cell. Endocrinol.* **382**, 460-465.

- Walker, C. G., Meier, S., Mitchell, M. D., Roche, J. R., and Littlejohn, M. (2009). Evaluation of real-time PCR endogenous control genes for analysis of gene expression in bovine endometrium. *BMC Mol. Biol.* **10**, 100.
- Wathes, D. C. (2012). Mechanisms linking metabolic status and disease with reproductive outcome in the dairy cow. *Reprod. Domest. Anim.* **47**, 304-312.
- Wehmeyer, L., Du Toit, A., Lang, D. M., and Hapgood, J. P. (2014). Lipid raft- and protein kinase C-mediated synergism between glucocorticoid- and gonadotropin-releasing hormone signaling results in decreased cell proliferation. *J. Biol. Chem.* **289**, 10235-10251.
- Young, J. M., Juengel, J. L., Dodds, K. G., Laird, M., Dearden, P. K., McNeilly, A. S., McNatty, K. P., and Wilson, T. (2008). The activin receptor-like kinase 6 Booroola mutation enhances suppressive effects of bone morphogenetic protein 2 (BMP2), BMP4, BMP6 and growth and differentiation factor-9 on FSH release from ovine primary pituitary cell cultures. *J. Endocrinol.* **196**, 251-261.